

CHALMERS



Impact of distributed generation on distribution systems and its protection

Master of Science Thesis in Electrical Power Engineering

Syed Sagheer Hussain Shah Jillani

Department of Energy and Environment
Division of Electric Power Engineering
CHALMERS UNIVERSITY OF TECHNOLOGY
Göteborg, Sweden 2012
Master's Thesis

MASTER'S THESIS

Impact of distributed generation on distribution systems and its protection

Master of Science Thesis in Electric Power Engineering

Syed Sagheer Hussain Shah Jillani

Department of Energy and Environment
Division of Electric Power Engineering
CHALMERS UNIVERSITY OF TECHNOLOGY
Göteborg, Sweden 2012

Impact of distributed generation on distribution system and its protection

Master of Science Thesis in Electric Power Engineering
SYED SAGHEER HUSSAIN SHAH JILLANI

© SYED SAGHEER HUSSAIN SHAH JILLANI, 2012

Master's Thesis
Department of Energy and Environment
Division of Electric Power Engineering
Chalmers University of Technology
SE-412 96 Göteborg
Sweden
Telephone: + 46 (0)31-772 1000

ABSTRACT:

Recent developments in the renewable energy sector suggest that the wind turbine and photo voltaic as Distributed Generation systems in the distribution network is gaining popularity as a new source of energy. One of the important factors associated with the traditional network is that their protection and setting scheme are inadequate when a distributed generation system is connected to the network as the protection and control requirement of the distributed generators is different than the transmission network. Thus, this interconnected system consistently imposes new challenges in the power system stability.

This study investigates the affect of distributed generators on distribution network during fault condition and includes voltage dips, transients and line short circuit fault current. The robust and effective fast switching of the circuit breakers acts as a protection system with respect to these fault conditions. This study is also valid for sources like photo voltaic, although only wind turbines are selected as an example.

ACKNOWLEDGEMENT:

This work has been carried out at ABB (Västerås) and KTH (Stockholm) with in the CIPOWER project of KIC-Inno Energy. At first I would like to thanks my supervisor at KTH, Nathaniel Taylor, for giving me the opportunity and support to perform the master thesis at ABB and for great help and assistant during the work. I would also like to give my special thanks to my supervisor Lars Liljestrand at ABB corporate research centre for his constant support and invaluable technical advices.

I would also like to express my deepest gratitude to Professor Ola Carlson at the division of Electrical Power Engineering, Chalmers University of technology for examining my thesis work and technical support.

Finally, I would like to thanks my friend Arslan Ashraf for his constant support whenever I need it.

Contents

1. INTRODUCTION.....	9
1.1. BACKGROUND.....	9
1.2. PURPOSE OF STUDY.....	9
1.3. AIM OF THE THESIS.....	10
2. REGULATION AND THEORY.....	11
2.1. VOLTAGE SAG.....	12
2.1.1 DEFINITION.....	12
2.1.2 CHARACTERISTIC OF VOLTAGE SAG.....	13
2.2. GRID COMPLIANCE.....	14
2.2.1 VOLTAGE CONTROL.....	14
2.2.2 FREQUENCY CONTROL.....	15
2.3. PRACTICAL LINE FAULTS.....	16
2.3.1. PHASE–PHASE SHORT CIRCUIT.....	17
2.3.2. SINGLE PHASE SHORT CIRCUIT TO EARTH.....	19
3. ANALYSIS OF A NETWORK.....	21
3.1. DESCRIPTION OF NETWORK.....	21
3.2. OBJECTIVE.....	22
3.3. NETWORK MODELING.....	23
3.3.1 NETWORK MODELING ASSUMPTION.....	23
3.3.2 CABLE DESIGNING.....	23
3.3.3 WIND TURBINE MODELING.....	23
3.3.3.1 LAYOUT OF GRID CONNECTED VSC.....	24
4. SIMULATION AND RESULTS.....	37
4.1. INTRODUCTION.....	37
4.2. SIMULATION RESULTS OF DISTRIBUTION SYSTEM WITHOUT WIND TURBINE.....	37
4.3. SIMULATION RESULTS WITH 3MW AND 6MW WIND TURBINE CAPACITY.....	48
4.3.1. DG ATTACHED AT FEEDER F11.....	48
4.3.2. DG ATTACHED AT FEEDER F12.....	54
4.3.3. DG ATTACHED AT FEEDER F2.....	83
4.3.4. DG ATTACHED AT FEEDER F3.....	89

4.3.5. DG ATTACHED AT FEEDER F4..... 94

4.4. SIMULATION RESULT WITH FAST SHORT CIRCUIT LIMITER 99

5. CONCLUSION AND FUTURE WORK..... 102

FUTURE WORK..... 103

BIBLIOGRAPGY..... 104

APPENDIX A..... 106

ABBREVIATIONS:

PSCAD/EMTDC	Power System Computer Aided Design/ Electromagnetic Transients Direct Current.
PCC	Point of Common Coupling
PCI	Point of Common Interface
LG	Single Line to Ground Fault
LLLG	Three Phase to Ground Fault
pu	Per Unit
DG	Distributed Generators
DR	Distributed Resources
EPS	Electrical Power System
SvK	Svenska Kraftnat
RMS	Root Mean Square

1. INTRODUCTION

1.1.BACKGROUND

The electrical power system has played a critical role in the development of human civilization. It has become a basic necessity in the lives of humans. These requirements have grown continuously and to cope with the demand, it has been achieved through best utilization of maximum energy resources and components to generate electricity to satisfy customer needs. With the increase in power demand, renewable energies such as wind turbines, solar panels and wave power plants have started to play a vital role in the global energy system. The integration of renewable energy into the power system can potentially cause severe challenges for the control and protection of large central generators and the distribution system. A careful design, planning, installation and operation of complex distribution system with renewable energy resources ought to be carried out. In this context, the electrical transmission and distribution plays a significant role in transporting energy from the generator site to customers. Despite the capacity of such a complex network, constant disturbances remain in the system which may be dangerous both for the customers and the power electronics equipment in the network. It is therefore recommended that the damage cause by disturbances should be limited and isolated by fast switching protection devices without affecting the rest of the distribution system.

1.2.PURPOSE OF STUDY

Advancement in the technology of renewable energy such as wind turbines in the MW range has developed more interest in general and its connection to the distribution network. Today large scale integration of wind turbine is connected to the Grid with high power density and controllability. As the quantity of distribution generation increases, as a result the distribution network becoming more like transmission network and the complexity of the network increases, thus a more complex protection system design cannot be ignored. A more adequate study is required for the stability and the protection of the distribution system with the impact of distribution generation (DG).

A fault on such a complex distribution network can have serious consequences on the stability of the power system. A fault in the distribution system creates severe voltage dips and transients which can cause instability. As these disturbances depend upon the location of the fault and the response of the equipment, it requires a deep network study to analyze all the fault condition and make a robust protect system according to the network layout. Also, to avoid reliability issues and network stability problem on the Grid, we assume that the wind farm should not have to cease its output power in the duration of the fault. To overcome such a scenario, the network protection system analysis has to be done including many fault condition.

The main objective of this thesis is to design and investigate the affect of DG in a medium voltage network for short circuit faults, voltage dips and transients which can cause an undesirable result on the distribution system protection system.

1.3.AIM OF THE THESIS

The primary objective of the thesis is divided in two main categories. The first is the impact of distributed generators on the distribution system during fault condition like voltage dips, and short circuit faults and their effect on power system stability. The second objective of the thesis is to design and operation of a robust protective system by fast switching of circuit breaker during faults for the protection of equipment in the distribution system.

In order to analyses the above scenario, a medium voltage 20kV network connected to 130kV is built in PSCAD. The simulation will be considered on different types of wind turbines with specification 3MW and 6MW, with constant output power and maximum current limiting of 1 p.u. The results will show how different line faults cause voltage dips and affect the protection system circuit breakers coordination in the distribution system with the integration of DG in the network, and what will be the best recommended protection of distribution system in-case of integration of DG in the network. The load flows and bus voltages and the magnitudes of voltage dips and transients due to line fault are also determined. These faults are applied at different locations and the response of each wind turbine stress before and during the fault is observed.

Chapter 1 briefly overview of the purpose of the study.

Chapter 2 introduces to the theoretical background and covers the mathematical analysis of the calculation of theoretical limit.

Chapter 3 presents the analysis and modeling of the network in the software and its response during each fault. It also analyses the stability of the derived network system.

Chapter 4 introduces the working simulation results

Chapter 5 briefly overviews the findings and ends up by giving the future prospects to be considered in this context.

2. REGULATION AND THEORY

Distributed resources (DR) or distributed generators (DG)— connected to the distribution systems provides a different type of possibilities for energy conversion and generation compared to large generators connected to the transmission system. For various renewable energy resources like wind turbines, small and micro size wind turbines, conventional diesel generators, internal combustion generators, gas-fired turbines, PV cells and energy storage technologies, converters are required to provide electricity from these resources.

Despite the different categories of these distributed resources, the behavior of a DR mainly depends upon the type of the converter that is connected with these DR in order to interact with the Electrical power system (EPS). These electrical converters are classified into three major types, depending on the type of DR with which are connected like synchronous generators, asynchronous (or induction) generators, and static (or electronic) inverters.

The rotating generators like synchronous and asynchronous generators can be driven by wind turbines, water turbines, steam turbines, internal combustion engines, combustion turbines or electric motors. The static inverters can be supplied by dc storage sources (such as batteries), by dc generating sources (such as fuel cells), or by an AC generating source and a converter (such as a high- or variable-speed combustion or wind turbine). These machines respond differently to changes because of their different mechanical and electrical inertias and the time constants of the regulators by which they are controlled.

Synchronous machines

The speed of the synchronous machine depends upon the number of poles of the machine and the frequency of the electrical power system with which it is connected. The real power produced by the machine is controlled by the governor of the prime mover whereas the reactive power produced is controlled by the excitation of the field.

The control of the synchronous machine is more difficult than the induction machine because it required both the control of field excitation and synchronization with the EPS (Electrical Power System). Thus it required a special protection system to isolate it during fault condition in the EPS. Its major advantage is that it has the ability to provide power during the outage of the EPS and control of power factor.

Asynchronous (induction) machines

In order to produce energy from the induction machine, the speed of the machine has to be slightly higher than the synchronous speed. If the speed drops below the synchronous speed, it will absorb power from the grid. The real power produced by the machine is controlled by the

governor of the prime mover. The induction machine always absorbs reactive power to cover its internal losses.

PMSG (Permanent Magnet Synchronous Generator)

The Permanent magnets generators are a distant class of synchronous generators. They employ fully rated back-to-back full power converters to get full power, fully rated, variable speed operation. The rating of the full power converter in these wind turbines depends upon the rated power of the generators. As the wind turbine is connected with the grid through the converter, thus all the power from the wind turbine is controlled and transferred by the converter.

The back-to-back full power voltage source converters of these wind turbines can be arranged in a number of ways. The generator side converter can be a diode rectifier or a PWM voltage source converter (PWM-VSC) in order to control the generator torque and speed whereas the grid side converter is typically a PWM voltage source converter which main purpose is to control the DC link voltage and giving the active and reactive power to the grid independently. In case of diode rectifier at the generator side a dc-booster is required to control the dc-link voltage.

Interfacing requirement for wind powered DR

For large wind farms with a nominal active power of more than 30 kW, there are some regulation techniques regarding its capacity to connect to the Electrical Power System (EPS) during different events. These events could also include faults which cause high fault current and voltage dips. Before the regulations are described in section 2.2, some useful information about voltage dips will be presented in section 2.1.

2.1.VOLTAGE SAG

The Power quality is a measure of the voltage, the current and the frequency. Power quality problem may be of different nature which includes interruption, under and over voltages, flickers, harmonics and voltage sags. (The term dip is also used instead of sag).

Constant voltage is the primary requirement of customers and the primary focus for this report. The main causes of the voltage sags which lead to permanent malfunctioning of the equipment are switching over-voltages, short-circuit faults (cause voltage dips) and lightning (cause transient overvoltages). A Voltage sag in a system is the result of a high current flowing in one branch of a network. The high current can be due to short circuits and starting of large motors.

2.1.1 DEFINITION

There are different standards for the definition of a voltage sag when it comes to magnitude and phase. According to standard IEEE std 1159-1995 [1], a voltage sag is a short duration

reduction in rms voltage between 0.1 p.u and 0.9 p.u for durations of 0.5 cycles to 1 minute. The amplitude of the voltage is the remaining value of the voltage during that time.

2.1.2 CHARACTERISTIC OF VOLTAGE SAG

Voltage sags are considered to be one of the severe disturbances to the industrial equipment [2]. A fault in a network produces severe voltage sags on phases which then propagate in the grid. As the fault propagates along the network its magnitude decreases because of the characteristic of network and transformer impedances which exist between the fault location and the generator. The high fault current produces a high voltage drop close to the fault location which as a result decreases the voltage drop across the generator end. Thus the voltage drop at the generator end is lower than the voltage drop at the fault location.

From the point of common coupling (PCC), the voltage sag will be propagated toward the customer end. This is the case when there is no generation connected at the customer end. When analyzing a balanced fault in order to calculate the sag magnitude at different points in the system, a simplified model using the voltage divider rule is used. Such a model is shown in figure 2.1. The voltage level at the PCC is calculated for a three phase fault.

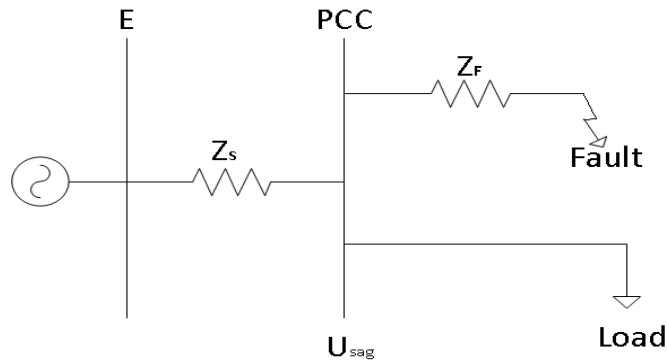


Figure 2.1: Model to calculate voltage dip magnitude

The sag magnitude depends on two impedances during a fault, the source impedance Z_s and fault impedance Z_f . The feeder impedance Z_f will have large value if the fault is located far away from the PCC and will have a small value if the fault is located close to the PCC. The voltage sag at the PCC is then calculated by using (2.1).

$$U_{sag} = E \frac{Z_f}{Z_s + Z_f} \quad (2.1)$$

The above equation is derived assuming that the load current is neglected before and during the fault and the pre-fault voltage at E is 1 p.u. and that the fault impedance is zero. The above equation indicates that the voltage sag will be more severe if the fault is located close to the PCC.

2.2.GRID COMPLIANCE

For the connection of a wind farm with the EPS there are some operational requirements and rules called grid codes which have to be fulfilled, these grid codes are given by the transmission system operators. Svenska Kraftnät (SvK) operates the Swedish national grid codes. Each country has its own grid code depending upon the national grid operators. Their main function is to provide electricity in a more reliable way to the customers.

In 2008 IEEE has published standards for interconnecting distributed resources with the electric power system in order to define criteria and requirements for interconnection of these DR with the Electrical Power System (EPS). The requirements shall be met at the point of common coupling (PCC). These standards address the methods used for DR performance and their impact on EPS, mitigating limitations of the Area EPS, operation, performance, and testing and safety consideration at PCC. [3]

The following outline the requirements from the IEEE-1547 standards especially for the control strategy of interfacing Distributed Generators (DG) in a distribution system.

2.2.1 VOLTAGE CONTROL

Voltage control describes the process with which the voltage is maintained within an acceptable range for the customers connected to the EPS. Thus large wind farms should be equipped with voltage control so that the DR shall not actively regulate the voltage level at the PCC and other local EPS. When connecting DR with EPS, the following points shall be observed for the control strategy of the voltage regulation.

1. The DR devices shall stop energizing the area when the voltage goes out of range. For the protection of DR devices the out of range voltage shall have a specified clearing time with an acceptable operating voltage range of 88% to 110% of nominal voltage.
2. The DR shall cease to energize the area when the area electrical power system is de-energized. The DR should not transfer power to the area of the EPS at the PCC when the area has been de-energized for any reason. Thus when the voltage and frequency of the area EPS is out of range, the DR shall cease to energize the area.
3. The grounding scheme of the DR should not cause over-voltages that exceed the protection rating of the equipment connected to the EPS and coordination of ground fault protection.
4. The DR shall operate in parallel to the EPS without causing voltage fluctuation at the PCC with an acceptable range of $\pm 5\%$ of the voltage level of EPS at the PCC point. Table 1 demonstrates that if any of the parameters are outside the acceptable ranges, the paralleling-device shall not energize the area.

Table1: Synchronization parameter limits for synchronous interconnection to an EPS or an energized local EPS to an energized area EPS (Given in IEEE 1547 [3])

Aggregate rating of DR units (KVA)	Frequency difference (Δf , Hz)	Voltage Difference (ΔV , %)	Phase angle difference ($\Delta\Phi$, °)
0-500	0.3	10	20
>500-1500	0.2	5	15
>1500-10000	0.1	3	10

1. When the voltage is in a range as given in table 2, the DR shall cease to energize the area EPS within the clearing time as indicated.

Table 2: Interconnection system response to abnormal condition (Given in IEEE 1547 [3])

Voltage range (% of the base voltage)	Clearing time (s)
$V < 50$	0.16
$50 \leq V < 88$	2.00
$110 < V < 120$	1.00
$V \geq 120$	0.16

2.2.2 FREQUENCY CONTROL

Abnormal conditions caused by short circuits, over voltages and transients can occur in any electrical power system. Thus it requires a quick response from the connected DR for the safety of public, utility maintenance personnel and equipment including DR.

During normal condition the following condition shall be fulfilled.

1. The DR shall be disconnected from the EPS prior to the reclosing of the area EPS.
2. When the system frequency at the PCC point is in a range as shown in [table 2], the DR shall cease to energize the area EPS within the clearing time as indicated in table 3.

Table 3: Interconnection system response to abnormal frequencies (Given in IEEE 1547 [3]).

DR size	Frequency Range (Hz)	Clearing time ^a (s)
$\leq 30\text{kW}$	>60.5	0.16
	<59.3	0.16
$>30\text{kW}$	>60.5	0.16
	$<\{59.8 \text{ to } 57.0\}$ (adjustable set point)	Adjustable 0.16 to 300
	<57.0	0.16

^a DR<30kW, maximum clearing times; DR>30kW, default clearing times.

2.3.PRACTICAL LINE FAULTS

Short circuit faults in the operation and planning of electrical network systems bring more changes to the operating level. The transition in this electrical network system caused by short circuit is classified in three different time frames: steady state, electromagnetic transients and electromechanical transients, which produce both over and under voltages. These voltages depend upon the magnitude and time variation of the short circuit current.

The transient produced by a short circuit depends on the instant at which the short circuit occurs, the location of the short circuit, its duration, topology of the network, the available short circuit power, the initial loading condition, and the rating and characteristic of the equipment involved in the network. Balanced three phase faults cause more severe voltage sags but are the least commonly occurring fault in the network, while single phase to ground faults are the most commonly occurring fault.

Unbalanced faults will be examined by using symmetrical components. This section has been inspired by [4], [5]. The circuit used for the fault analysis is shown in the figure 2.2.

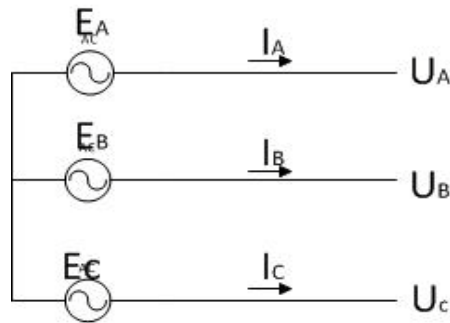


Figure 2.2: Circuit used for fault analysis

The phase currents will be denoted by I_A, I_B, I_C and the sequence components for both currents and voltages are I_1, I_2, I_0 and U_1, U_2, U_0 where I_1 represents the positive sequence, I_2 represents the negative sequence and I_0 represents the zero sequence. The same applies for voltages. The phase (fault) current can be expressed as

$$I_A = I_1 + I_2 + I_0 \quad (2.2)$$

$$I_B = a^2 I_1 + a I_2 + I_0 \quad (2.3)$$

$$I_C = a I_1 + a^2 I_2 + I_0. \quad (2.4)$$

Which states

$$I_1 = 1/3 (I_A + a I_B + a^2 I_C) \quad (2.5)$$

$$I_2 = 1/3 (I_A + a^2 I_B + a I_C) \quad (2.6)$$

$$I_0 = 1/3 (I_A + I_B + I_C). \quad (2.7)$$

Let phase A be chosen as a reference thus $E = E_A$ which is the voltage at phase A at no-load condition. The Thevenin equivalents of the network are shown in the figure 2.3,

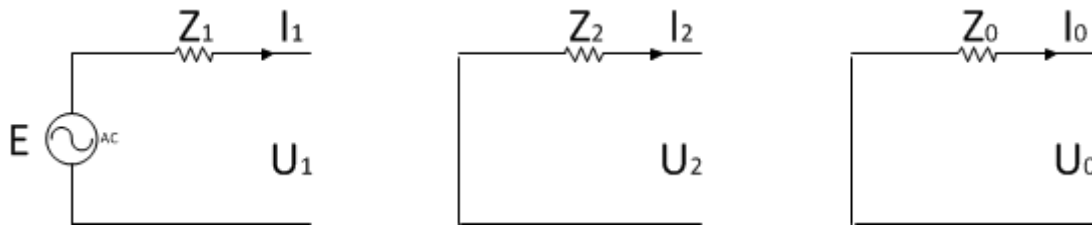


Figure 2.3: Thevenin equivalent of three sequences

The voltage representation of the three sequence circuit is

$$U_1 = E - I_1 Z_1 \quad (2.8)$$

$$U_2 = - I_2 Z_2 \quad (2.9)$$

$$U_0 = - I_0 Z_0 \quad (2.10)$$

2.3.1. PHASE-PHASE SHORT CIRCUIT

A Phase to phase fault occurs when two of the three phases are short circuited together. Let us assume that phase B and C are short circuited. When doing a short circuit calculation we assume that the generator was initially at no load condition. The fault impedance Z_F is calculated with the following boundary conditions.

$$U_A = 0$$

$$U_B = U_C$$

Such that,

$$U_B - U_C = Z_F I_B$$

$$I_B = - I_C \text{ and } I_A = 0$$

The network representation for Phase to Phase fault is shown in the fig 2.4.

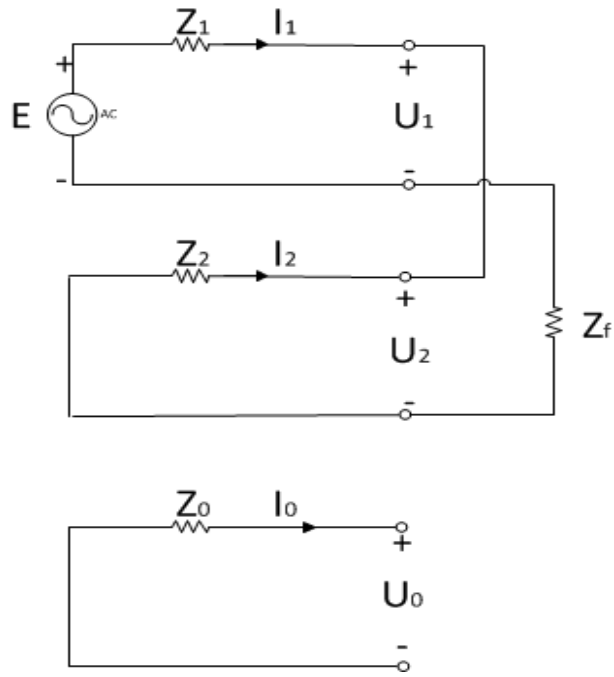


Figure 2.4: Equivalent circuit of the symmetrical-component systems for a line to line fault.

The result in sequence current will be

$$I_1 = -I_2 = E / (Z_1 + Z_2 + Z_F) \quad (2.11)$$

From Eq 2.8 to Eq 2.10 , Eq 2.5 to Eq 2.7 can be written as,

$$I_1 = 1/3 (a I_B + a^2 I_C) = 1/3(a - a^2) I_B \quad (2.12)$$

$$I_2 = 1/3 (a^2 I_B + a I_C) = 1/3(a^2 - a)I_B \quad (2.13)$$

$$I_0 = 0 \quad (2.14)$$

Since $I_1 = -I_2$ and $U_1 + U_2 + U_0 = 0$

By using transformation matrix for the component theory along with the relation $E_A = E_1$, $E_B = a^2 E_1$, $E_C = a E_1$. The phase voltages and current will be,

$$U_A = E_1 - [(Z_1 + Z_2) / (Z_1 + Z_2 + Z_F)] E_1 \quad (2.15)$$

$$U_B = a^2 E_1 - [(a^2 Z_1 + a Z_2) / (Z_1 + Z_2 + Z_F)] E_1 \quad (2.16)$$

$$U_C = a E_1 - [(a Z_1 + a^2 Z_2) / (Z_1 + Z_2 + Z_F)] E_1 \quad (2.17)$$

As $I_A = 0$.

The short circuit current will be

$$I_B = -I_C = (a^2 - a) I_1 = E_B - E_C / (Z_1 + Z_2 + Z_F) \quad (2.18)$$

Let us assume that the fault impedance is zero ($Z_F = 0$) and the positive and negative sequence impedance are equal ($Z_1 = Z_2 = Z$) and the zero sequence impedance is zero. Thus the phase voltage on the conductors will be

$$U_A = E_1 = E_A \quad (2.19)$$

$$U_B = a^2 E - [(a^2 - a) Z / (2Z + Z_F)] E = \frac{1}{2}(E_B + E_C) = -\frac{1}{2}E_A \quad (2.20)$$

$$U_C = a E - [(a + a^2) Z / (2Z + Z_F)] E = \frac{1}{2}(E_C - E_B) = \frac{1}{2}E_A \quad (2.21)$$

2.3.2. SINGLE PHASE SHORT CIRCUIT TO EARTH

When doing short circuit calculations we assume that the generator was initially at no load condition. The fault impedance Z_F is calculated with the following boundary conditions.

$$U_A = Z_F I_A \quad (2.22)$$

$$I_B = I_C = 0 \quad (2.23)$$

The network representation for single line to ground fault is shown in the fig 2.5

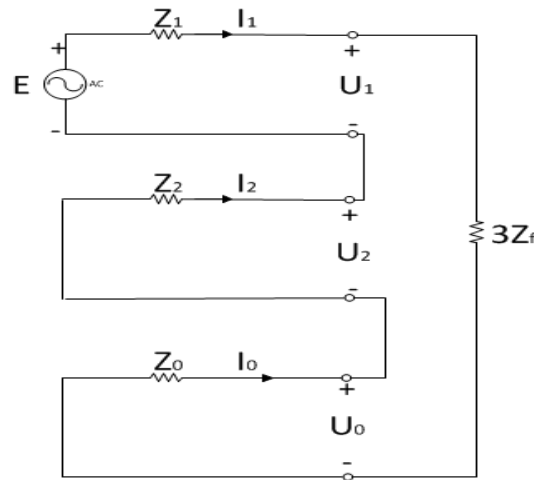


Figure 2.5: Equivalent circuit of the symmetrical-component systems for a single line to ground fault.

The results in sequence currents will be

$$I_1 = I_2 = I_0 = E / (Z_1 + Z_2 + Z_0 + 3Z_F) \quad (2.24)$$

From Eq 2.8 to Eq 2.10, Eq 2.5 to Eq 2.7 can be written as,

$$I_1 = 1/3 (I_A + a I_B + a^2 I_C) = 1/3 I_A \quad (2.25)$$

$$I_2 = 1/3 (I_A + a^2 I_B + a I_C) = 1/3 I_A \quad (2.26)$$

$$I_0 = 1/3 (I_A + I_B + I_C) = 1/3 I_A \quad (2.27)$$

Since $I_1 = I_2 = I_0$ and $U_1 = U_2 = U_0 = 0$

By using transformation matrix for the component theory, the phase voltages and current will be,

$$U_A = E_1 - [(Z_1 + Z_2 + Z_0) / (Z_1 + Z_2 + Z_0 + 3Z_F)] E_1 \quad (2.28)$$

$$U_B = a^2 E_1 - [(a^2 Z_1 + a Z_2 + Z_0) / (Z_1 + Z_2 + Z_0 + 3Z_F)] E_1 \quad (2.29)$$

$$U_C = a E_1 - [(a Z_1 + a^2 Z_2 + Z_0) / (Z_1 + Z_2 + Z_0 + 3Z_F)] E_1 \quad (2.30)$$

As

$$I_A = 3I_0.$$

The short circuit currents will be,

$$I_A = I_F = 3I_0 = 3E / (Z_1 + Z_2 + Z_0 + 3Z_F) \quad (2.31)$$

$$I_B = 0, I_C = 0. \quad (2.32)$$

Let us assume that the fault impedance is zero ($Z_F = 0$) and the positive and negative sequence impedance are equal ($Z_1 = Z_2$) and the zero sequence impedance is large. Thus the phase voltages on the conductors will be

$$U_A = 0 \quad (2.33)$$

$$U_B = a^2 E - [(Z_0 + Z_1) / (Z_0 + 2Z_1)] E = (a^2 - 1) E = E\sqrt{3} \angle -150^\circ \quad (2.34)$$

$$U_C = a E - [(Z_0 + Z_1) / (Z_0 + 2Z_1)] E = (a - 1) E = E\sqrt{3} \angle 150^\circ \quad (2.35)$$

3. ANALYSIS OF A NETWORK

3.1.DESCRPTION OF NETWORK

The studied network consists of a 20 kV distribution station where all the loads are connected to the main bus bar through cables. The distribution station is connected to the 130 kV grid station through a 5.5 km cable. The outgoing cable is operated at high voltage to reduce the transmission to feed the same load area. The distribution station has a transformer rated 130/20kV and 20MVA. The high voltage side of the transformer is directly connected with the ground for the protection of the transformer during faults and lightning whereas the low voltage side of the transformer is impedance grounded through a high impedance 1500Ω resistance [5] in order to minimize the magnitude of a fault current.

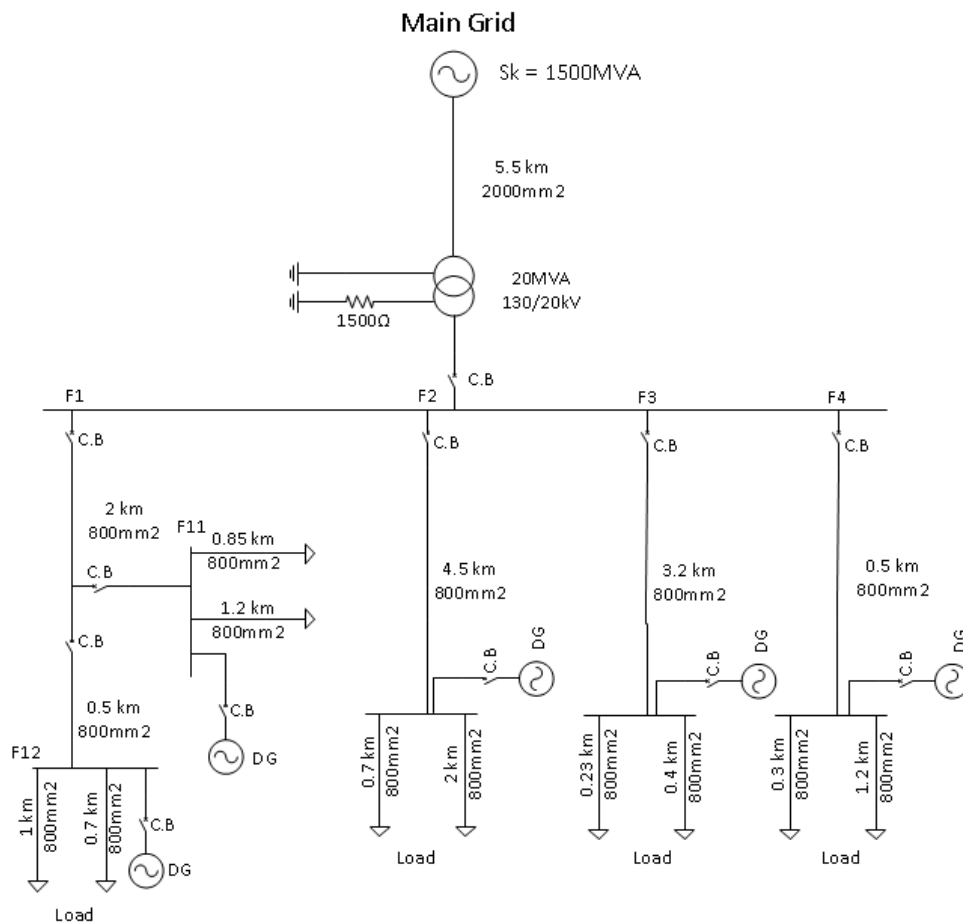


Fig 3.1: Single line view of the distribution system

The reason of the high voltage side to be directly connected with ground is to minimize the voltage rise at the non-faulted phases in case of a line to ground fault and to keep the insulation

level of the equipment as low as possible because the higher the insulation level the higher will be the cost of the equipment.

The short circuit power of the grid which the network is connected to is 1500MVA. The main grid is modeled as a voltage source with a short circuit impedance of $R= 0.5626\Omega$ and $X= 11.2441\Omega$ representing the Thevenin equivalent at the point of connection of the grid with the medium voltage distribution network. The distribution network consists of four feeders from the distribution network bus with which a minimum 3MW to 6MW wind generation capacity is installed. The design of the wind turbines will be discussed in section 3.3.3. A total load of 11.36MVA is installed. The load in the feeder of the network is distributed through different length of 20kV cables with different load capacity so that the effect of the wind turbine can be analyzed on each feeder. The layout of the distribution system is shown in figure 3.1.

For simplicity of the network the installed feeders are radially connected and all the breakers are connected at the beginning of each feeder. The relays in the network for the protection system of each feeder are constant-time over-current relays. Wind turbines of different capacity are connected to the distribution system. The installed capacity of the wind turbines on each feeder is proportional to the strength of the grid, which is proportional to the short circuit ratio of the system short circuit power (S_k) and the short circuit power of the generators (S_n) (S_k/S_n) at the point of common coupling (PCC). The grid should be strong enough in order to recover voltage quickly when the fault is cleared. For a strong grid concept the SCR ratio of the grid is minimum to be kept 5.

3.2.OBJECTIVE

The main objective of this study is as follow,

- 1) Study of the control strategies and performance evaluation of the wind turbines.
- 2) Designing and Modeling of Full Power Converter to attain the desired results.
- 3) Understanding the behavior of the converter during fault conditions, and the increase of power quality by the converter.
- 4) The variation in voltage level with rise in current at different location of the network by applying faults.
- 5) Simulation of a distribution system with a combination of cable lines and fault protection of the lines and the effect of Wind Turbines during fault conditions and their protection system.

3.3.NETWORK MODELING

3.3.1 NETWORK MODELING ASSUMPTION

- 1) In Sweden, a large extent of power loads are Industrial loads. These loads behave as constant power loads during fault condition. Thus the industrial loads are therefore modeled as constant power load with power factor of 0.9.
- 2) The wind turbine is modeled as constant current source with unity power factor. The purpose of constant current source is to limit the output current during fault conditions and provide constant current during nominal condition.
- 3) It is assumed that the wind turbine has fault handling capability (damping resistor) and not disconnected from the network during different line fault conditions.
- 4) It is assumed that the wind turbine will only be disconnected when the feeder circuit breaker is disconnected from the line due to fault.
- 5) The transformer magnetization losses are neglected.
- 6) The negative sequence, positive sequence and zero sequence impedance of the transformer is the same.
- 7) The negative sequence, positive sequence and zero sequence impedance of the grid source is the same.
- 8) Throughout the thesis, all the faults are applied at the end of the downstream feeder to maintain uniformity in the fault. Also all the applied faults are solidly grounded with 10m Ω grounding resistance.

3.3.2 CABLE DESIGNING

The purpose of this section is to illustrate the actual modeling of cable in PSCAD in order to represent the actual behavior of the cable. For this purpose, the cable description has been taken from a manufacture site where the data sheets are attached in the appendix. Some further calculation has been done to model the cable close to the cable in a real cable system. The calculation of the cable parameters and its calculation are explained in appendix A1.

3.3.3 WIND TURBINE MODELING

The connection of large wind turbines to the distribution system create problem of constant power and power system stability on the distribution system. However if the wind power plant has a control on its output power that is how much power it need to inject during normal and fault condition and how it should operate during fault conditions is the main limitation as described in grids codes will cease to exist. Today the wind power plants with forced commutated voltage source converters (VSC) make the possibility of independently controlling the active and reactive power of the variable speed wind turbine.

In this project the structure of grid connected converter VSC is implemented as a full power converter. The major advantage of a full power converter is that the active and reactive output power can be controlled independently. The control system of grid connected VSC full power converter for voltage dip mitigation and short circuit faults will be carried out. The control system consists of two controllers: a vector current controller and a voltage/power controller. A brief analysis of the control system will be carried out in this chapter. Simulation result of the controller for voltage dips and balance short circuit will also be carried out.

3.3.3.1 LAYOUT OF GRID CONNECTED VSC

To derive the control system it is necessary how the grid connected VSC acts to mitigate the voltage dips. The three phase diagram of a grid connected VSC is shown in Figure 3.2. This section has been inspired by [14], [16] and [17].

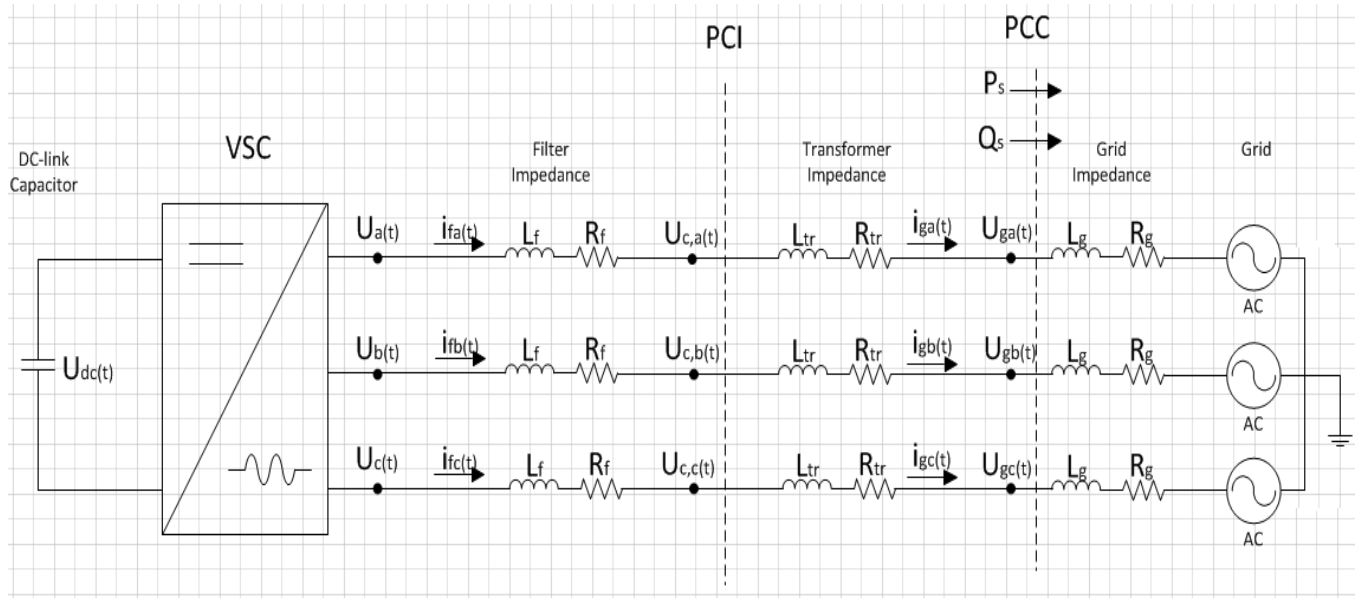


Figure 3.2: Grid Connected VSC

The three phase voltage of the grid is denoted by $E_{g,a}(t)$, $E_{g,b}(t)$ and $E_{g,c}(t)$. While the voltage and current at the point of common coupling (PCC) is denoted by $U_{g,a}(t)$, $U_{g,b}(t)$ and $U_{g,c}(t)$ and $i_{g,a}(t)$, $i_{g,b}(t)$ and $i_{g,c}(t)$. The three phase voltage at the point of common interface (PCI) is represented by $U_{c,a}(t)$, $U_{c,b}(t)$ and $U_{c,c}(t)$, whereas the three phase voltage and current for the VSC can be denoted by $U_a(t)$, $U_b(t)$ and $U_c(t)$ and $I_{fa}(t)$, $I_{fb}(t)$, and $I_{fc}(t)$. AC-filter of first order is denoted by L_f and R_f respectively. A capacitor C is added later with the RL filter in order to remove the voltage harmonics and make the voltage at the PCI more stable and sinusoidal. The DC-link voltage is denoted by $U_{dc}(t)$.

The reason to mount an LCL filter at the output of the VSC is to remove the current and voltage harmonics. The filter inductance, capacitance and the transformer impedance make the LCL

filter. The cutoff frequency of the filter determines the number of harmonics to be injected in the grid by the VSC. As the main purpose of the VSC is to maintain the voltage constant at the PCC point thus for simplicity the transformer inductance is neglected.

Control System

As mentioned earlier the control system of the VSC consists of two controllers, the current controller and the voltage controller. These controllers will be connected in cascade by making an assumption that the inner controller (Current Controller) will be ten times faster than the outer controller (voltage controller). The inner controller controls the current through the filter inductor and sends a reference signal proportional to the VSC output voltage controller, while the voltage controller controls the voltage at the PCC point by sending a reference current signal to the current controller.

Current Controller

In this section the inner current controller will be derived. It is assumed that the injected voltage is equal to the voltage across the PCI point and the transformer is ideal with 1:1 turn ratio.

Thus the single line view of the LC filter with ideal VSC is as shown below.

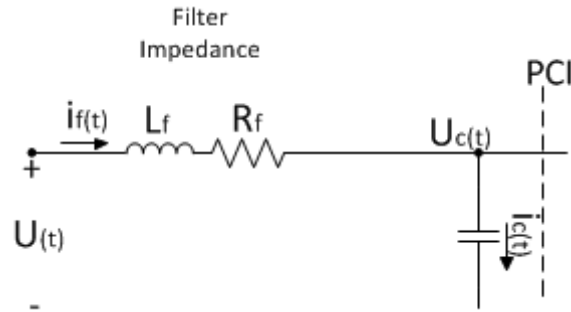


Figure 3.3: Single line view of LC filter

By applying Kirchhoff's current law, we get

$$U_a(t) - R_f i_{fa}(t) - L_f \frac{d}{dt} i_{fa}(t) - U_{ca}(t) = 0 \quad (2.36)$$

$$U_b(t) - R_f i_{fb}(t) - L_f \frac{d}{dt} i_{fb}(t) - U_{cb}(t) = 0 \quad (2.37)$$

$$U_c(t) - R_f i_{fc}(t) - L_f \frac{d}{dt} i_{fc}(t) - U_{cc}(t) = 0 \quad (2.38)$$

By applying Clark's transformation, we can transform the above three phase quantities into two phase quantities (see Appendix A) i.e $\alpha\beta$ system without losing information.

$$U^{\alpha\beta}(t) - R_f i_f^{\alpha\beta}(t) - L_f \frac{d}{dt} i_f^{\alpha\beta}(t) - U_c^{\alpha\beta}(t) = 0 \quad (2.39)$$

By using the grid angle through PLL we can transform the above equation into dq coordinate system by substituting $\frac{d}{dt} = \frac{d}{dt} + j\omega$

Thus the above equation can be written as

$$U^{dq}(t) - R_f i_f^{dq}(t) - L_f \frac{d}{dt} i_f^{dq}(t) - j\omega L_f i_f^{dq}(t) - U_c^{dq}(t) = 0 \quad (2.40)$$

Taking the Laplace transform and neglecting the cross coupling and the feed forward terms, the above equation can be written as

$$U^{dq}(s) - R_f i_f^{dq}(s) - sL_f i_f^{dq}(s) = 0 \quad (2.41)$$

$$U^{dq}(s) - (R_f + sL_f) i_f^{dq}(s) = 0 \quad (2.42)$$

By assuming that the output voltage of the VSC is pure sinusoidal, thus the U_{dq} voltage can be equal to the reference voltage U_{dq}^* . The above equation can be written as,

$$U^{dq*}(s) - (R_f + sL_f) i_f^{dq}(s) = 0 \quad (2.43)$$

So

$$G_{cc}(s) = \frac{I_{fdq}(s)}{U_{dq}(s)} = \frac{1}{(R_f + sL_f)} \quad (2.44)$$

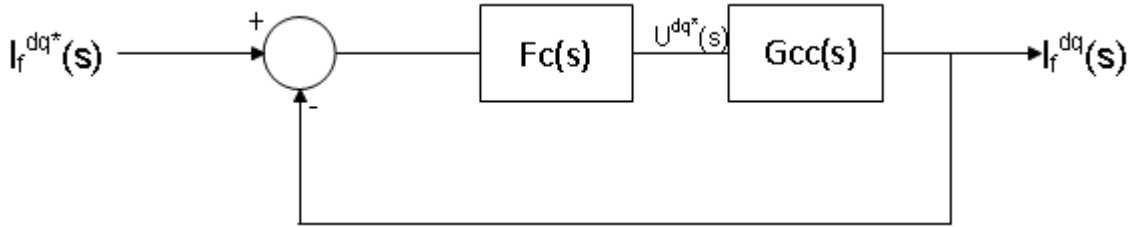


Figure 3.4: Current Controller

Since $G_{cc}(s)$ is the transfer's function of a model for which the current controller can be designed.

Where $F_c(s)$ is the current controller, $I_{fdq}(s)$ is the output and $I_{fdq}^*(s)$ is the reference output from the output of the voltage controller. Since the close loop system to be a first order low pass system. The transfer function will be

$$G_{CC}(s)_{close\ loop} = \frac{I_{fdq}(s)}{U_{dq}(s)} = \frac{Fc(s)G_{cc}(s)}{1 + Fc(s)G_{cc}(s)} = \frac{\frac{\alpha_c}{s}}{1 + \frac{\alpha_c}{s}} \quad (2.45)$$

$$Fc(s)G_{cc}(s) = \frac{\alpha_c}{s}$$

$$Fc(s) = \frac{\alpha_c}{s} G_{cc}^{-1}(s)$$

$$Fc(s) = \frac{\alpha_c}{s} (R_f + sL_f) = K_{pc} + \frac{K_{ic}}{s} \quad (2.46)$$

Which yields,

$$K_{pc} = \alpha_c L_f \quad (2.47)$$

$$K_{ic} = \alpha_c R_f \quad (2.48)$$

Since PI controller is appropriate for control of current controller. The current controller has a proportional part with a gain of K_{pc} and integral gain of K_{ic} , in order to remove steady-state errors.

The complete implementation of current controller by adding the feed forward and cross coupling terms, eq. (3.5) can be expressed as

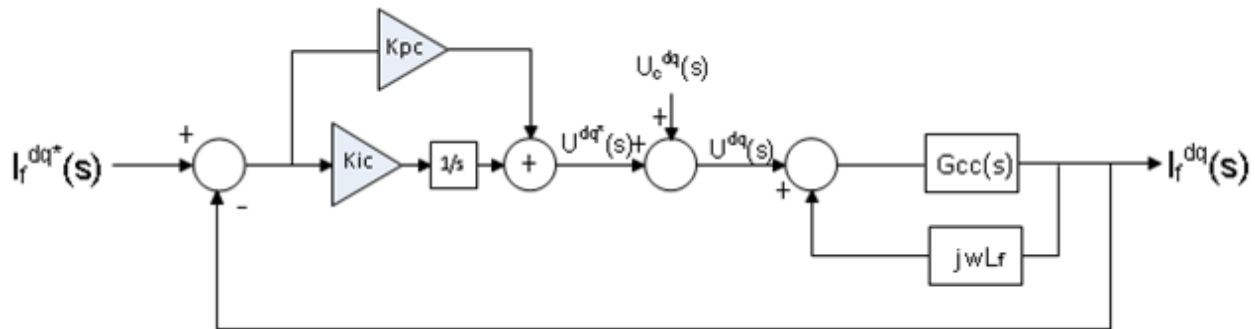


Figure 3.5: Current Controller Implementation

The current controller has a rise time of t_r (time required for an output signal to rise from 10% to 90% of the field value)

$$Fc(s) = \frac{\ln(9)}{\alpha_c} \quad (2.49)$$

Where α_c is the bandwidth of the current controller.

Improvement in Current controller by adding Active Damping term:

We assume perfect parameters for the designing of the current controller, although in a real case the perfect parameters can never be possible. Thus a disturbance error $U_c^{dq^*}(s)$ always exist and it can never be zero. A feed forward term of estimated capacitance $U_c^{dq^*}(s)$ should be added to cancel the effect of filter capacitor disturbance. Thus the current controller can be expressed as,

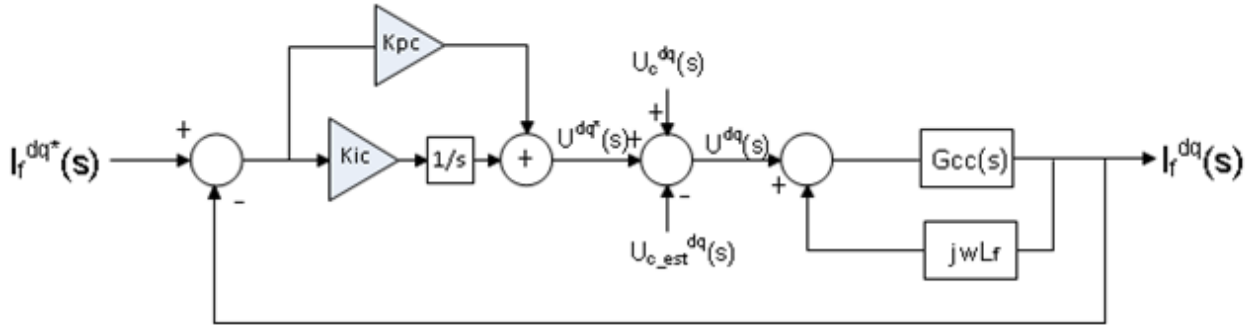


Figure 3.6: Current Controller Implementation with feed forward voltage vector and decoupling term

By changing the response of the integrator an active damping resistance R_a should be added with the integrator in order to remove the small errors and damping of the system.

So the modified transfer function will be

$$G_{cc}'(s) = \frac{1}{R_f + R_a + sL_f} \quad (2.50)$$

$$G_{cc}'(s) = \frac{\frac{\alpha_c}{s}}{1 + \frac{\alpha_c}{s}} = \frac{\frac{1}{L_f}}{s + \frac{R_a + R_f}{L_f}} = K_{pc} + \frac{K_{ic}}{s} \quad (2.51)$$

Thus $\alpha_c = \frac{R_a + R_f}{L_f} \Rightarrow R_a = \alpha_c L_f - R_f$

The PI controller can now be expressed as

$$G_{cc'}(s) = \frac{\frac{\alpha_c}{s}}{1 + \frac{\alpha_c}{s}} = \frac{\alpha_c}{s} * (R_f + R_a + sL_f) = K_{pc} + \frac{K_{ic}}{s} \quad (2.52)$$

$$K_{pc} = \alpha_c * L_f$$

$$K_{ic} = \alpha_c^2 * L_f$$

Thus the net block diagram of the current controller with limited output voltage of 1.1% of nominal voltage can be expressed as.

$$U_s^{dq}(s) = \left(K_{pc} + \frac{K_{ic}}{s} \right) \left(I_f^{dq*}(s) - I_f^{dq}(s) \right) + j\omega L_f * I_f(s) + U_c^{dq}(s) \quad (2.53)$$

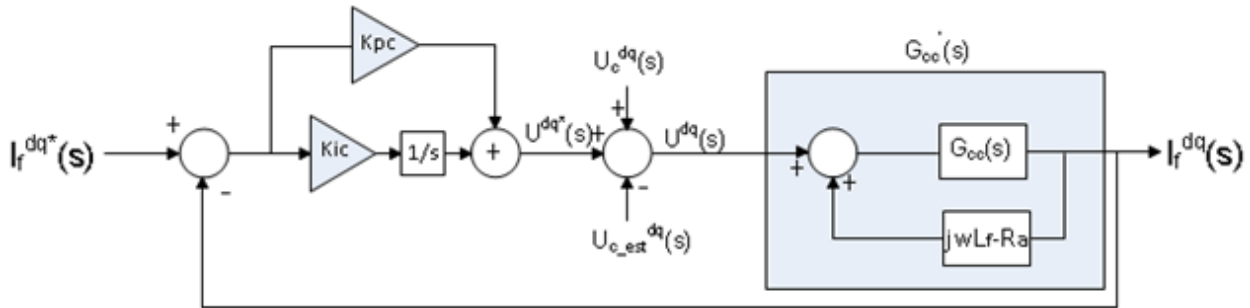


Figure 3.7: Current Controller Implementation with feed forward voltage vector, decoupling term and active damping

Dynamic Model of Real and Reactive Power Controller (Voltage Controller)

The real and reactive power deliver to the AC system at the point of PCC can be expressed as,

$$P_s(t) = \frac{3}{2K^2} [V_{sd} i_d(t) + V_{sq}(t) i_q(t)] \quad (2.54)$$

$$Q_s(t) = \frac{3}{2K^2} [-V_{sd} i_q(t) + V_{sq}(t) i_d(t)] \quad (2.55)$$

If the Phase lock loop (PLL) is in steady state then $V_{sq} = 0$. Thus the above equation can be written as,

$$P_s(t) = \frac{3}{2K^2} [V_{sd} i_d(t)] \quad (2.56)$$

$$Q_s(t) = \frac{3}{2K^2} [-V_{sd} i_q(t)] \quad (2.57)$$

Thus $P_s(t)$ and $Q_s(t)$ can be controlled by $I_d(t)$ and $I_q(t)$. As the output of the power controller is current reference signal which is used as an input of voltage controller. So,

$$I_{d_ref}(t) = \frac{2K^2}{3*V_{sd}} [P_{s_ref}(t)] \quad (2.58)$$

$$I_{q_ref}(t) = -\frac{2K^2}{3*V_{sd}} [Q_{s_ref}(t)] \quad (2.59)$$

For the designing of power controller we assume that the power controller should be a closed loop first order low pass system.

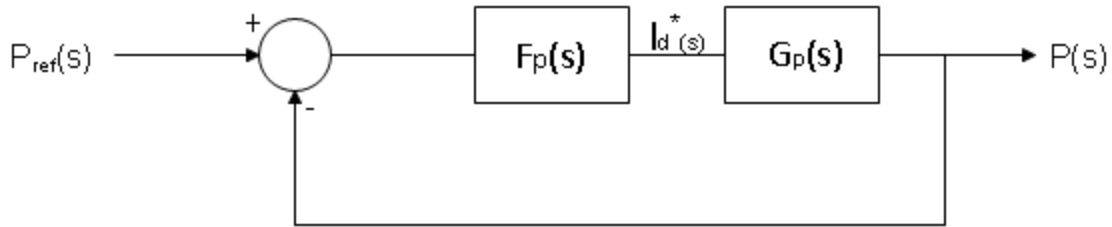


Figure 3.8: Power Controller Implementation

$$G(s)_{closed\ loop} = \frac{P(s)}{P_{ref}(s)} = \frac{Fp(s)Gp(s)}{1 + Fp(s)Gp(s)} = \frac{\alpha_p}{s + \alpha_p} \quad (2.60)$$

$$Fp(s)Gp(s) = \frac{\alpha_p}{s} \quad (2.61)$$

$$Fp(s) = \frac{\alpha_p}{s} Gp^{-1}(s) \quad (2.62)$$

Since

$$Gp(s) = \frac{P(s)}{I_d(s)} = \frac{3}{2} V_{sd}(s) \quad (2.63)$$

Thus the control system of the power controller can be expressed as,

$$Fp(s) = \frac{\alpha_p}{s} \frac{2}{3V_{sd}(s)} \quad (2.64)$$

Thus,

$$I_{d_ref}(s) = (P_{ref} - P) \frac{\alpha_p}{s} \frac{2}{3V_{sd_ref}(s)} \quad (2.65)$$

Similarly,

$$I_{q_ref}(s) = (Q_{ref} - Q) \frac{\alpha_p}{s} \frac{2}{3V_{sd_ref}(s)} \quad (2.66)$$

Where α_p is the gain of the power controller which is ten times smaller than the gain of the current controller.

At the point of PCC, the AC system voltage can be expressed as,

$$V_{sa}(t) = V_s \cos(\omega t + \theta_0) \quad (2.67)$$

$$V_{sb}(t) = V_s \cos(\omega t + \theta_0 - 2\pi/3) \quad (2.68)$$

$$V_{sc}(t) = V_s \cos(\omega t + \theta_0 - 4\pi/3) \quad (2.69)$$

Where

V_s = Peak value of line to ground voltage

ω = grid angular frequency

θ_0 = Initial phase angle.

Applying Kirchhoff's voltage law at figure 3.7

$$V_t(t) - R_g I_g(t) - L_g \frac{d}{dt} I_g(t) - V_s(t) = 0 \quad (2.70)$$

In $\alpha\beta$ co-ordinate system, the above equation can be written as

$$L_g \frac{d}{dt} I_g^{\alpha\beta}(t) = V_t^{\alpha\beta}(t) - V_s^{\alpha\beta}(t) - R_g I_g^{\alpha\beta}(t) \quad (2.71)$$

By expressing in dq Coordinate system, the above equation can be expressed as

$$L_g \frac{d}{dt} I_g^{dq}(t) + j\omega L_g I_g^{dq}(t) = V_t^{dq}(t) - V_s^{dq}(t) - R_g I_g^{dq}(t) \quad (2.72)$$

Separating the real and imaginary

$$L_g \frac{d}{dt} I_g^d(t) - \omega L_g I_g^q(t) = V_t^d(t) - V_s^d(t) - R_g I_g^d(t) \quad (2.73)$$

$$L_g \frac{d}{dt} I_g^q(t) + \omega L_g I_g^d(t) = V_t^q(t) - V_s^q(t) - R_g I_g^q(t) \quad (2.74)$$

If it is assumed that the grid resistance is quite small compared to the grid inductance, thus by neglecting the grid resistance from the above equation

$$L_g \frac{d}{dt} I_g^d(t) - \omega L_g I_g^q(t) = V_t^d(t) - V_s^d(t) \quad (2.75)$$

$$L_g \frac{d}{dt} I_g^q(t) + \omega L_g I_g^d(t) = V_t^q(t) - V_s^q(t) \quad (2.76)$$

If it is assumed that the PLL is perfectly aligned with the grid angular frequency thus the error is $\omega_0 = 0$ and it can be assumed that there is no change in voltage across the PCI terminal. Thus the above equation can be expressed as,

$$V_s^d(t) = L_g \frac{d}{dt} I_g^d(t) - \omega_0 L_g I_g^q(t) \quad (2.77)$$

$$V_s^q(t) = L_g \frac{d}{dt} I_g^q(t) - \omega_0 L_g I_g^d(t) \quad (2.78)$$

If there is a load attached between that PCC and the grid with load current I_L , then the grid current can be expressed as

$$I_{gd} \cong I_{Ld}$$

$$I_{gq} \cong I_q - I_{Lq}$$

By transforming the above equation in Laplace transform and substituting the value of grid current we obtain,

$$V_s^d(s) = -L_g s I_L^d(s) - \omega_0 L_g I_L^q(s) - \omega_0 L_g I^q(s) \quad (2.79)$$

Since

$$V_s^d(s) = -G_d I_L^d(s) + G_g I_L^q(s) + G_g I^q(s) \quad (2.80)$$

From above equation, the first two terms represent the load effect and the last term represents the control effect.

Thus,

$$G_d(s) = L_g s$$

$$G_g(s) = -L_g \omega_0$$

Thus the control block diagram of the PCC voltage regulator base on the above calculation is

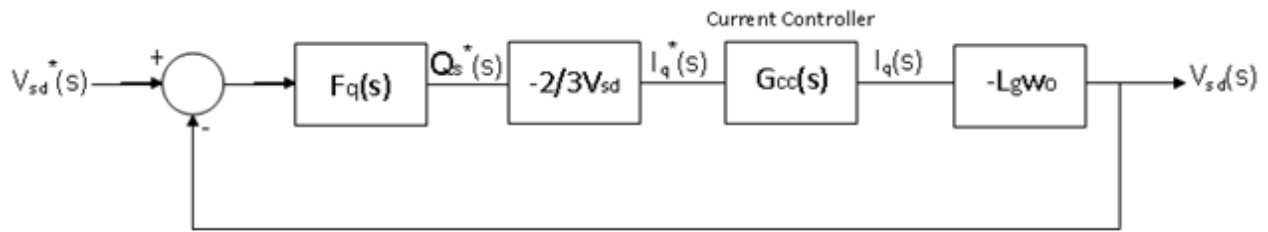


Figure 3.9: Control Block diagram of PCC Voltage Regulator

Stability Analysis

The performance and stability of the entire control system depends upon the parameter of the control system. To ensure the stability and performance of the system, the transfer function of the closed loop control system should be calculated. For the stability of the system, the pole of the close-loop system should be located at the left side of the s-plane within the ± 45 degree in the continuous time domain.

Impact of Controller Bandwidth

As the stability of the system mainly depends upon the system parameter and controller bandwidth thus the controller should operate in a well damped region which depends upon the damping ratio ' ζ ' representing the overshoot of the system. For a well damped system the damping ratio is selected between $(0.5 < \zeta < 1)$. To investigate the dynamic performance between the two controllers, the bandwidth of the two controllers should be selected carefully for the stability of the system. For this purpose a unit step function has been considered.

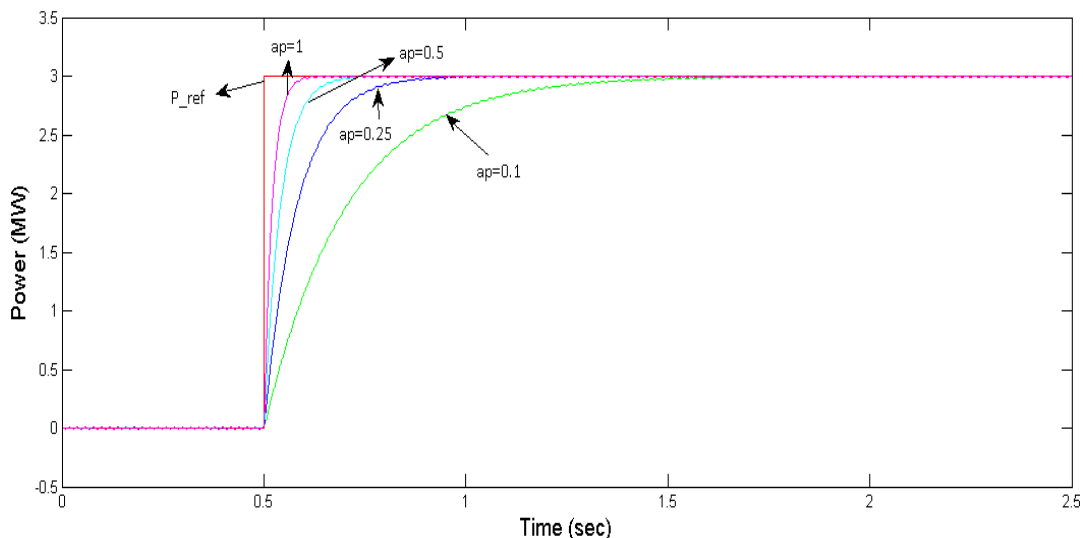


Fig 3.10: Step response of power controller from Power as a reference value to Power as an actual value at variation of power controller bandwidth "ap" by keeping the current controller bandwidth "ac" constant.

Similarly the step response of current controller bandwidth performance has been carried out by applying a unit step response at $t= 0.1\text{s}$ by keeping the power controller bandwidth “ a_p ” constant whereas the current controller bandwidth has been changed. The result is shown in fig 3.11. From the figure it is seen that by increasing the current controller bandwidth as a reference to power controller bandwidth the performance of the control system increases.

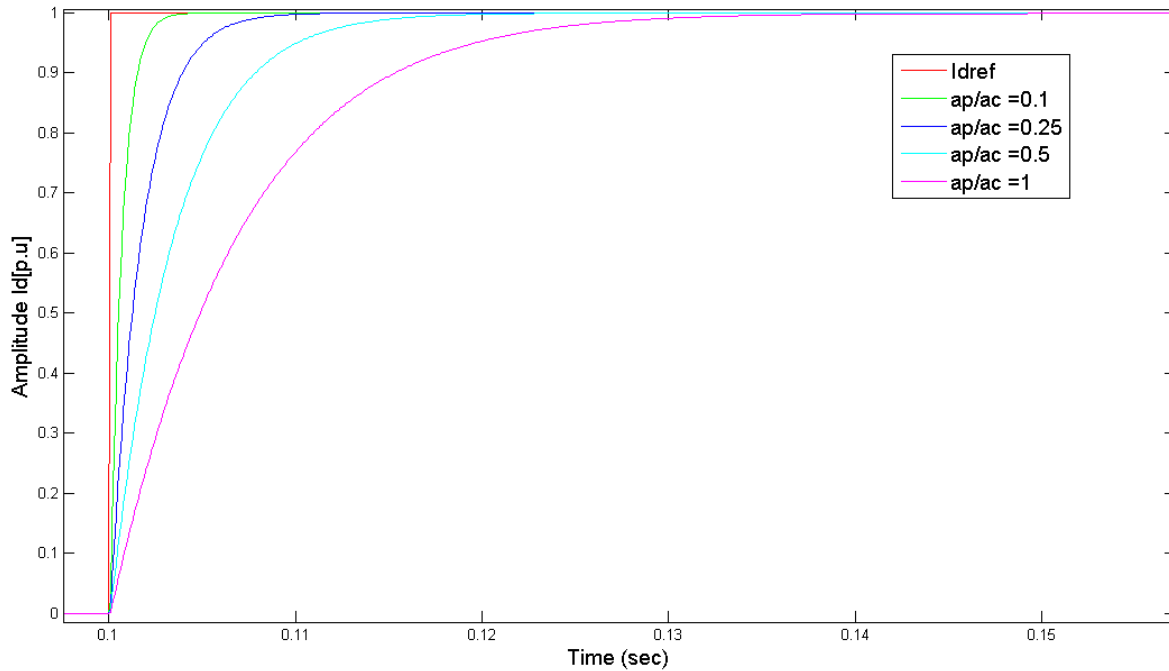


Fig 3.11: Step response of controller from d-component of current controller as a reference d-component of actual value at variation of current controller bandwidth “ a_c ” by keeping the power controller bandwidth “ a_p ” constant.

A unit step in the d-component of the cascade controller has been applied at $t= 0.1\text{ s}$ and the response of the controller from reference to actual d-voltage component has been depicted with a change in current controller and voltage controller bandwidth. The results are shown in figure 3.12.

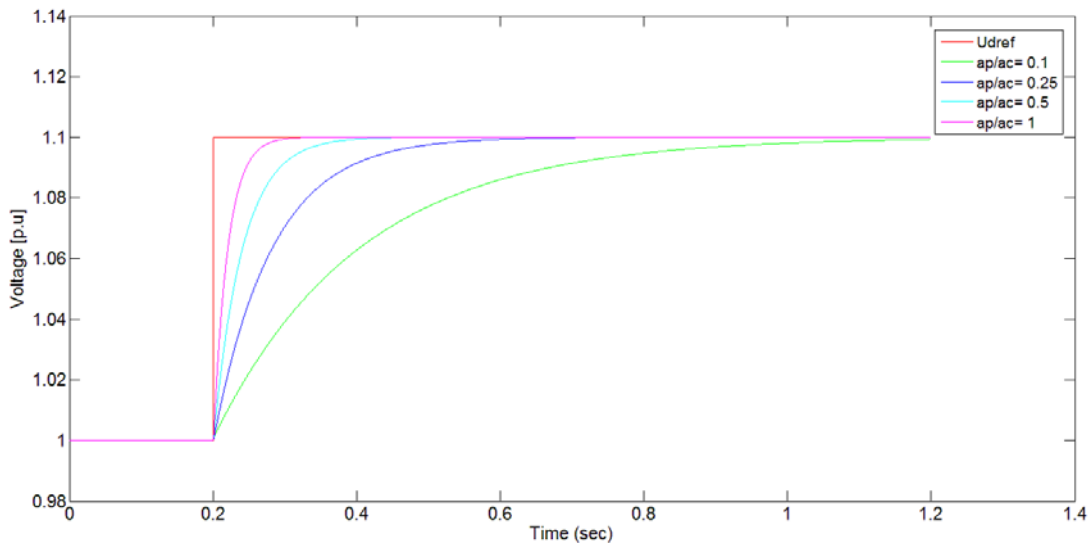


Fig 3.12: Step response of controller from d-component of current controller as a reference d-component of actual value with a variation of a_p/a_c .

The same response of the bandwidth of the current and the power controller has been applied on the system and the response of the d- component of the converter voltage has been analyzed by keeping the bandwidth of the current controller “ a_c ” constant and changes only the power controller bandwidth. The result has been shown in figure 3.13.

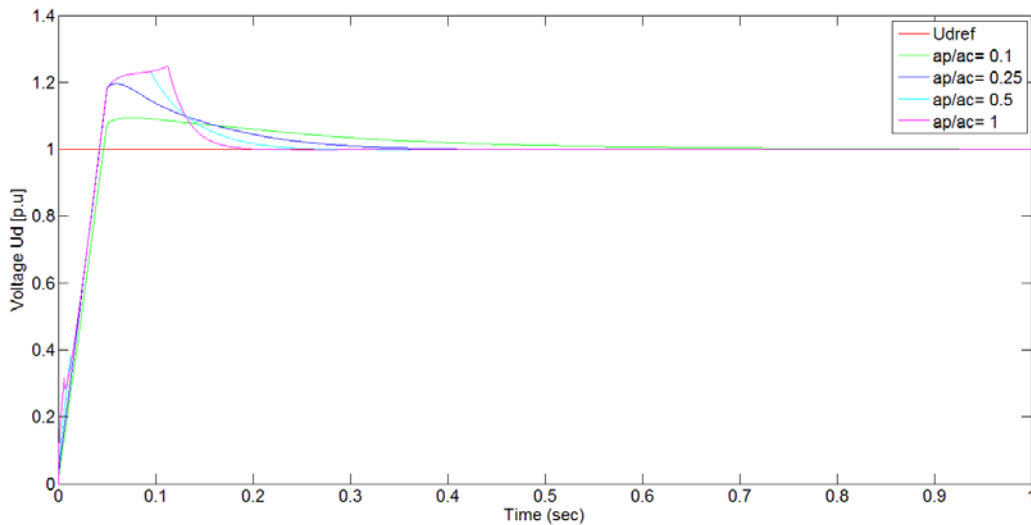


Figure 3.13: Voltage response of d-component of converter output with variation of bandwidth of power controller “ a_p ” by keeping the current controller bandwidth “ a_c ” constant.

From the figure it is possible to notice that increasing the power controller bandwidth the actual voltage closely follow the reference voltage and the response of the converter is faster but with the cost of higher overshoot which represents the stability analysis of the system.

From the above analysis it is possible to design and highlight the basic rule of selecting the parameter of the converter controller design that the inner controller should be faster than the outer controller. Typically the bandwidth of the inner controller is selected to be 10 times the outer controller.

Impact of Frequency Deviation

The above converter is subjected to Grid frequency change to see the response of the grid side wind turbine converter. It has been observed that during the start the simulation takes 0.31s to reach its steady state. The simulation has been run for 3s during which a sudden change in grid frequency from 50Hz to 47Hz has been implemented in order to check the response of the converter. At the steady state the turbine produces 3MW with zero reactive power to the grid. The results are shown in figure 3.14

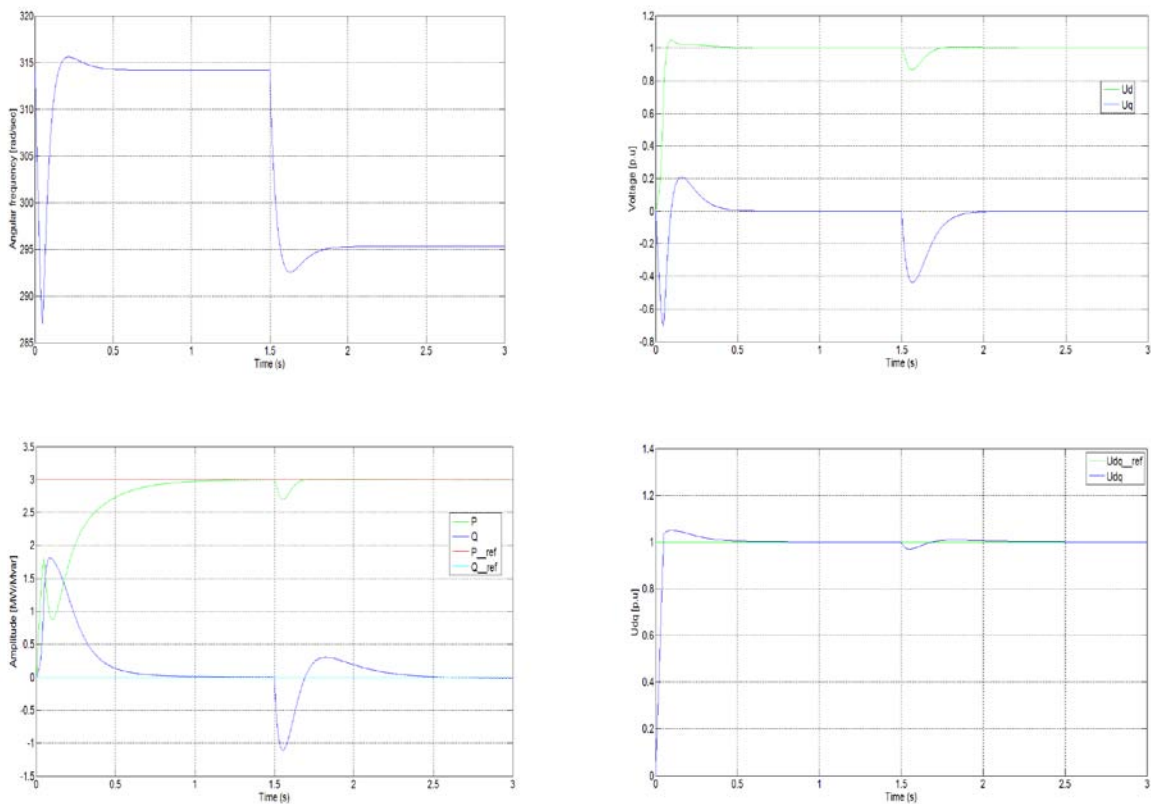


Figure 3.14 Response of a converter with a change in grid frequency.

4. SIMULATION AND RESULTS

4.1. INTRODUCTION

The duration of a voltage dip depends upon the protection system fault clearing time. The clearing time of the circuit breaker is inversely proportional to the magnitude of fault current. In this section a voltage dip is caused by applying line to ground fault, the most occurring, and a three phases to ground fault.

In this section, the change in voltage magnitude during and after the fault having different load has been observed with 3MW and 6MW DG installed in the distribution system. The feeder where the fault is applied is assumed to have a wind power generation in order to see the worse effect on the distribution network during fault condition.

4.2. SIMULATION RESULTS OF DISTRIBUTION SYSTEM WITHOUT WIND TURBINE

Before the installation of wind power capacity in the distribution system, the magnitude of the fault current and the circuit breaker tripping time for all the feeders have been calculated. The fault current is selected from any of the three phases which has the highest magnitude of fault current during the case of a three phase fault. For the protection of the distribution system all the protection relays are Inverse-time over-current relays. For the protection of distributed system with DG other relays are also used like directional relays as a secondary protection but in this thesis the emphasis is only done on inverse time over current relay. An extremely inverse-time over current characteristic have been selected for the relay [18]. The relay tripping time will depend upon the magnitude of the current. Higher the magnitude of the fault current, smaller will be the tripping time. The analytical equation of the relay tripping time will be,

$$t(I) = \left(\frac{A}{M^p - 1} + B \right)$$

Where

$T(I)$ is the tripping time in sec

M is the I_{input}/I_{pickup} (I_{pickup} is the relay current set point)

A, B, p constants to provide selected curve characteristic

As we know that in a cable system a single line to ground fault in a distributed system lead to a three phase permanent fault thus a reclosing of circuit breaker is never applied. Although during this study a reclosing is applied in order to analyze the behavior of the converter recovering from faults condition.

Table 4.1 shows the magnitude of fault current on each faulted feeder and the pre-fault nominal rms current of each feeder.

Fault Location	Fault Type	Current through Feeder (kA_rms)					Current before Fault (kA_rms)
		F11	F12	F2	F3	F4	
F11	LG	3.512	0.36	0.385	0.279	0.343	0.2622
	LLLG	11.126	0.083	0.052	0.041	0.089	
F12	LG	0.5072	3.421	0.627	0.445	0.54	0.3049
	LLLG	0.082	10.17	0.08	0.081	0.069	
F2	LG	0.4329	0.531	3.307	0.434	0.53	0.3246
	LLLG	0.109	0.105	9.514	0.052	0.063	
F3	LG	0.4903	0.539	0.622	3.819	0.538	0.2328
	LLLG	0.0679	0.068	0.084	10.24	0.0750	
F4	LG	0.5105	0.557	0.646	0.459	3.54	0.285
	LLLG	0.0310	0.0305	0.0385	0.0278	12.178	

Fault at Feeder F11

As feeder F1 is divided into two sub feeder F11 and F12 as shown in figure 4.1. Thus a single line to ground fault at phase A is applied at feeder F11. The magnitude of fault current and the tripping time of the circuit breaker are calculated. Figure 4.2 and figure 4.3 shows the magnitude of fault current and voltage dip on each feeder when a line to ground fault at 0.1sec is applied at feeder F11.

Table 4.2: Voltage across F11 for a pre-fault, during fault and post-fault voltages when a fault is applied at the end of the feeder F11.

Faulted Location		Fault Type	Voltage across the Feeder F11 in p.u		
			Pre-Fault	During Fault	Post Fault
F11	Without DG	LG	0.9882	0.7756	0.99
		LLLG	0.9882	0.225	0.99

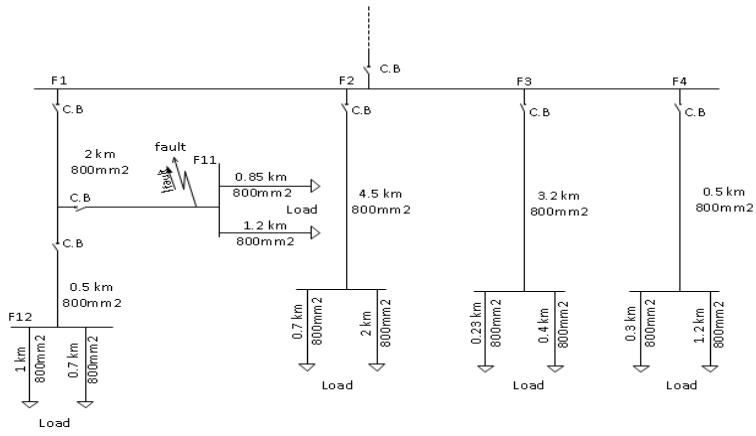


Fig 4.1: Single line diagram of the distribution system when a fault is applied at F11.

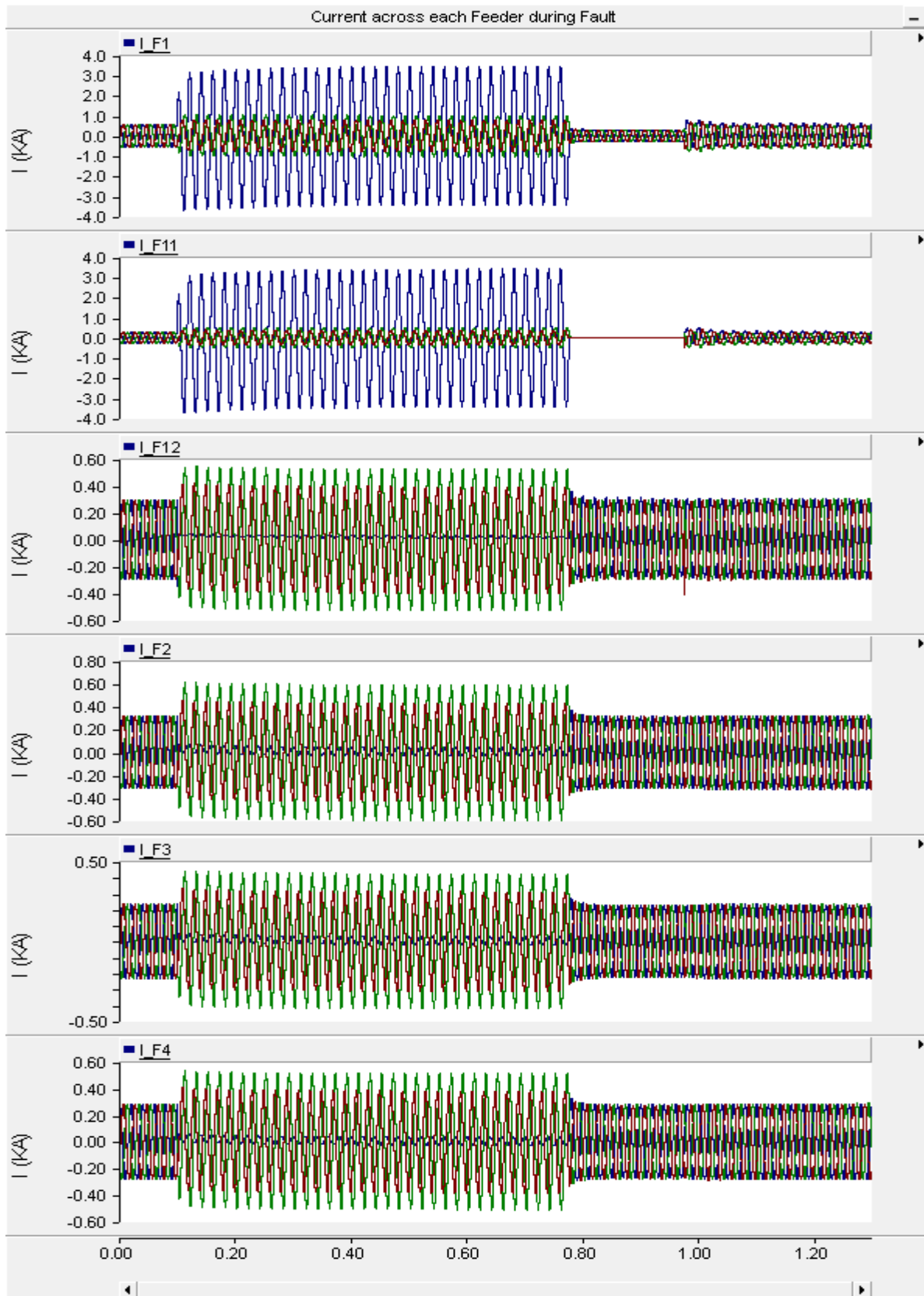


Figure 4.2 Magnitude of currents through each feeder during line to ground fault at F11.

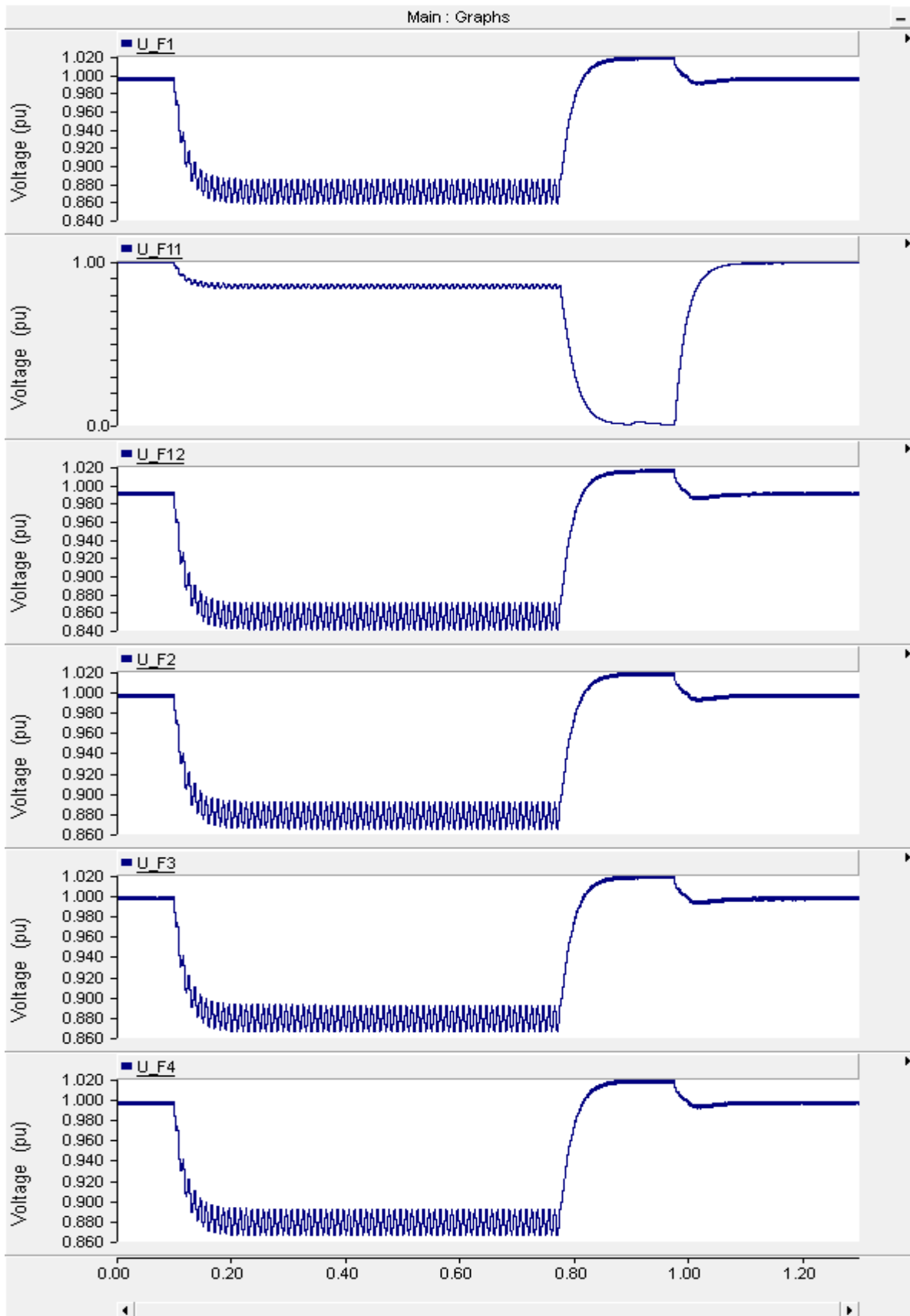


Figure 4.3 Feeder voltages due to a single line to ground fault at feeder F11.

From table 4.2, it is observed that when the feeder F11 is tripped due to a fault at the end of the feeder F11, the change in pre-fault and post-fault voltage is only about 0.18% at F11 and all the other feeders. It is also observed that the voltage at the load buses decreases from the main bus bar downstream toward the load feeders because of the line impedance as the cable length increases. From figure 4.4 it is observed that the circuit breaker will take 0.67s to trip the fault whereas the simulation has run for duration of 1.3s.

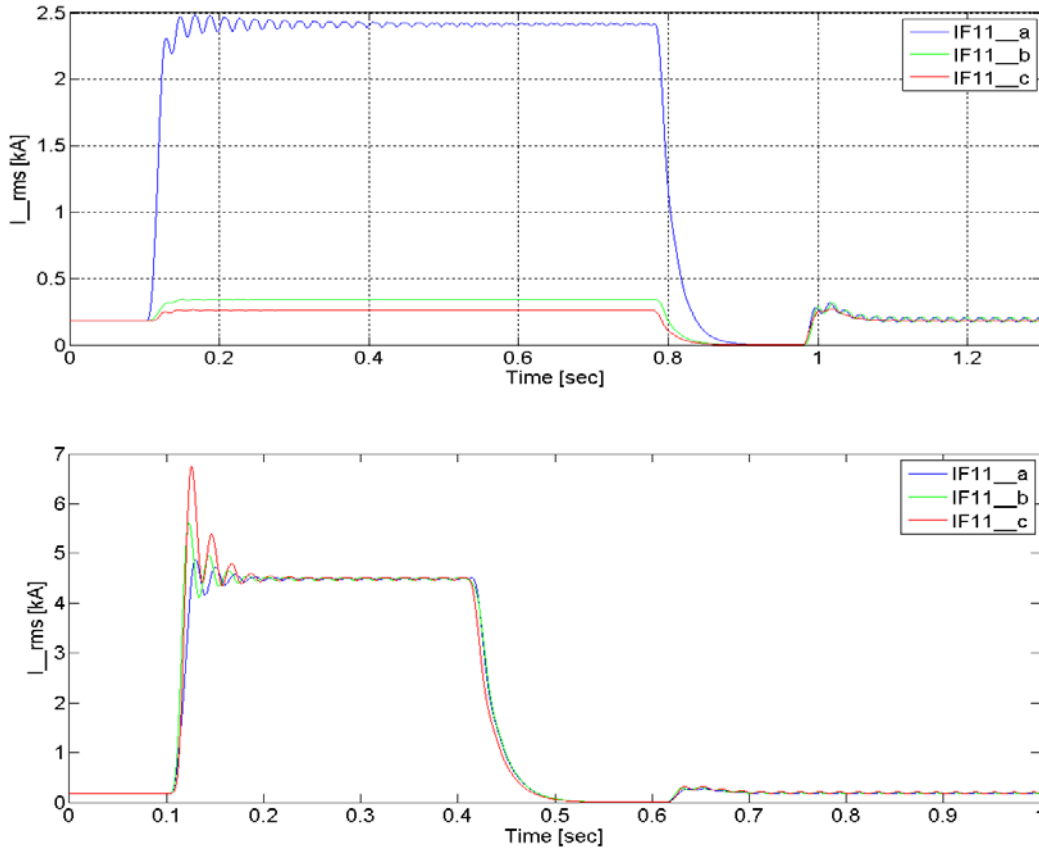


Figure 4.4 Current magnitudes at F11 when a three phase fault is applied at Feeder F11.

Fault at Feeder F12

The total length of feeder F12 is 2.5km which is 500m more than feeder F11. In this case the fault is applied at feeder F12. It is observed that when the feeder F12 is tripped due to a fault at the end of the feeder F12, the change in pre-fault and post-fault voltages is only about 3.27% at F12. The difference is higher because the load at feeder F12 is higher than the load at feeder F11. The nominal current drawn by feeder F12 is 0.3049kA whereas the current drawn by feeder F11 is 0.2644kA. Thus when feeder F12 is disconnected from the network due to tripping of the circuit breaker, the voltage in the network rises as shown in figure 4.6 for a particular time when the feeder F12 remained disconnected from the network.

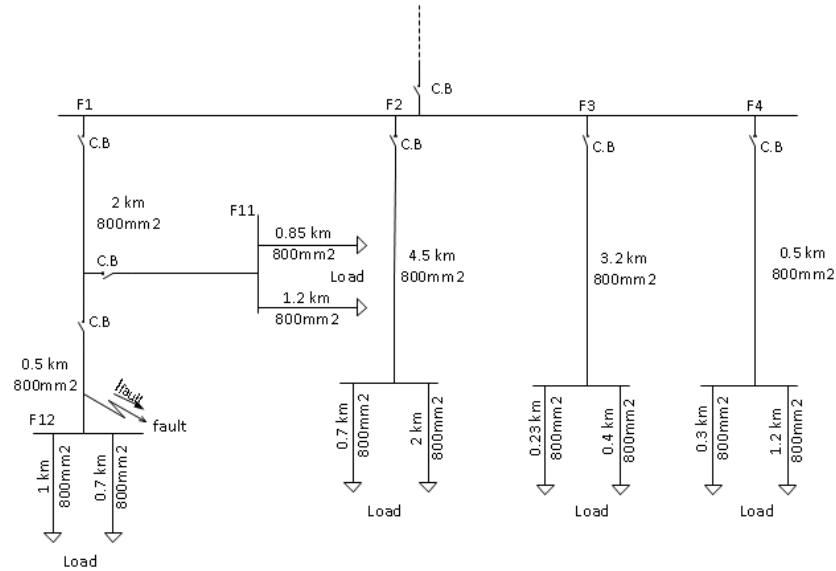


Fig 4.5: Single line diagram of the distribution system when a fault is applied at F12

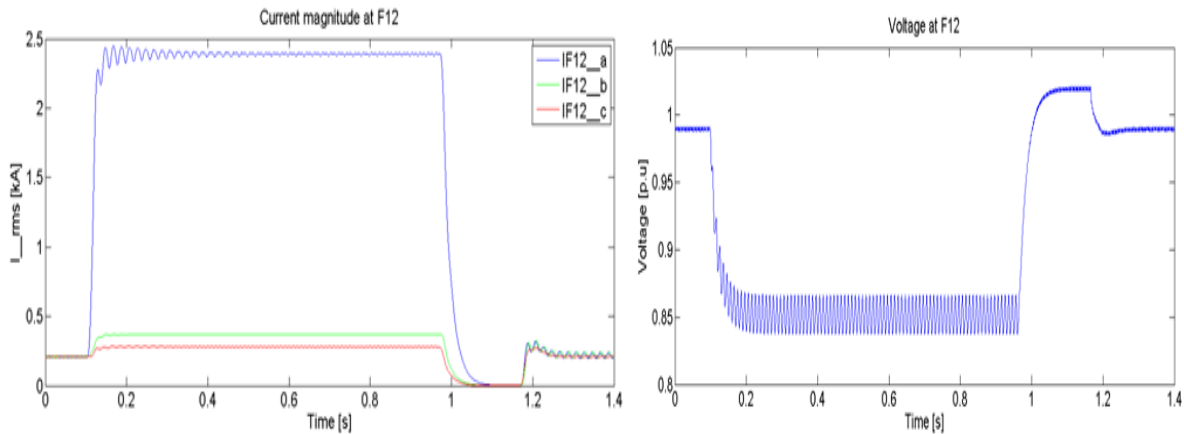


Figure 4.6 Current and Voltage magnitude at F12 when a Line to Ground fault is applied at F12.

From figure 4.6, it is observed that the circuit breaker will take 0.87s to trip after the fault occurs. It is noted that as the feeder F12 is far away from the main bus bar thus it will take longer time for the circuit breaker to detect the fault.

Table 4.3: Voltage at F11 for a pre-fault, during fault and post-fault when a fault is applied at the end of the feeder F12.

Faulted Location		Fault Type	Voltage across the Feeder F12 in p.u		
			Pre-Fault	During Fault	Post Fault
F12	Without DG	LG	0.9841	0.764	1.0024
		LLLG	0.9841	0.1634	1.0024

When the fault occurs at the end of the feeder F12, the voltage is reduced by 22% of the pre-fault voltage. The same procedure is applied for three phase fault and the results are noted in table 4.3.

Fault at Feeder F2

The total length of the feeder F2 is 4.5 km. This is the longest feeder in the network. The nominal current of the feeder is 0.3246kA. Thus when the feeder F2 is tripped due to a fault at the end of the same feeder, the change in pre-fault and post-fault voltage is only about 2.18%. The circuit breaker will take 0.998 sec to detect the fault and remove the faulted feeder from the network. The same procedure is applied for a three phase fault where the magnitudes of voltage dips are shown in table 4.4.

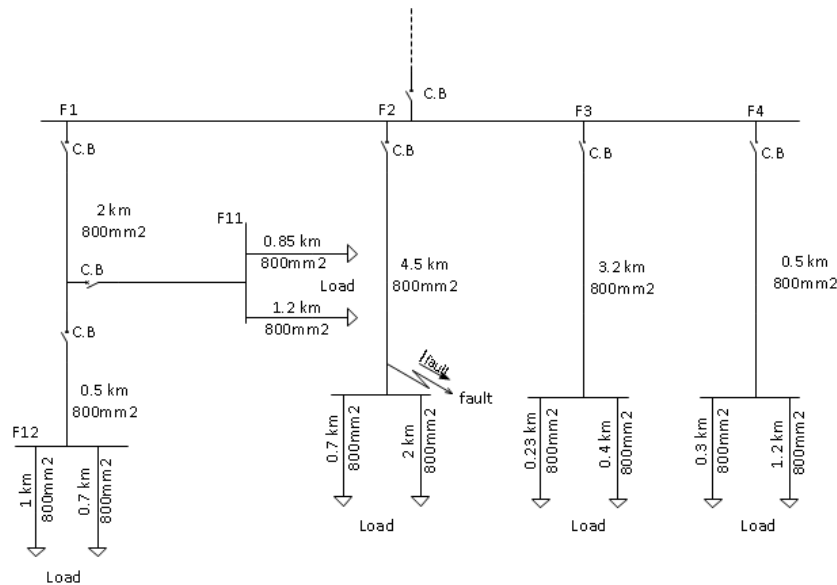


Fig 4.7: Single line diagram of the distribution system when a fault is applied at F2

Table 4.4: Voltage at F2 for a pre-fault, during fault and post-fault when a fault is applied at the end of the feeder F2.

Faulted Location		Fault Type	Voltage across the Feeder F2 in p.u		
			Pre-Fault	During Fault	Post Fault
F2	Without DG	LG	0.9845	0.8484	1.008
		LLLG	0.9841	0.2144	1.008

As shown in table 4.2 the nominal current of feeder F2 is higher than feeder F12 and F11. But still the fault detection time of feeder F2 circuit breaker is longer than the rest of the circuit breaker of feeder F1 as shown in figure 4.8. The main reason is that as feeder F2 is the longest feeder in the network, thus if a fault occur far away from the main bus bar then the detection time of the fault will be longer and it will produce less voltage dip on the main bus bar. As shown in table 4.4, the voltage dip on the main bus bar is only 13.6% of the pre-fault voltage as compare to the 22% voltage drop at feeder F12. Figure 4.5 shows the magnitude of voltage dip and current when a line to ground fault is applied at feeder F2.

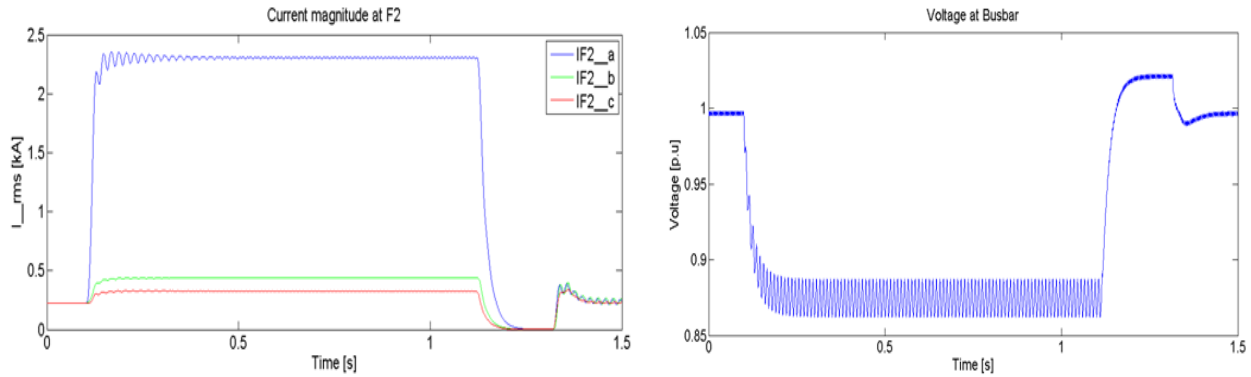


Figure 4.8 Current and Voltage magnitude at F2 when a Line to Ground fault is applied.

Fault at Feeder F4

The length of feeder F4 is 0.5km which is the shortest feeder in the network. Thus if a fault occurs on this feeder it will severely affect the main bus bar, as a result the entire feeder on the main bus bar will be affected. The nominal current of the feeder is 0.285kA. Thus when the feeder F2 is tripped due to a fault at the end of the feeder F4, the change in pre-fault and post-fault voltage is only about 2.37%. The voltage dip on the main bus bar is 13.32% of the pre-fault voltage and will be same on all the other feeders. The circuit breaker takes 0.7278s to trip after the fault occurs. The same procedure is done for a three phase to ground fault. The results are shown in table 4.5. Figure 4.10 shows the voltage and current magnitude when a line to ground fault is applied at the end of the feeder.

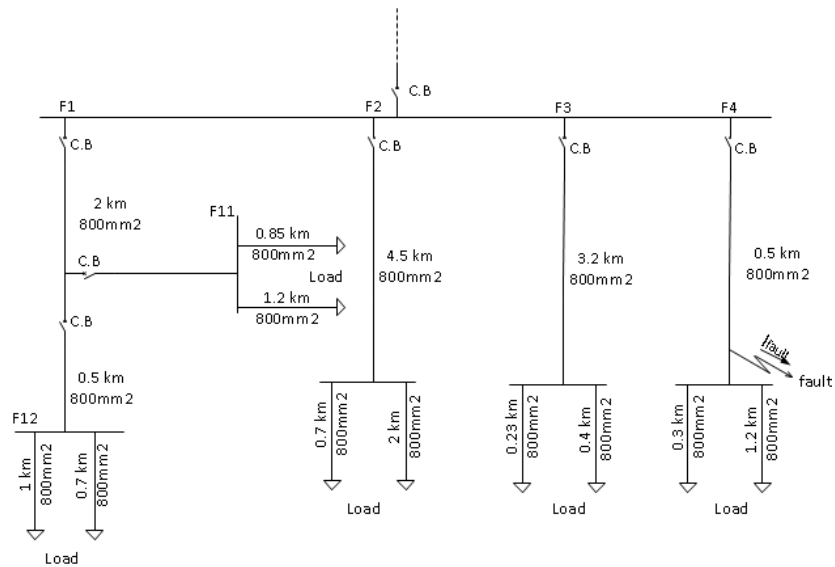


Fig 4.9: Single line diagram of the distribution system when a fault is applied at F4

Table 4.5 Voltage at F4 for a pre-fault, during fault and post-fault when a fault is applied at the end of the feeder F4.

Faulted Location		Fault Type	Voltage across the Feeder F4 in p.u		
			Pre-Fault	During Fault	Post Fault
F4	Without DG	LG	0.9845	0.8622	1.0211
		LLLG	0.9841	0.0607	1.0211

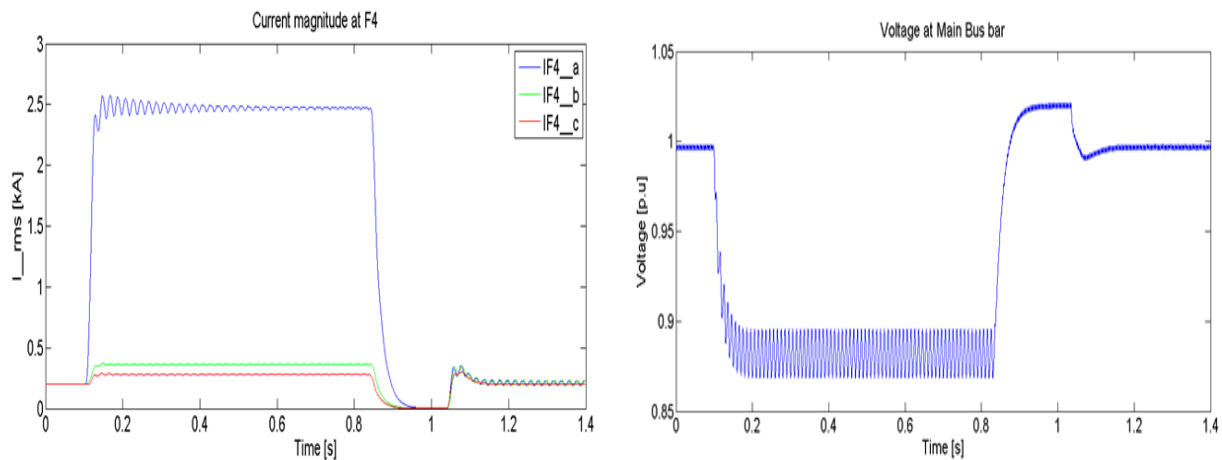


Figure 4.10 Current and Voltage magnitude at F4 when a Line to Ground fault is applied.

After applying faults on each feeder, the tripping times of the circuit breakers are calculated and the results are shown in table 4.6. The tripping times of the circuit

breakers will be helpful in order to realize the effect of different wind power capacities on the distribution system and the behavior of the protection system during fault conditions.

Table 4.6 Circuit Breaker Tripping Time of the distribution system.

Fault Location	Fault Type	Circuit Breaker Trip Time (sec)
F11	LG	0.57
	LLLG	0.3036
F12	LG	0.86
	LLLG	0.35
F2	LG	1.0123
	LLLG	0.43
F3	LG	0.58
	LLLG	0.282
F4	LG	0.72
	LLLG	0.298

4.3. SIMULATION RESULTS WITH 3MW AND 6MW WIND TURBINE CAPACITY

The effect of DG in a distribution system may impact the fault detection and protection of the circuit breakers in the distribution system. It mainly depends upon the protection, designing and location of DG in a distribution system. Typical possible problem may be protection blinding, sympathetic tripping and loss of coordination between the protection systems [6] [7]. The main goal of this section is to analyze the performance of the protection devices and the fault location in networks when distributed generators of 3MW and 6MW are attached in the network.

Each feeder in the distribution system is equipped with 3MW and 6MW wind turbine capacity individually. Each feeder is subjected to a single line to ground fault and a three phase fault where the results are compared with the case when there is no wind turbine installed on the network as studied in section 4.2. Since each turbine is designed with a converter, the converter provides the first degree of protection to the wind turbine and the distribution system. In case of protection, the main purpose of a converter is to limit the current during nominal operation and even in the fault condition by using a hard limiter in the designing of the voltage and current controllers. Thus for a 3MW wind turbine, the maximum current the turbine inject in a 20kV distribution system is 121A whereas a 6MW wind turbine will inject 242A to the current feeder. The wind turbine on each feeder is installed in such a way that the net capacity of the wind turbine cannot exceed the total load demand of the current feeder. The entire wind turbines are directly connected with the feeder in order to neglect the line losses at the point of common coupling. The pre-fault, during fault and post-fault voltages are calculated. The post-fault voltage represent when a faulted feeder being removed from the distribution system, thus the post-fault voltage will always be slightly greater than the pre-fault voltage due to the removal of load from the distribution system which will bring the system voltage closed to 1 p.u.

4.3.1. DG attached at Feeder F11

Single line to Ground Fault at F11

A 3MW wind turbine is attached at feeder F11. A fault is applied at 0.1s in order to check the behavior of the protection system in the distribution system. The simulation runs for 1.4s with a time step of 5 μ s. When a line to ground fault is applied on the same feeder it is observed that the protection system will take 104ms more to detect the fault compared to the case without the wind turbine. In a similar way when a wind turbine of 6 MW is attached with the feeder F11, the circuit breaker will take a longer time of approximately 160ms to detect a line to ground fault on the same feeder. The results are shown in figure 4.12. The reasons are that the currents are lower when wind turbines are connected and that an inverse time relay is used.

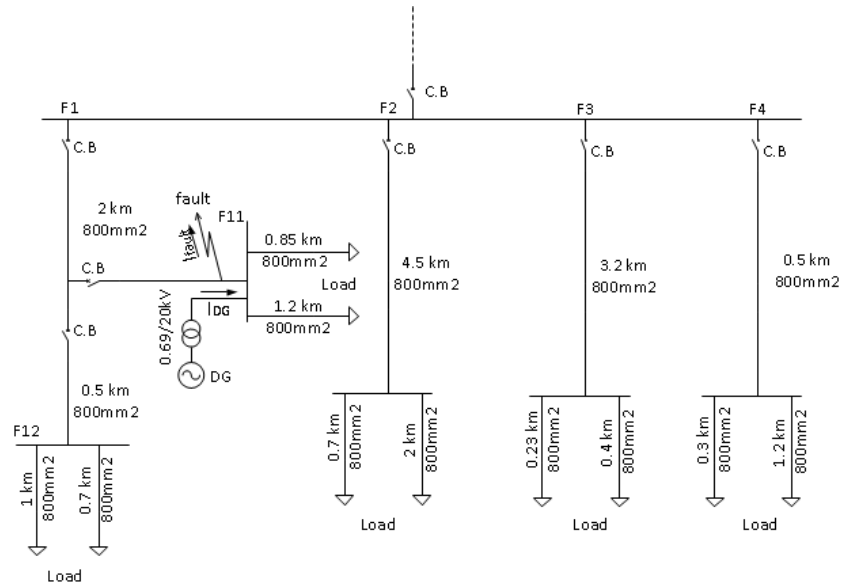


Fig 4.11: Single line diagram of the distribution system when a fault is applied at F11 with DG attached at F11

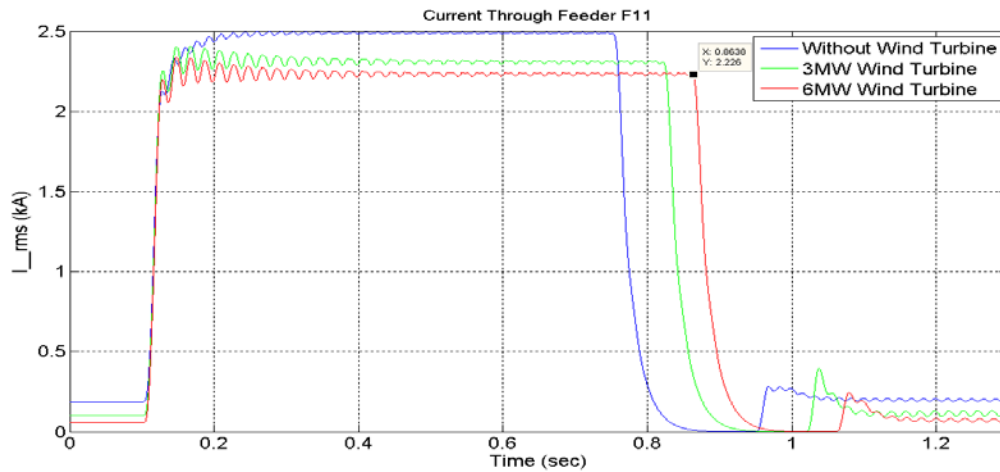


Figure 4.12 Magnitude of fault current at adjacent feeder with a wind turbine of 3MW and 6MW capacity by applying Line to Ground fault at F11.

As the magnitude of the nominal current and fault current decreases by the addition of wind turbine, thus the protection system will take longer time to detect the fault and the fault will stay in the line for a longer duration. As shown in the above figure, before the fault applied on the line, the nominal current of the line feeder without wind turbine is 262A which decrease to 144A with a case of 3MW wind turbine and 74A with a 6MW wind turbine. Thus as a result the magnitude of the fault current also decreases. Since the larger the magnitude of the fault current, the shorter the clearing time of the circuit breaker but as the magnitude of fault current decreases as a result the tripping time of the circuit breaker on that feeder increases. The results are shown in table 4.7.

Table 4.7 Magnitude of fault current on F11 during 3MW and 6MW wind turbine capacity and the time taken by the protection system to detect the fault.

Fault Location	Wind Power Capacity	Fault Type	Current through the Feeder F11			cycles
			Nominal Current (kA)	Fault Current (kA_rms)	Fault Detection Time (ms)	
F11	No Wind Power	LG	0.262	2.438	629	31.5
	3 MW Wind Power	LG	0.144	2.296	733	36.6
	6 MW Wind Power	LG	0.077	2.21	789	39.45

The duration of a voltage dip depends upon the protection system fault clearing time. With the addition of a wind turbine the magnitude of the voltage dips decreases as shown in figure 4.13. The wind turbine will stiff the voltage to 1 p.u during normal operation and the voltage dip on the main bus bar is only 13% of the pre-fault voltage as compared to 22.4% voltage drop in case of without wind turbine.

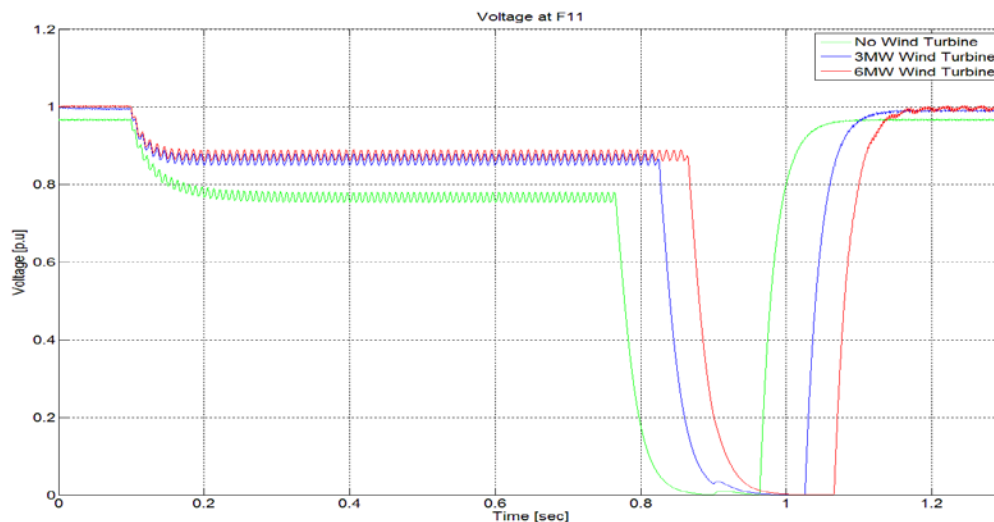


Figure 4.13: Magnitude of voltage dips with wind turbine of 3 MW and 6 MW capacities when a Line to Ground fault is applied at F11.

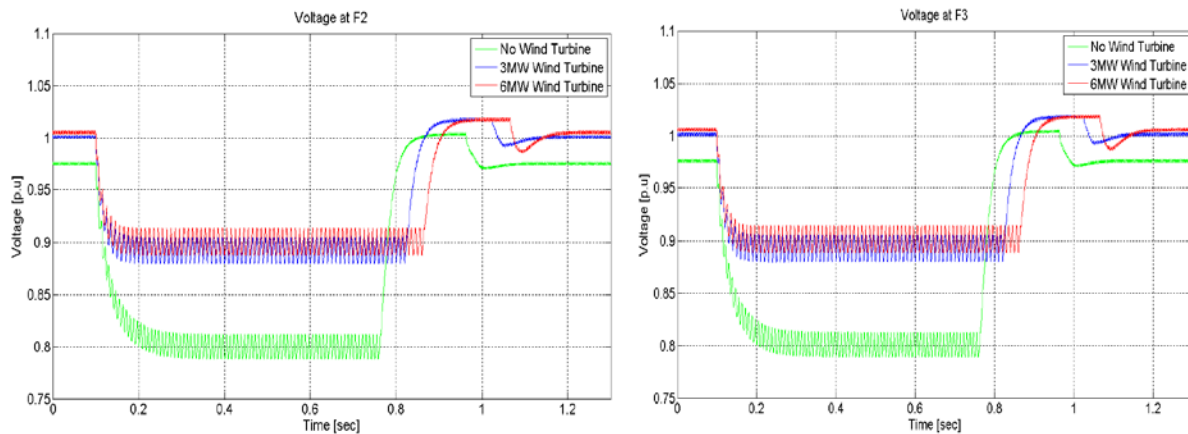
Table 4.8 shows the pre-fault, during fault, post-fault voltages and the tripping times of the circuit breaker when a fault is detected by the circuit breaker. In case of a three phase fault, the magnitude of the fault current is higher than the magnitude of the fault current when there is no wind turbine attached with the feeder. It is totally opposite to the case of single line to ground fault where the magnitude of the fault current is smaller than the magnitude when there is no wind turbine attached with the feeder as shown in the figure 4.12. Thus the circuit breaker will produce a false tripping because of the high

magnitude of the fault current which will make the circuit breaker to trip faster. In case of three phase fault, the wind turbine is also contributing in the fault and as a result the magnitude of the fault current rises, this is not desirable and can be prevented by installing a directional over current relay at the feeder where wind turbine is attached at the PCC point. The second option is to change the pickup current setting in the over current relay in order to prevent unwanted disconnection due to short circuit at the adjacent feeder. [6] [7]

Table 4.8: Magnitude of Voltage dips and circuit breaker tripping time at F11 for a pre-fault, during fault and post-fault when a fault is applied at the end of the feeder F11.

Fault Location	Wind Power Capacity	Fault Type	Voltage across F11 [p.u]			Fault detection Time (ms)
			Pre- Fault	During Fault	Post-fault	
F11	No Wind Power	LG	0.98	0.76	1.0	629
		LLLG	0.98	0.16	1.0	375.8
	3 MW Wind Power	LG	0.99	0.86	1.02	733
		LLLG	0.99	0.10	1.02	312.6
	6 MW Wind Power	LG	1	0.89	1.02	789.4
		LLLG	1	0.10	1.02	303.5

As the maximum capacity of the wind turbine on feeder F11 is not more than 50% of the load capacity. Thus it will produce less effect on the other feeders. The magnitude of the voltage drop on rest of the other feeder will be shown in figure 4.14.



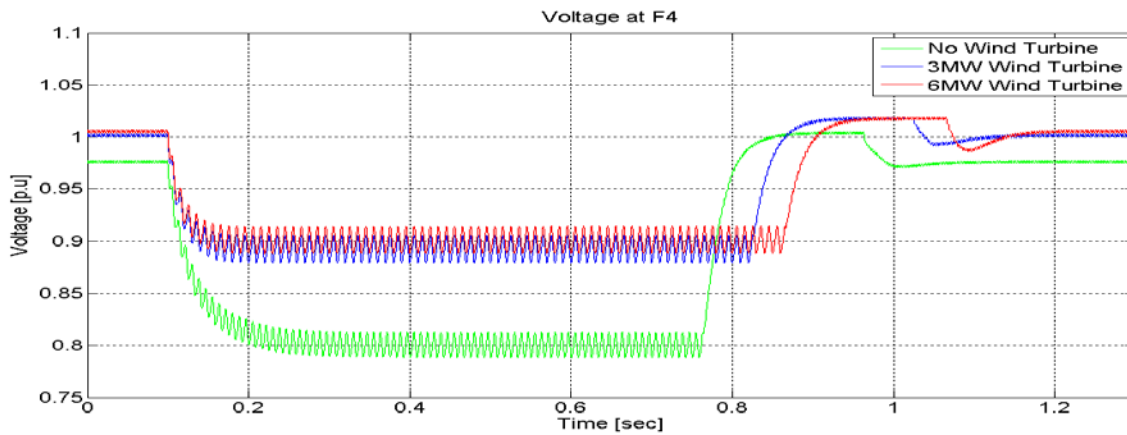


Figure 4.14: Magnitude of voltage dips at adjacent feeders when a Line to Ground fault is applied at F11.

The current through main bus bar and feeder F1 is shown in fig. 4.15.

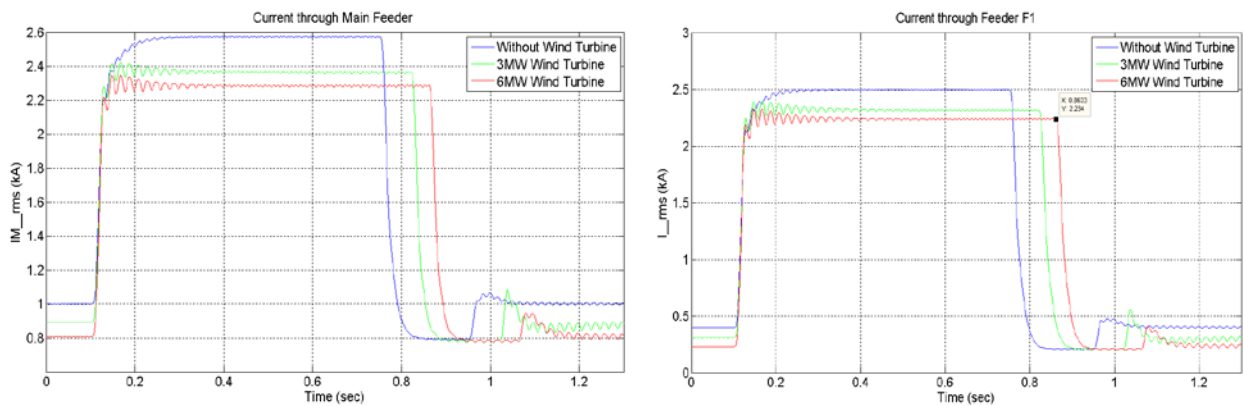


Figure 4.15: Magnitude of fault current when a Line to Ground fault is applied at F11.

Three phase to Ground Fault at F11

Now the above system is subjected to a 3 phases to Ground fault. A fault is applied at 0.1s whereas the simulation runs for 1s with a time step of $5\mu s$. When a fault is applied on the same feeder it is observed that the magnitude of the fault current increases. The protection system tripping time depends upon the magnitude of the fault current. The higher the magnitude of fault current the smaller will be the tripping time of the circuit breaker.

In case of a 3 phases to ground fault the magnitude of the fault current increases which will trip the circuit breaker 61.6ms earlier in case when there is 3MW wind turbine attached on the same feeder. As the power capacity of the turbine increases the magnitude of three phases to ground fault increases because of the saturation of the turbine inner current converter. During three phase faults, the inner converter of the turbine saturate as a result the converter will take more reactive power from the grid in

order to provide active power. Thus the circuit breaker will produce a false tripping. Table 4.9 shows the magnitude of fault current.

Table 4.9: Magnitude of fault current on F11 during 3MW and 6MW wind turbine capacity and the time taken by the protection system to detect the fault.

Fault Location	Wind Power Capacity	Fault Type	Current through the Feeder F11			cycles
			Nominal Current (kA)	Fault Current (kA_rms)	Fault Detection Time (ms)	
F11	No Wind Power	LLLG	0.26	3.77	374.4	18.72
	3 MW Wind Power	LLLG	0.14	4.49	312.8	15.64
	6 MW Wind Power	LLLG	0.08	4.50	303.2	15.16

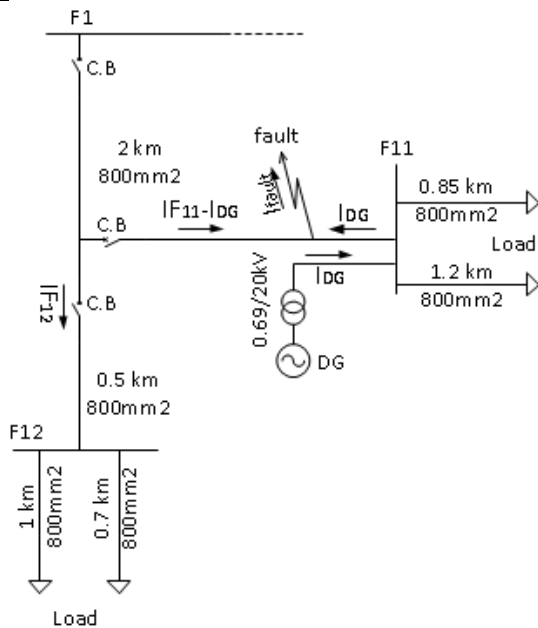


Figure 4.16(a): [Magnitude of single line to Ground fault at F11]

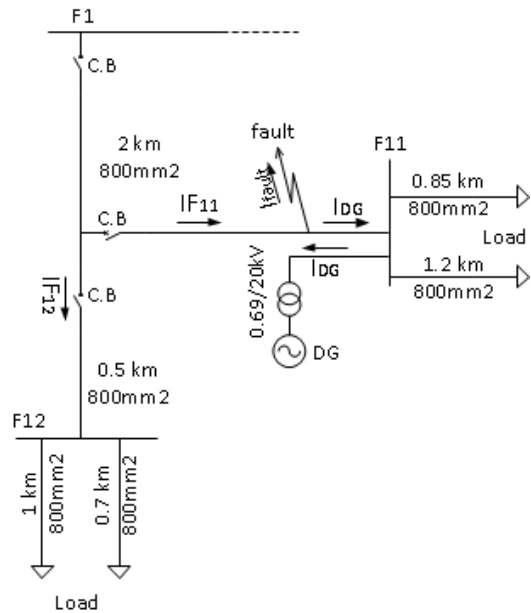


Figure 4.16(b): [Magnitude of three phases to Ground fault at F11]

Figure 4.16(a) and 4.16(b) shows the flow current in case of a single line to ground fault and a three phases to ground fault. The magnitude of the fault current in F11 and the other feeders are shown in figure 4.17.

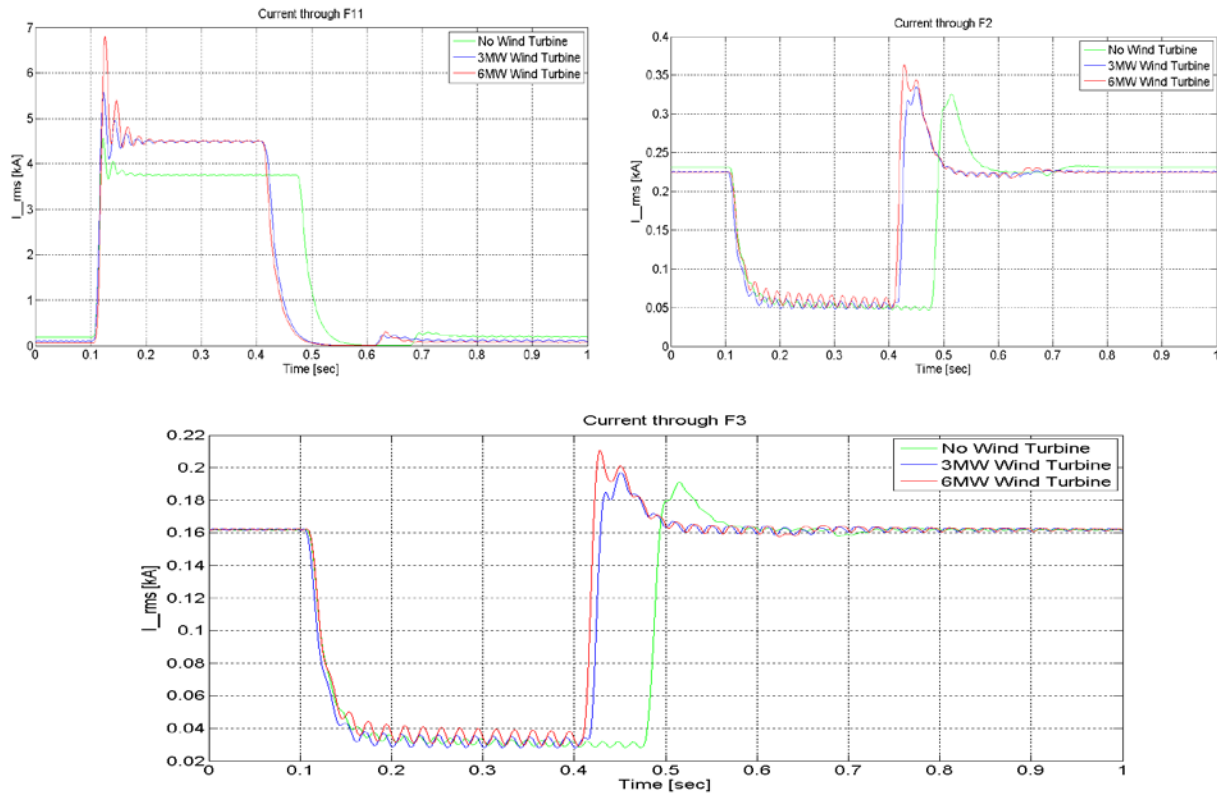


Figure 4.17 Magnitude of 3ph to ground fault current at 3MW and 6MW wind turbine installed on feeder F11 and the time taken by the protection system to trip the line.

4.3.2. DG attached at Feeder F12

Single line to Ground Fault at F11

A 3MW wind turbine is attached at feeder F12. The simulation runs for 1.4s with a time step of 5 μ s. A single line to ground fault at 0.1s is applied at Feeder F11. As a fault is applied on an adjacent feeder, it is observed that the protection system will take only 690ms to detect the fault. In case of a 6MW wind turbine, the circuit breaker will take 703.1ms to detect the fault which cause 13ms delay in detecting the same fault. Figure 4.19 shows the magnitude of line to ground fault current at F11.

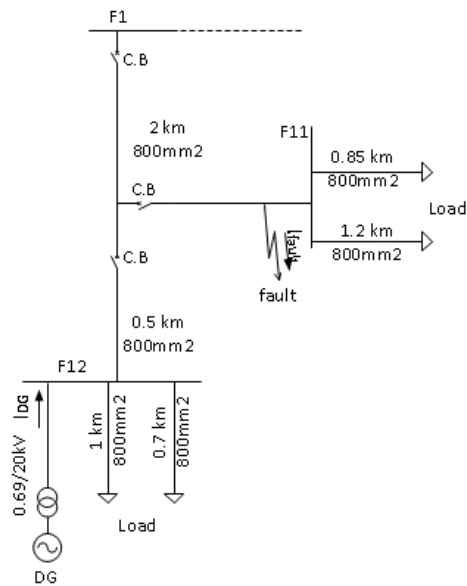


Fig 4.18: Single line diagram of the distribution system when a fault is applied at F11 with DG attached at F12

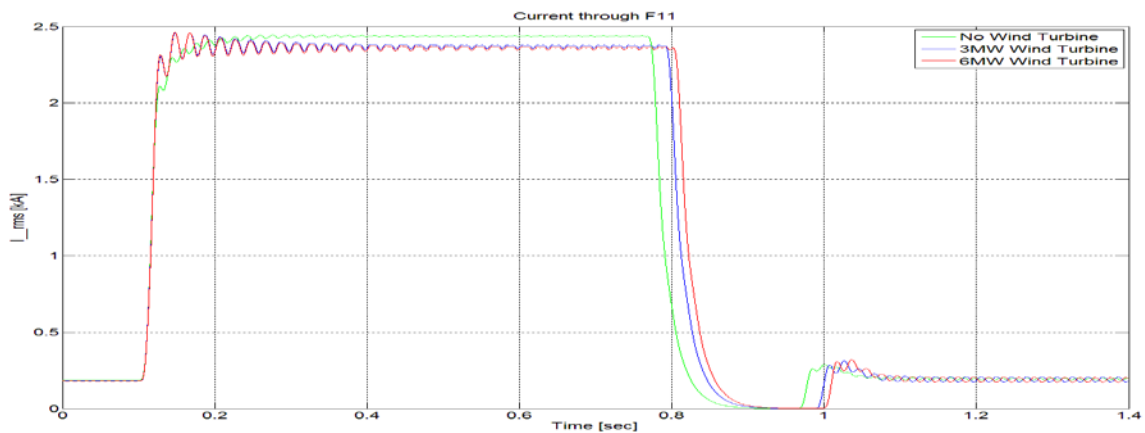


Figure 4.19 Magnitude of line to ground fault current at 3MW and 6MW wind turbine installed on feeder F12 and the time taken by the protection system to trip the line.

As the magnitude of the nominal current and fault current decreases by the addition of the wind turbine, thus the protection system will take longer time to detect the fault. As shown in the above figure the magnitude of nominal current remain the same before the fault whereas the magnitude of the fault current decreases only to 76A during fault when a wind turbine of 3MW capacity is installed at feeder F12. As the load is a constant power load, the magnitude of the fault current will have to remain the same, but as it is observed that with the addition of the wind turbine the voltage drop of the line decreases during the fault as shown in figure 4.20 which as a result will demand less current during the fault case as shown in the figure.

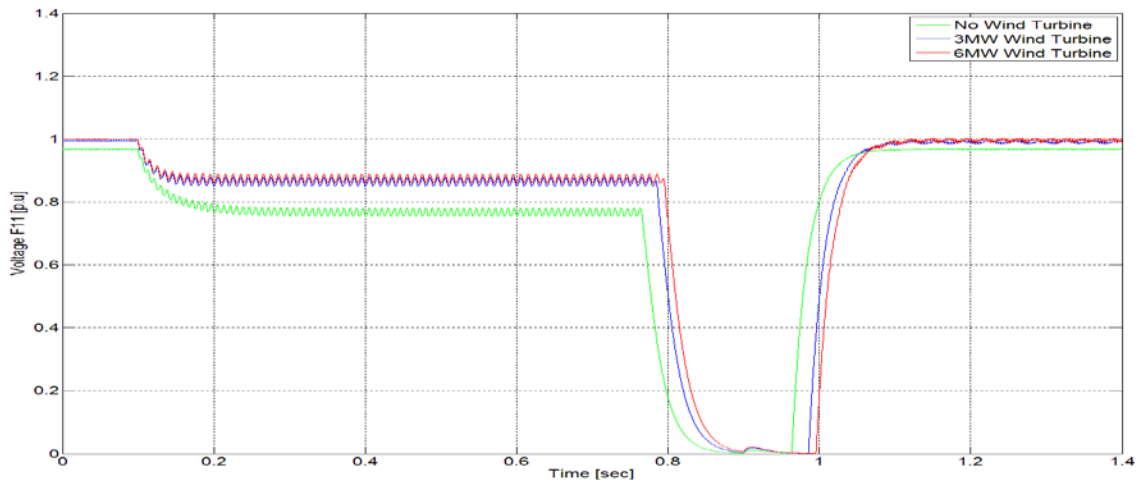


Figure 4.20 Magnitude of voltage dips at F11 when a Line to Ground fault is applied at F11.

Since the magnitude of the fault current decreases on feeder F11, as a result the tripping time of the circuit breaker increases. Table 4.11 shows the magnitude of Line to ground fault current at F11.

Table 4.10: Magnitude of fault current on F11 during 3MW and 6MW wind turbine capacity and the time taken by the protection system to detect the fault.

Fault Location	Wind Power Capacity	Fault Type	Current through the Feeder F11			cycles
			Nominal Current (kA)	Fault Current (kA _{rms})	Fault Detection Time (ms)	
F11	No Wind Power	LG	0.187	2.44	662	33
	3 MW Wind Power	LG	0.183	2.36	690	34.5
	6 MW Wind Power	LG	0.181	2.34	703.1	35.15

During line to ground fault at F11, the magnitude of the fault current at F12 decreases with the same amount as injected by the wind turbine. The magnitude of the fault current at F12 and rest of the other feeders are shown in figure 4.21.

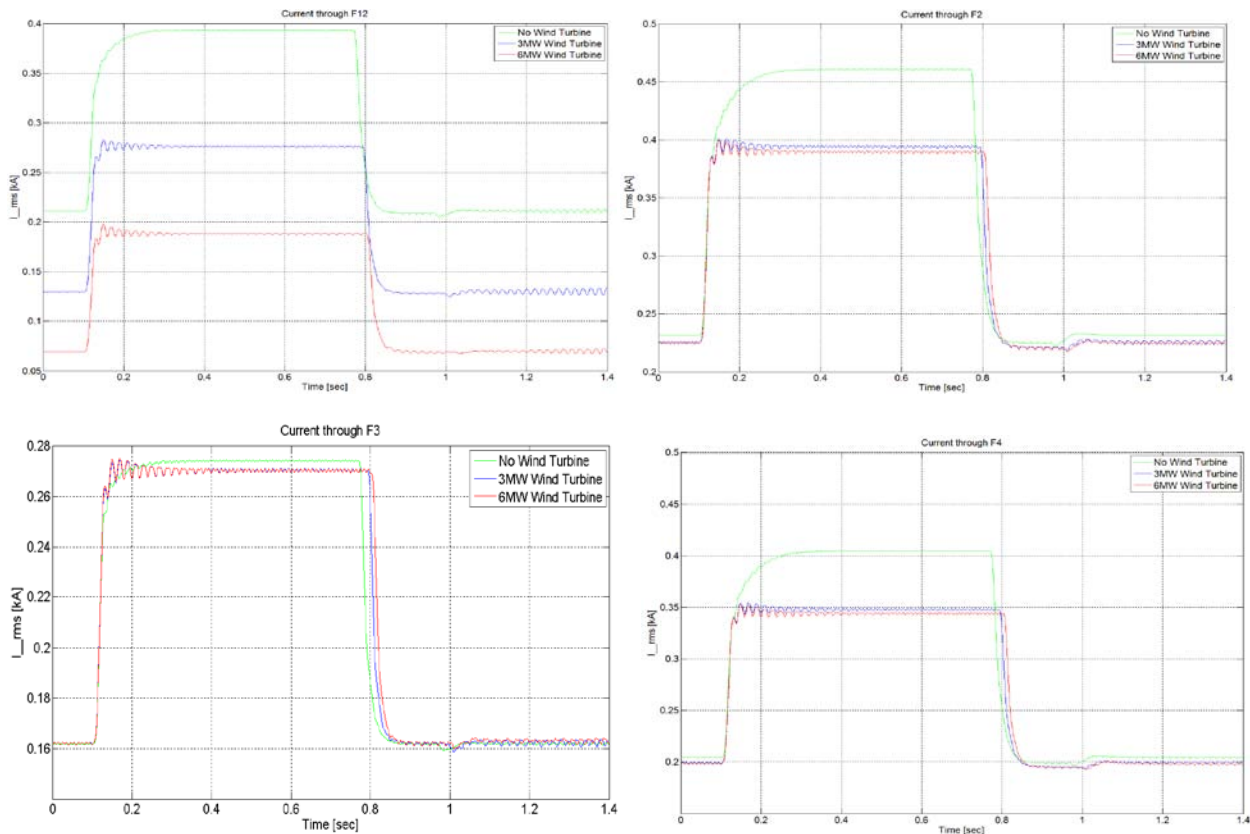


Figure 4.21 Magnitude of line to ground fault current when 3MW and 6MW wind turbine installed on feeder F12.

As feeder F12 is 2.5 km away from the main bus bar, thus the voltage dip on the F12 will be more as compare to F11. The wind turbine will stiff the voltage to 1p.u during nominal operation. When a 3MW wind turbine is attached at F12, the voltage dip on the main bus bar is only 14% of the pre-fault voltage as compare to 20.5% voltage drop in case of without DG. Whereas in case of 6MW DG capacities installed, the voltage drop on the main bus bar will reduce to 11% of the pre-fault voltage. Table 4.11 shows the pre-fault, during fault and the post-fault voltages and the tripping times when a fault is disconnected from the distribution system by tripping of the circuit breaker.

Fault Location	Wind Power Capacity	Fault Type	Voltage across F11 [p.u]			Fault detection Time (ms)
			Pre- Fault	During Fault	Post-fault	
F11	No Wind Power	LG	0.97	0.77	1.0	662
	3 MW Wind Power	LG	0.99	0.86	1.02	690
	6 MW Wind Power	LG	1	0.89	1.02	703.1

Table 4.11 Magnitude of Voltage dips and circuit breaker tripping time at F11 for a pre-fault, during fault and post-fault when a fault is applied at the end of the feeder F11.

The magnitudes of the voltage drop at F12 and rest of the other feeders when a line to ground fault is applied at F11 are shown in figure 4.22. As the fault is applied on the feeder F11 which is 500m away from the feeder where the DG is installed, thus it will produce less effect on the distribution protection system

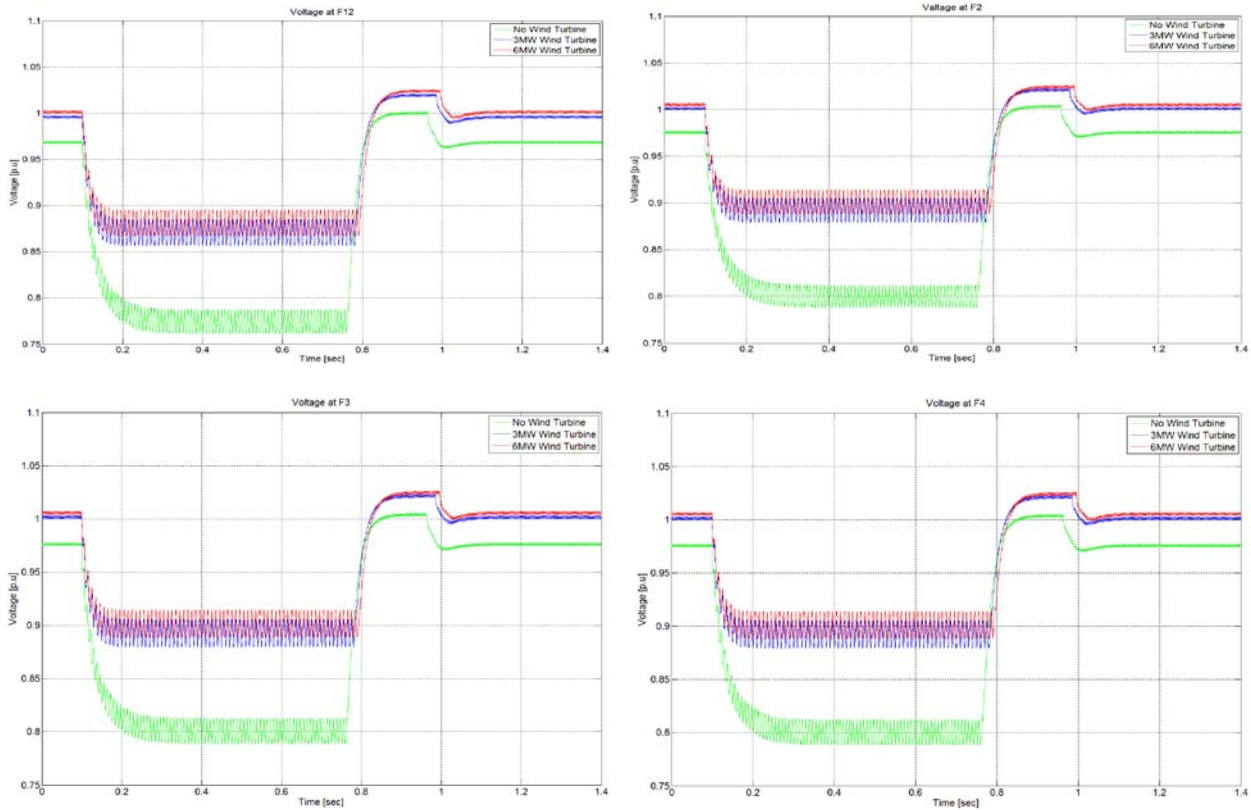


Figure 4.22: Magnitude of voltage dips when a Line to Ground fault is applied at F11.

Three phase to ground fault at F11

In this case, the magnitude of the fault current increases and as a result the tripping time of the circuit breaker decreases because of the contribution of DG current in the faulted area. As the capacity of the turbine increases, the magnitude of the fault current increases. Thus the circuit breaker F11 will trip 66.1ms earlier when a 3MW DG is attached at F12. Table 4.12 shows the magnitude of fault current at F11 and the protection system fault clearing time.

Table 4.12: Magnitude of fault current on F11 during 3MW and 6MW DG and the time taken by the circuit breaker to detect the fault.

Fault Location	Wind Power Capacity	Fault Type	Current through the Feeder F11			cycles
			Nominal Current (kA)	Fault Current (kA _{rms})	Fault Detection Time (ms)	

F11	No Wind Power	LLLG	0.18	3.77	375	7.5
	3 MW Wind Power	LLLG	0.18	4.55	319.8	6.4
	6 MW Wind Power	LLLG	0.18	4.66	301	6

The nominal pre-fault current of the load will remain the same. The load current demand of the of feeder F1 will decrease during normal operation because of the injection of wind turbine current in load area as shown in figure 4.36 pre-fault current across F1.

The first transient produced by the fault current is higher in case of 6MW DG as shown in figure 4.23 because of the high power rating of the turbine. At steady state the fault current of both the 3MW and 6MW DG approximately remain the same because of the converter limiter and short circuit capacity.

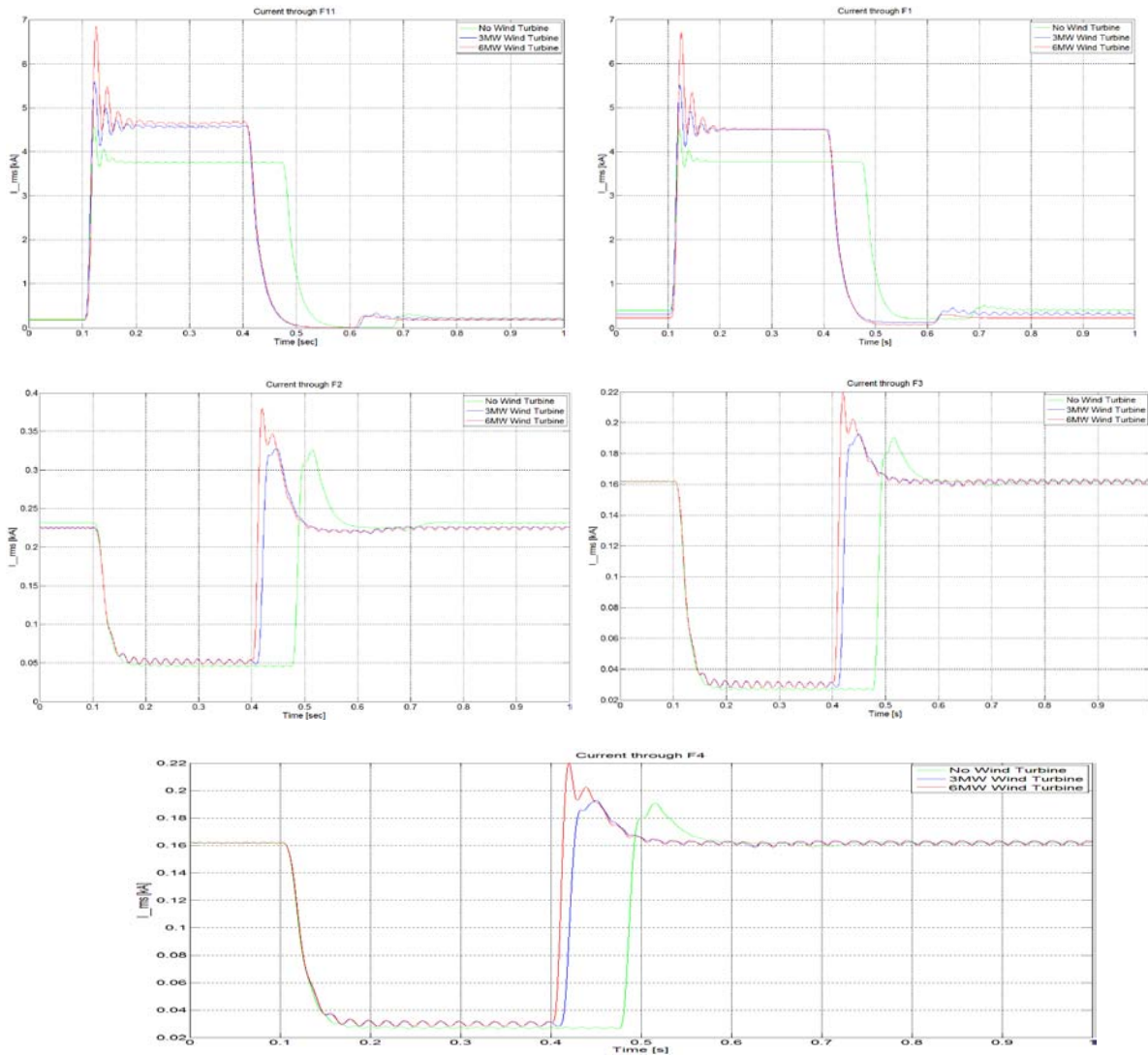


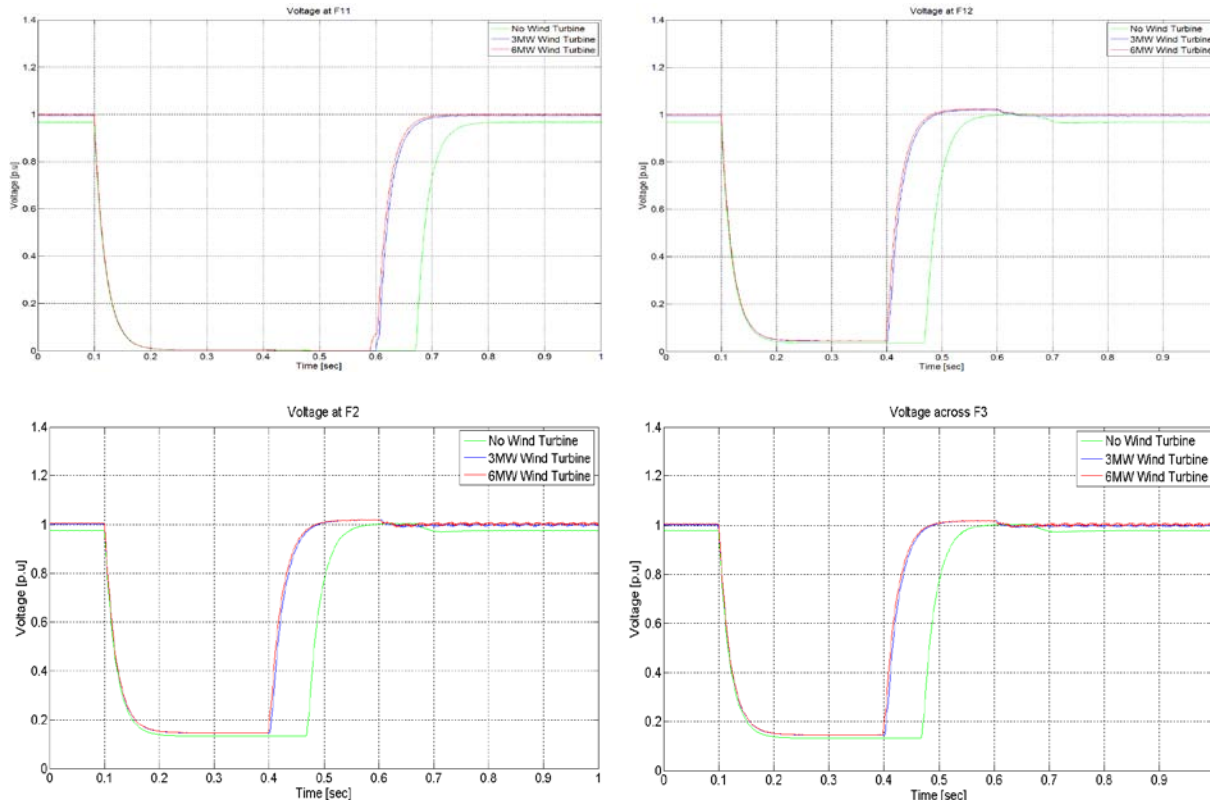
Figure 4.23: Magnitudes of the three phase fault current at F11 with 3MW and 6MW DG installed at feeder F12.

As feeder F11 is 500m away from the F12, thus during 3phase fault at F11 will experience less voltage drop on the line as compared to when DG is attached at F12. In case of a three phase fault, the voltage drop on the main bus bar is 85.69% of the three phase voltage with 3MW wind turbine as compare to 86.41% voltage drop without wind power generation in the distribution system. For a 6MW wind turbine capacity installed at F12, the voltage drop on the main bus bar is only reduced to 84.4% of the pre-fault voltage in case of a three phase fault. The results are shown in table 4.13.

Table 4.13 Magnitude of Voltage dips and circuit breaker tripping time at F11 for a pre-fault, during fault and post-fault when a fault is applied at the end of the feeder F11.

Fault Location	Wind Power Capacity	Fault Type	Voltage across F11 [p.u]			Fault detection Time (ms)
			Pre- Fault	During Fault	Post-fault	
F11	No Wind Power	LLLG	0.97	0.13	1.0	7.5
	3 MW Wind Power	LLLG	0.99	0.14	1.02	6.4
	6 MW Wind Power	LLLG	1	0.16	1.03	6

The magnitudes of the voltage drop at F12 and rest of the other feeders when a line to ground fault is applied at F11 is shown in figure 4.24.



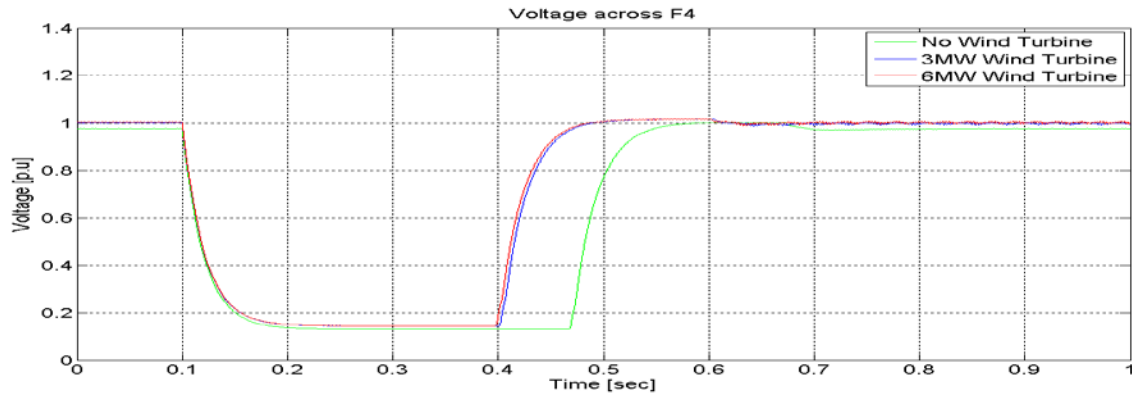


Figure 4.24: Magnitude of voltage dips when a three phase to ground fault is applied at F11.

Single line to Ground Fault at F12

As the wind turbine is attached with feeder F12 which is 2.5km away from the main bus bar, thus the effect of the fault will be more on this feeder as compare to fault at F11. The simulation runs for 1.4s with a time step of $5\mu s$. A single line to ground fault is applied at 0.1s. The results are shown in table 4.14.

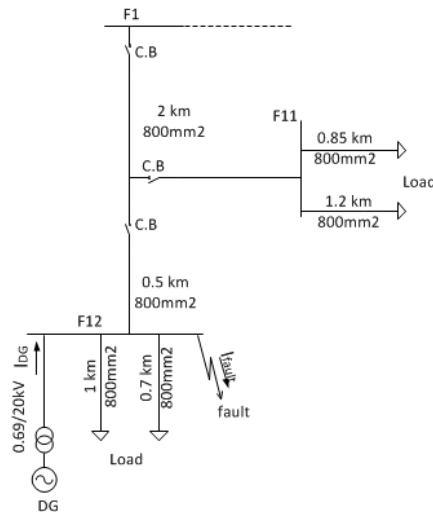


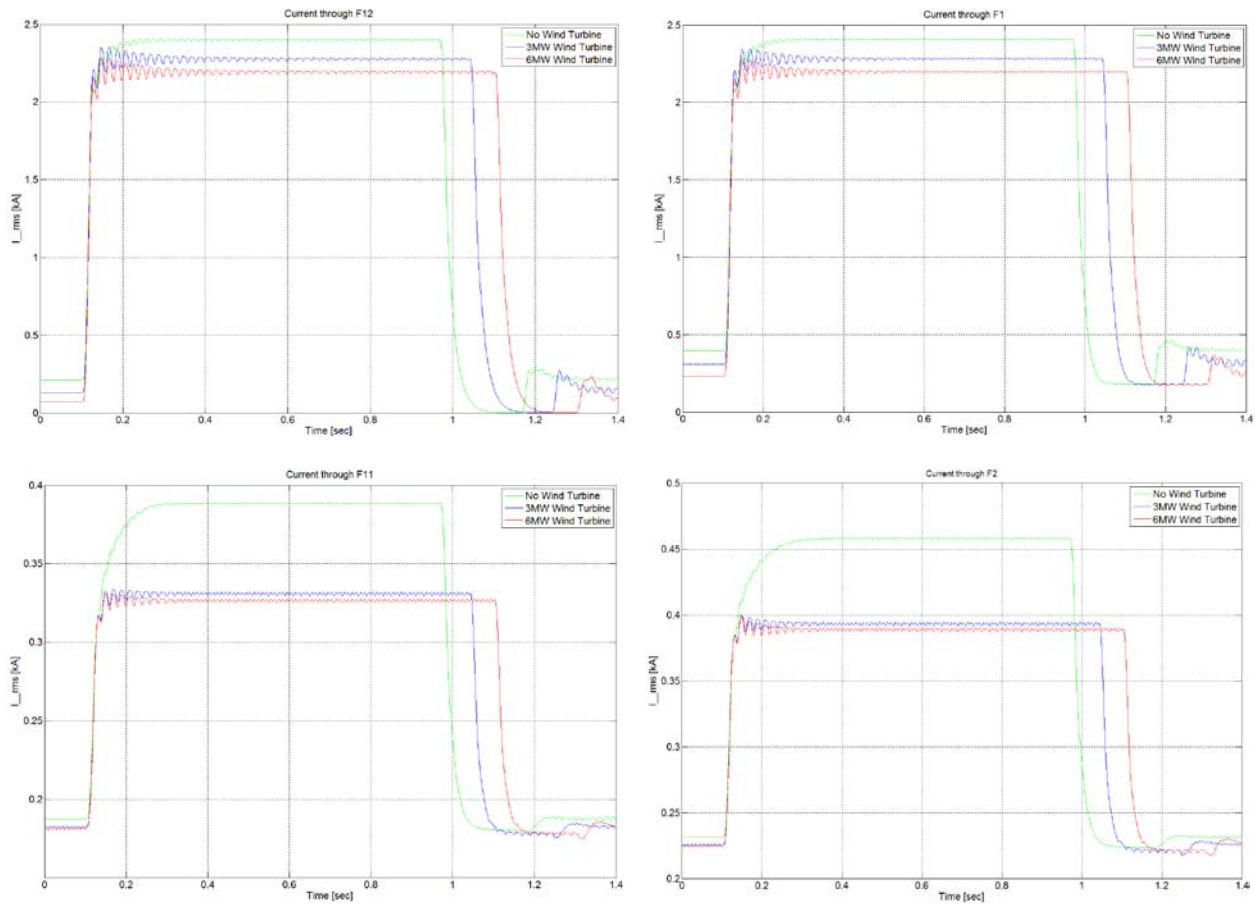
Fig 4.25: Single line diagram of the distribution system when a fault is applied at F12 with DG attached at the same feeder.

Table 4.14: Magnitude of fault current at F12 when 3MW and 6MW wind turbine are attached at F12 and the time taken by the protection system to detect the fault.

Fault Location	Wind Power Capacity	Fault Type	Current through the Feeder F12			cycles
			Nominal Current (kA)	Fault Current (kA _{rms})	Fault Detection Time (ms)	

F12	No Wind Power	LG	0.21	2.40	868.9	43.4
	3 MW Wind Power	LG	0.13	2.28	943.3	47.2
	6 MW Wind Power	LG	0.07	2.18	1013	50.65

From table 4.14, it is observed that the circuit breaker will take 943.3ms to detect the fault in case of 3MW DG installed on F12. When the capacity of the DG is increased to 6MW, the tripping time of the circuit breaker will increase to 1013ms. As the magnitude of the nominal current and the fault current decreases by the addition of a wind turbine, thus the circuit breaker will take longer time to detect the fault on the line. By comparing with table 4.11, it is observed that by increasing the distance from the main bus bar the circuit breaker fault detection time increases. Figure 4.26 shows the magnitude of the fault currents at F12 and the rest of other feeders.



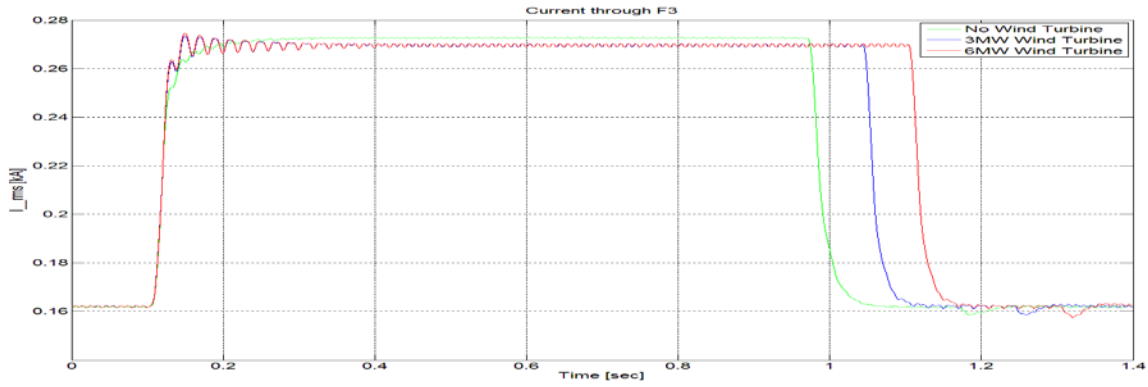


Figure 4.26: Magnitude of line to ground fault at F12 with 3 MW and 6 MW DG installed at feeder F12.

As feeder F3 is a constant current load, thus during fault the magnitude of the fault current will remain the same as compared to F2 and F4 constant power load. Because of the constant power load at F2 and F4, with the addition of 3MW and 6MW DG in the network the magnitude of voltage drop across the line decrease during the fault and as a result the fault current of F2 and F4 decrease compared to F3.

When a DG of 3MW capacity installed at F12, the voltage drop on F12 is only 12.75% of the pre-fault voltage compared to 20.43% voltage drop in case of without DG in the network. In case of 6MW DG capacity installed at the same feeder, the voltage drop on the bus will reduce to 11.56% of the pre-fault voltage. Table 4.15 shows the pre-fault, during fault and the post-fault voltages and the tripping time of the circuit breaker.

Table 4.15 Magnitude of Voltage dips and circuit breaker tripping time at F12 for a pre-fault, during fault and post-fault when a fault is applied at the end of the feeder F12.

Fault Location	Wind Power Capacity	Fault Type	Voltage across F12 [p.u]			Fault detection Time (ms)
			Pre- Fault	During Fault	Post-fault	
F12	No Wind Power	LG	0.97	0.77	1.0	868.9
	3 MW Wind Power	LG	0.99	0.87	1.01	943.3
	6 MW Wind Power	LG	1.0	0.89	1.02	1013

The magnitude of voltage drop at F12 and rest of the other feeders are shown in figure 4.27.

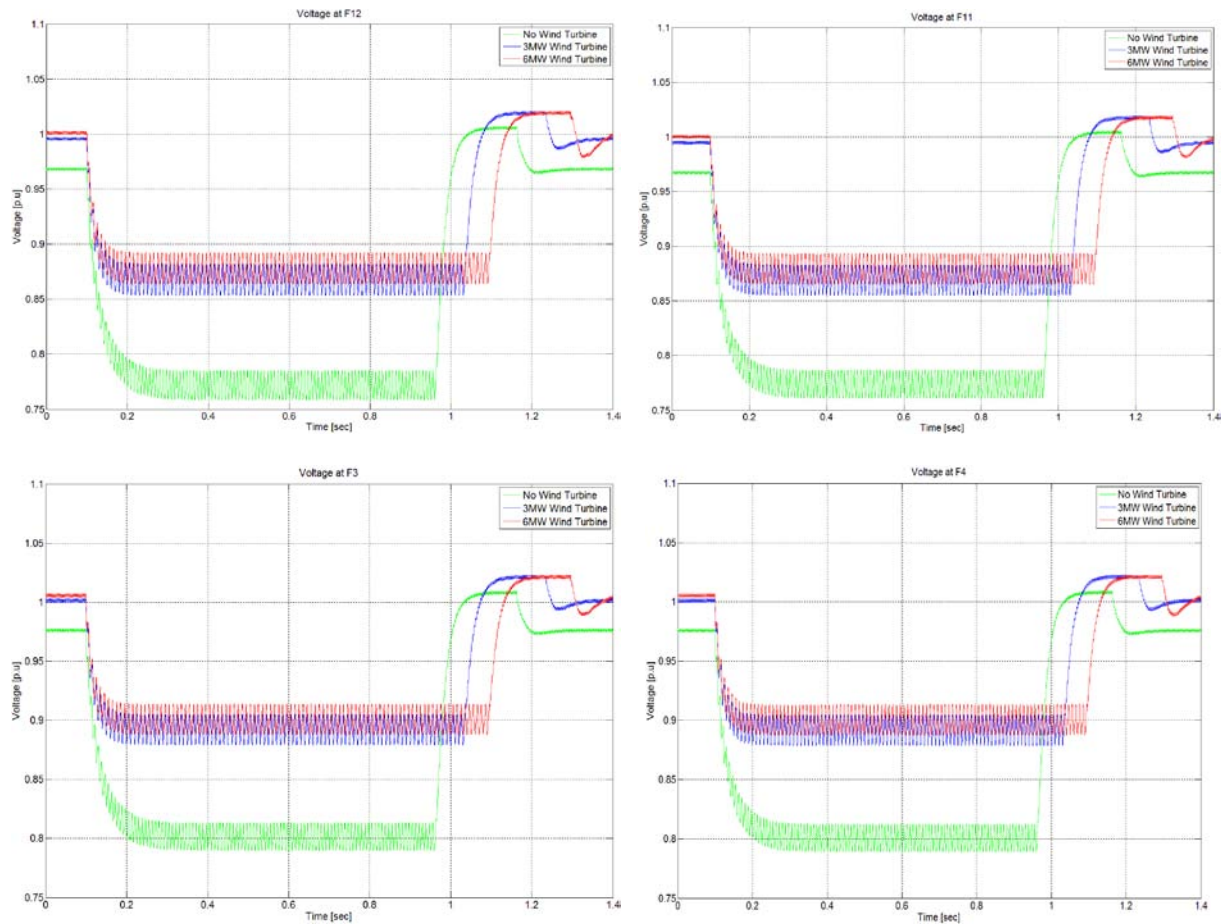


Figure 4.27: Magnitude of voltage dips when a line to ground fault is applied at F12.

Three phase to ground fault at F12

In case of a three phase fault, the magnitude of the fault current increased and as a result the tripping time of the circuit breaker will decrease. The magnitude of the fault current is increased because of the contribution of the DG current in the faulted area. As the capacity of the wind turbine increased, the magnitude of the fault current increased as explained in the case of three phases to ground fault at F11. Thus the circuit breaker F11 will trip 66.1ms earlier when a 3MW turbine is attached at F12. Table 4.16 shows the magnitude of fault current at F11 and the protection system fault clearing time during three phases to ground fault.

Figure 4.28 shows the magnitude of the fault current and voltage at F12. The first peak of the fault current will always be high because of the transient. The instantaneous values of the fault current are shown in figure 4.29. The higher the power capacity of the turbine, the higher will be the first peak of fault current. The hard limiter in the converter will limit the fault current thus after the first peak the magnitude of 3MW and 6MW DG fault current will approximately remain the same because of the saturation of the current controller in the case of a three phase fault.

Table 4.16 Magnitude of fault current on F12 during 3 MW and 6 MW wind turbine capacity and the time taken by the protection system to detect the fault.

Fault Location	Wind Power Capacity	Fault Type	Current through the Feeder F12			cycles
			Nominal Current (kA_rms)	Fault Current (kA_rms)	Fault Detection Time (ms)	
F12	No Wind Power	LLLG	0.21	3.66	457.7	22.8
	3 MW Wind Power	LLLG	0.13	4.36	380.7	19.035
	6 MW Wind Power	LLLG	0.07	4.40	370.4	18.52

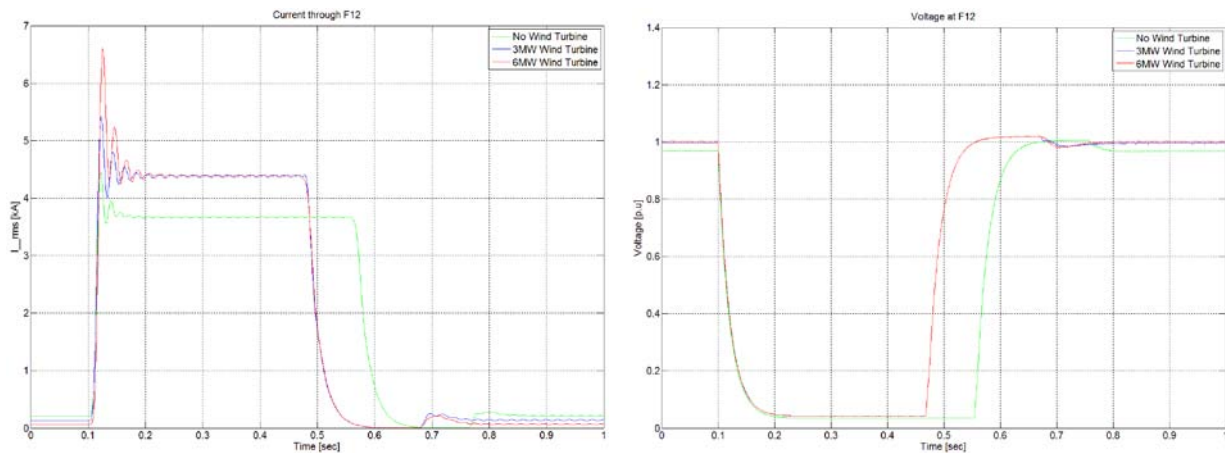
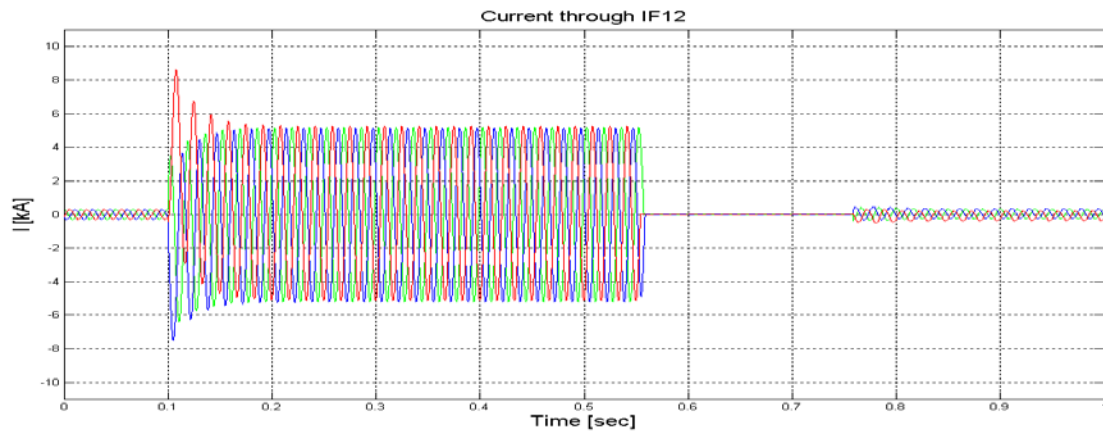
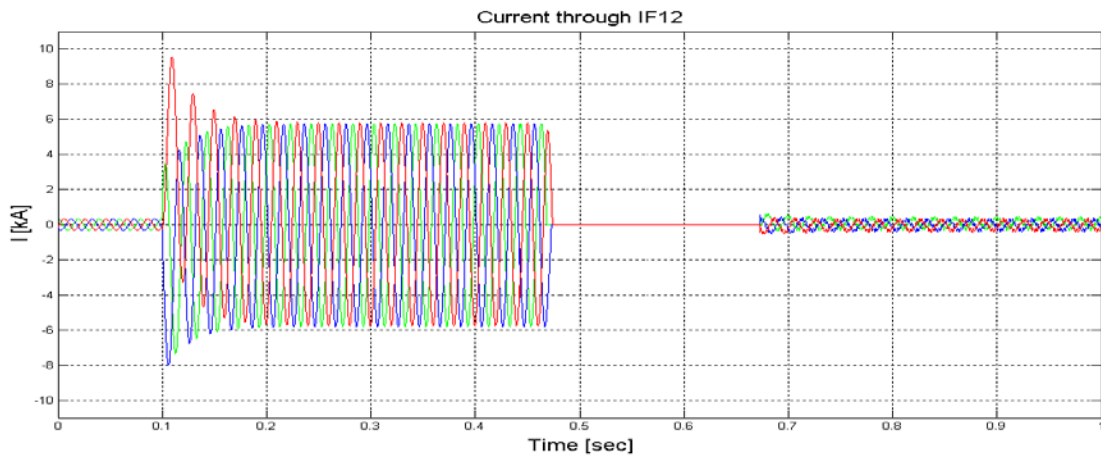


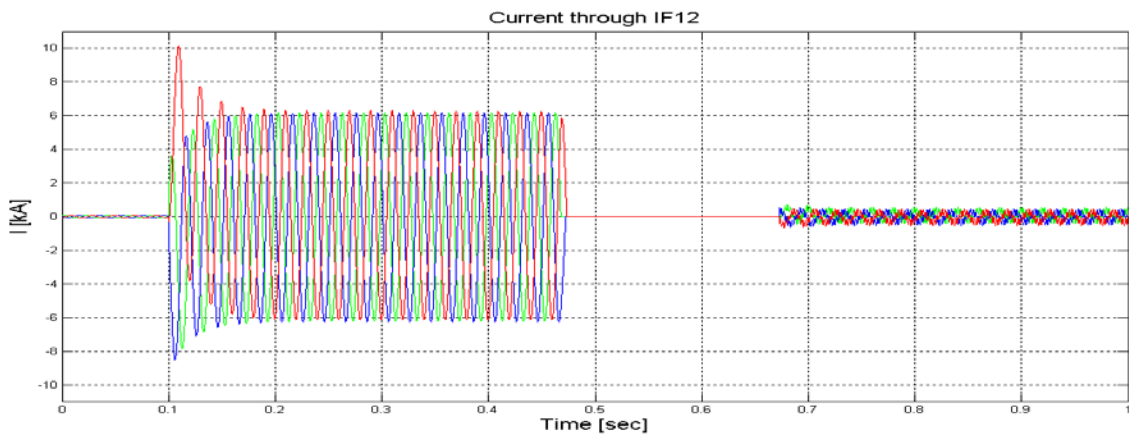
Figure 4.28: Magnitude of three phases to ground fault at F12 with 3MW and 6MW wind turbine installed at feeder F12.



(a) Without DG attached at F12



(b) With 3MW DG attached at F12



(c) With 6MW DG attached at F12

Figure 4.29: Instantaneous value of fault current when a three phases to ground fault is applied at F12.

Single line to Ground Fault at F2

It is observed that if a fault is far away from the main bus bar, the longer will be the time taken by the protection system to detect the fault. As feeder F2 is 4.5km away from the main bus bar, thus if a fault is apply on F2, the time taken by the circuit breaker to detect the fault will be longer as compare to fault at F11 and F12. In order to analyze the effect of single line to ground fault at F2, the simulation runs for 1.5s with a time step of 5 μ s.

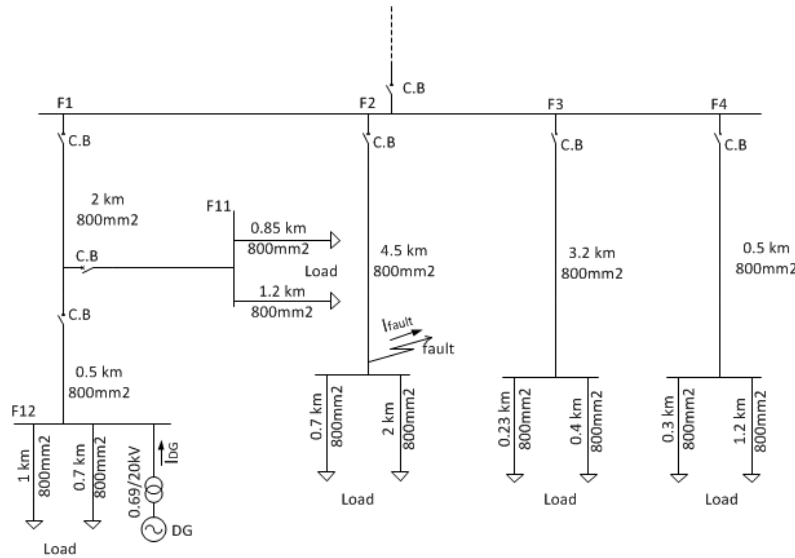


Fig 4.30: Single line diagram of the distribution system when a DG is attached at F12 and a fault is applied at F2 feeder.

As the wind turbine is installed at F12, thus the fault at F2 will put less effect on the network because the fault is far away from the distribution generation. Figure 4.31 shows the magnitude of fault current at F2.

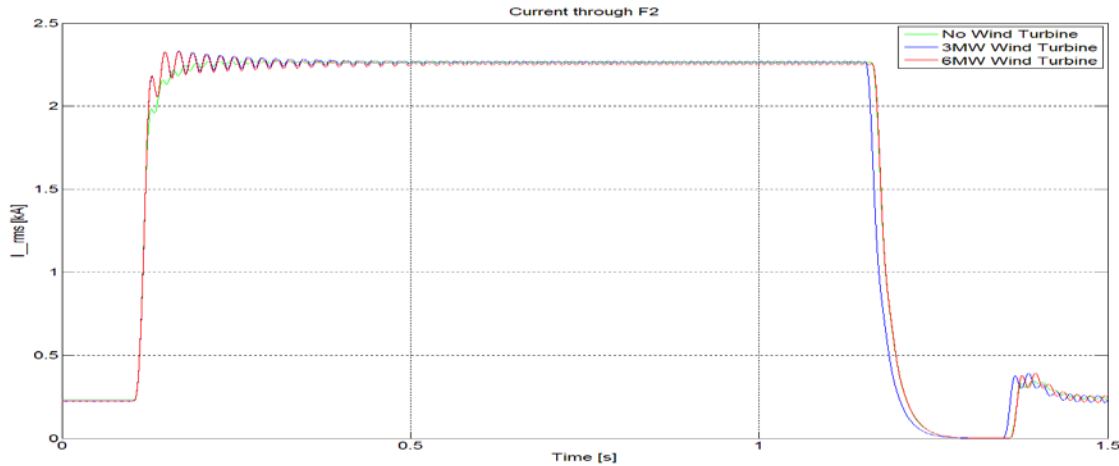


Figure 4.31: Magnitude of line to ground fault at F2 with 3MW and 6MW wind turbine installed at feeder F12.

It is observed that the magnitude of the nominal current at F2 is approximately same. A small change in the nominal current occur because of the wind turbine which brings the voltage of the main bus bar close to 1p.u, thus as the voltage is close to 1p.u as a result the load current decreases. The same effects apply on the fault current as shown in figure 4.32. Table 4.17 shows the magnitude of fault current at F2.

Table 4.17: Magnitude of fault current at F2 when 3MW and 6MW wind turbine are attached at F12 and the time taken by the protection system to detect the fault.

Fault Location	Wind Power Capacity	Fault Type	Current through the Feeder F2			cycles
			Nominal Current (kA_rms)	Fault Current (kA_rms)	Fault Detection Time (ms)	
F2	No Wind Power	LG	0.23	2.27	1044	52.2
	3 MW Wind Power	LG	0.23	2.26	1050	52.5
	6 MW Wind Power	LG	0.23	2.25	1055	52.75

From table 4.17, it is observed that the circuit breaker will take 1050ms to detect the fault in case of 3MW DG. When the capacity of the DG is increase to 6MW, the tripping time of the circuit breaker will increase to 1055ms. Thus a small change occurs in the detection time of the circuit breaker which effect is negligible on the distribution system protection system.

The magnitude of the voltage drop at F2 during pre-fault, during fault and post-fault are shown in table 4.18. With 3MW wind power capacity, the voltage drop on F2 is only 12.95% of the pre-fault voltage as compare to 18.08% voltage drop without DG. In case of 6MW wind power capacity in the distribution system, the voltage drop on the bus will reduce to 10.22% of the pre-fault voltage. Table 4.18 shows the pre-fault, during fault and the post-fault voltages and the tripping time of the circuit breaker.

Table 4.18 Magnitude of Voltage dips and circuit breaker tripping time at F2 for a pre-fault, during fault and post-fault when a fault is applied at the end of the feeder F2.

Fault Location	Wind Power Capacity	Fault Type	Voltage across F2 [p.u]			Fault detection Time (ms)
			Pre- Fault	During Fault	Post-fault	
F2	No Wind Power	LG	0.97	0.80	1.00	52.2
	3 MW Wind Power	LG	0.99	0.87	1.02	52.5
	6 MW Wind Power	LG	1.0	0.90	1.03	52.75

Figure 4.32 shows the magnitude of voltage dip at F2 when a line to ground fault is applied. It is observed that the voltage dip on the line decreases when a DG are installed in the network which is the cause of decrease in current as explain earlier.

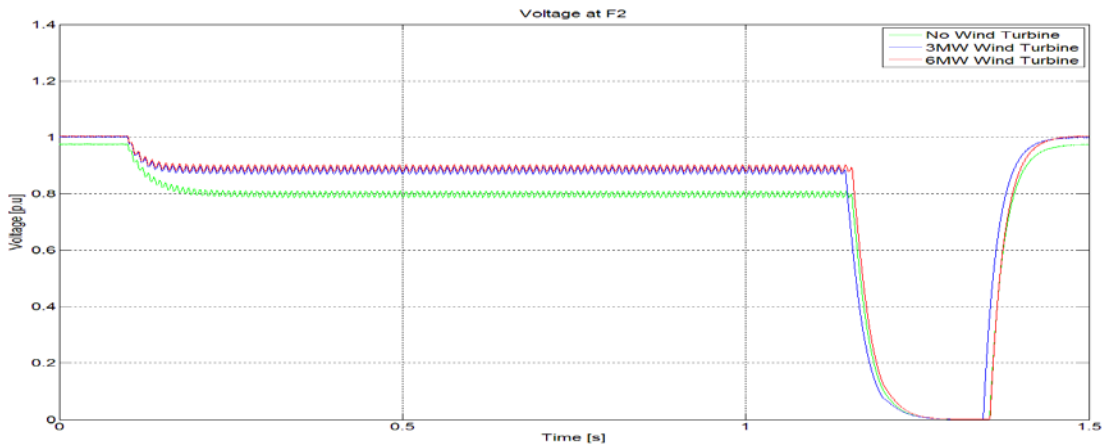


Figure 4.32 Magnitude of voltage dips when a line to ground fault is applied at F2

Three phase to ground fault at F2

When feeder F2 is subjected to three phase to ground fault as shown in table 4.19. It can be seen that the magnitude of fault current increases as a result the tripping time of the circuit breaker decreases. By comparing with table 4.12 and 4.16 during a three phase fault at F11 and F12, the magnitude of fault current decreases because of the long distance between the fault location and the DG end which will result in line losses.

Table 4.19: Magnitudes of fault currents at F2 when 3MW and 6MW wind turbine are attached at F12 and the time taken by the protection system to detect the fault.

Fault Location	Wind Power Capacity	Fault Type	Current through the Feeder F2			cycles
			Nominal Current (kA_rms)	Fault Current (kA_rms)	Fault Detection Time (ms)	
F2	No Wind Power	LLLG	0.231	3.36	562.6	28.13
	3 MW Wind Power	LLLG	0.226	4.04	439.5	22
	6 MW Wind Power	LLLG	0.225	4.10	431.4	21.5

Figure 4.33 shows the magnitude of fault current at F2.

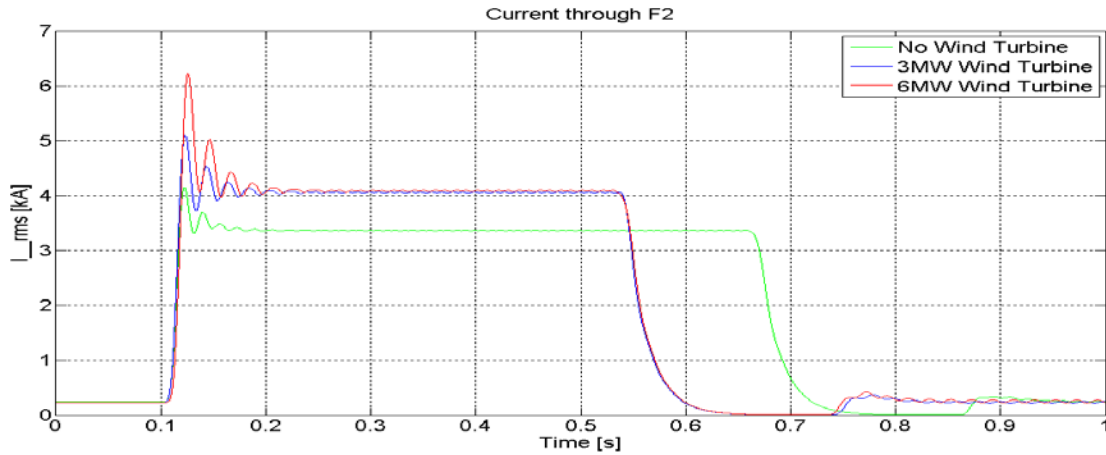


Figure 4.33: Magnitude of three phases to ground fault at F2 with 3MW and 6MW wind turbine installed at feeder F12.

The magnitude of the voltage drops at F2 during pre-fault, during fault and post-fault are shown in table 4.20. With 3MW wind power capacity, the voltage drop on F2 is only 79.9% of the pre-fault voltage as compare to 89% voltage drop without DG. In case of 6MW wind power capacity installed in the distribution system, the voltage drop on the bus will reduce to 79.8% of the pre-fault voltage. Table 4.20 shows the pre-fault, during fault and the post-fault voltages and the tripping time of the circuit breaker.

Table 4.20: Magnitude of Voltage dips and circuit breaker tripping time at F2 for a pre-fault, during fault and post-fault when a fault is applied at the end of the feeder F2.

Fault Location	Wind Power Capacity	Fault Type	Voltage across F2 [p.u]			Fault detection Time (ms)
			Pre- Fault	During Fault	Post-fault	
F2	No Wind Power	LLLG	0.98	0.11	1.0	562.6
	3 MW Wind Power	LLLG	0.99	0.20	1.02	439.5
	6 MW Wind Power	LLLG	1.0	0.20	1.03	431.4

Figure 4.34 shows the magnitude of voltage dip at F2 during fault condition. It can be seen that at 0.539s when a faulted feeder is remove from the distribution network, the voltage across the load goes to zero. The circuit breaker will take 0.2s to reconnect when the fault is removed from the network according to IEEE 1547 [1] standard.

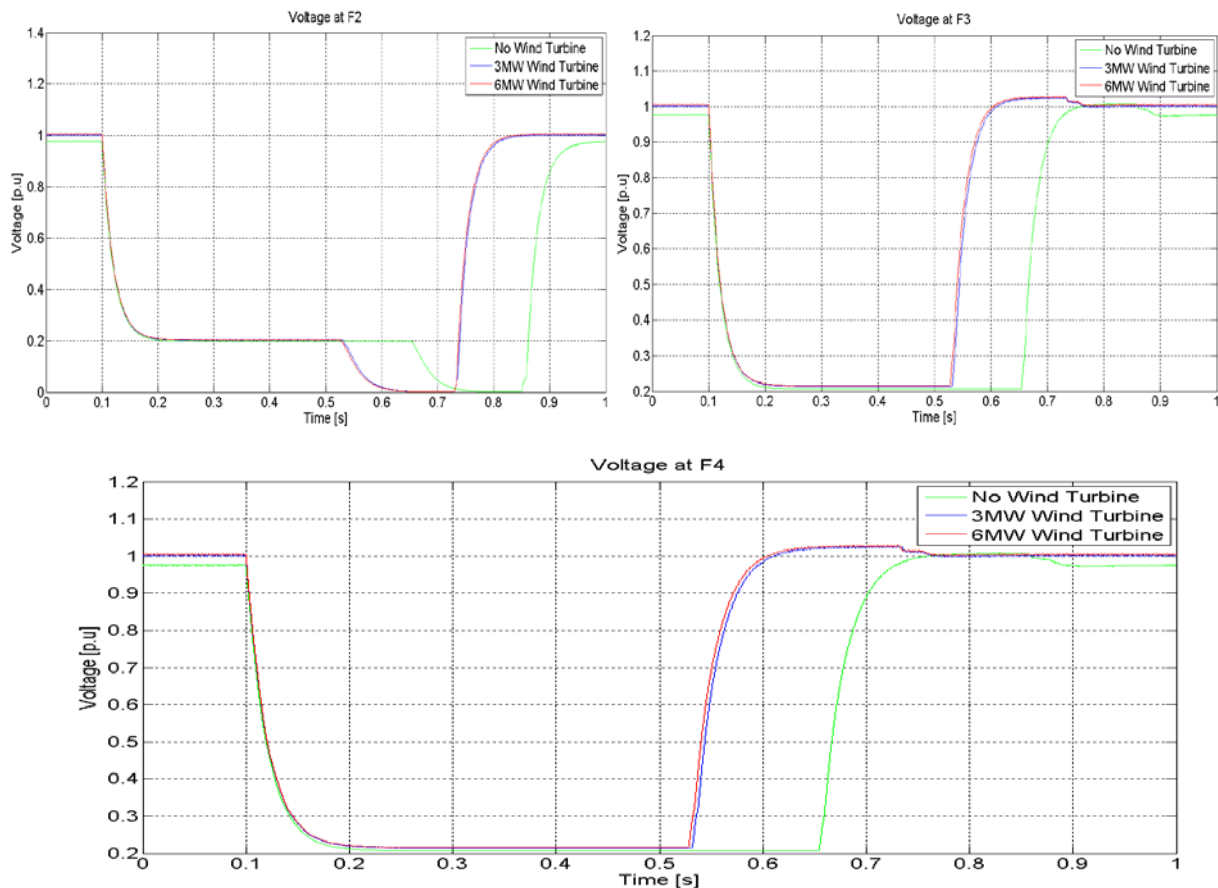


Figure 4.34: Magnitude of voltage dips when a three phase to ground fault is applied at F2

Single line to Ground Fault at F3

As the fault location is far away from the DG which is attached at F12, thus is a fault occur far away from DG it will produce less effect on the protection system of the distribution system. Since the capacity of DG is selected in such a way that it should not increase 50% of the load capacity. From figure 4.36, it can be observed that when feeder F3 is subjected to fault, the circuit breaker fault detection time is less affected. As F3 load is a constant current load, thus if a fault occur on the line the magnitude of the fault current remains the same as observed. A small difference occurs because of the decrease of voltage dip on the line due to addition of DG in the network.

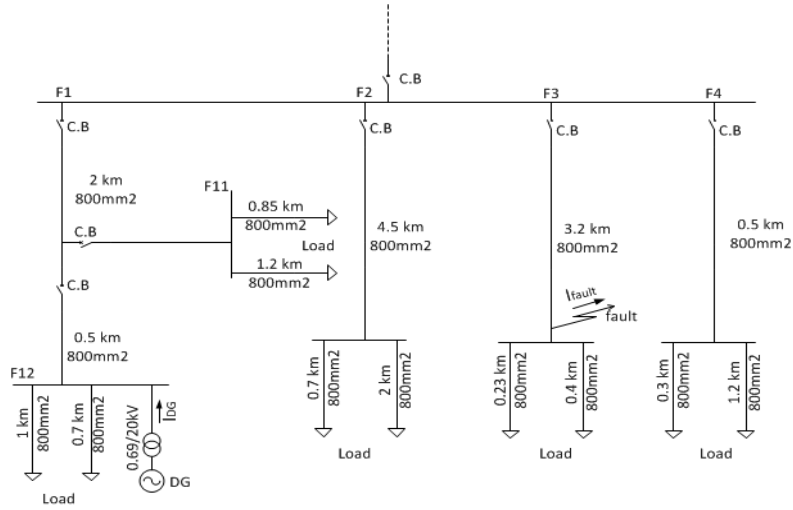


Fig 4.35: Single line diagram of the distribution system when a DG is attached at F12 and a fault is applied at F3 feeder.

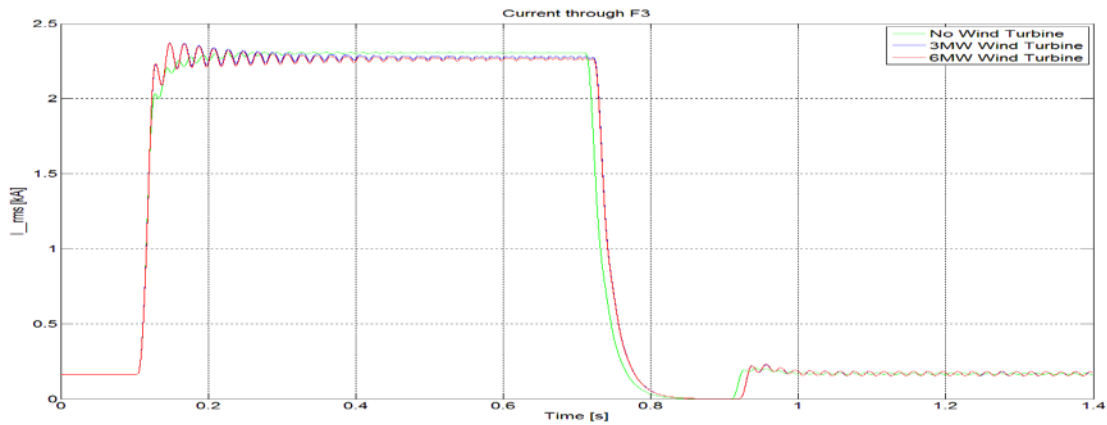
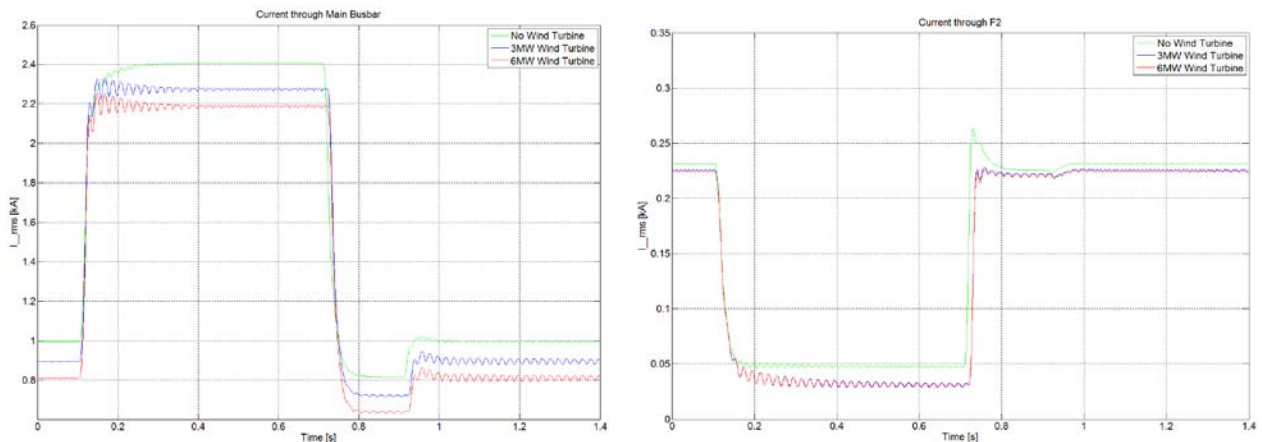


Figure 4.36: Magnitude of line to ground fault at F3 with 3MW and 6MW wind turbine installed at feeder F12.

Figure 4.37 shows the magnitude of fault current at phase 'A' when a line to ground fault at phase 'A' is applied at F3.



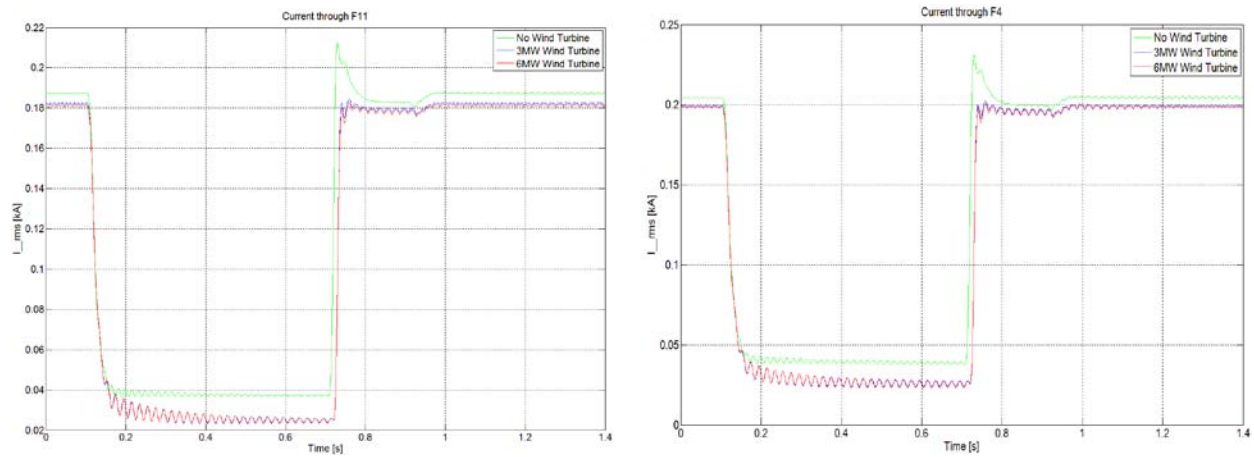


Figure 4.37: Magnitude of fault current when F3 is subjected to line to ground fault.

The nominal current of F3 remains the same regardless of any DG in the distribution system. As shown in table 4.21, the magnitudes of fault current approximately remain the same.

Table 4.21: Magnitude of fault current at F3 when 3MW and 6MW DG attached at F12 and the time taken by the protection system to detect the fault.

Fault Location	Wind Power Capacity	Fault Type	Current through the Feeder F3			cycles
			Nominal Current (kA)	Fault Current (kA _{rms})	Fault Detection Time (ms)	
F3	No Wind Power	LG	0.16	2.30	603.7	30.185
	3 MW Wind Power	LG	0.16	2.28	614	30.7
	6 MW Wind Power	LG	0.16	2.27	614	30.7

The magnitudes of the voltage drops at F3 during pre-fault, during fault and post-fault are shown in table 4.22. With 3MW wind power, the voltage drop on F3 is only 10.56% of the pre-fault voltage as compare to 17.08% voltage drop without wind turbine. In case of 6MW wind power capacity in the distribution system, the voltage drop on the bus will reduce to 10.22% of the pre-fault voltage.

Table 4.22 Magnitude of Voltage dips and circuit breaker tripping time at F3 for a pre-fault, during fault and post-fault when a fault is applied at the end of the feeder F3.

Fault Location	Wind Power Capacity	Fault Type	Voltage across F3 [p.u]			Fault detection Time (ms)
			Pre- Fault	During Fault	Post-fault	
F3	No Wind Power	LG	0.98	0.80	0.99	603.7
	3 MW Wind Power	LG	0.99	0.89	1.02	614
	6 MW Wind Power	LG	1.0	0.90	1.02	614

The magnitude of voltage dip at F3 and rest of the other feeders when a line to ground fault is applied at the end of the feeder is shown in figure 4.38.

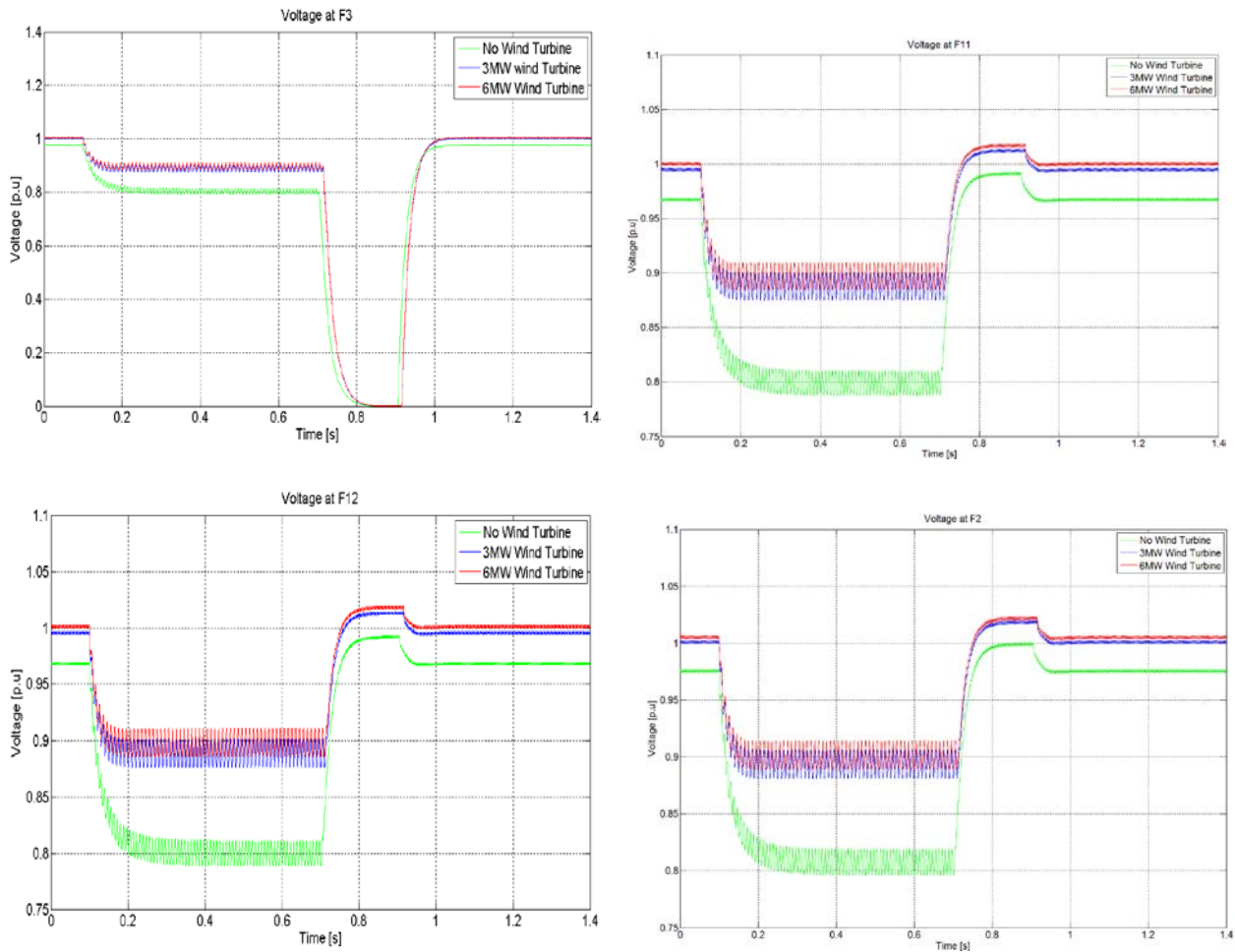


Figure 4.38: Magnitude of voltage dips when a line to ground fault is applied at F3

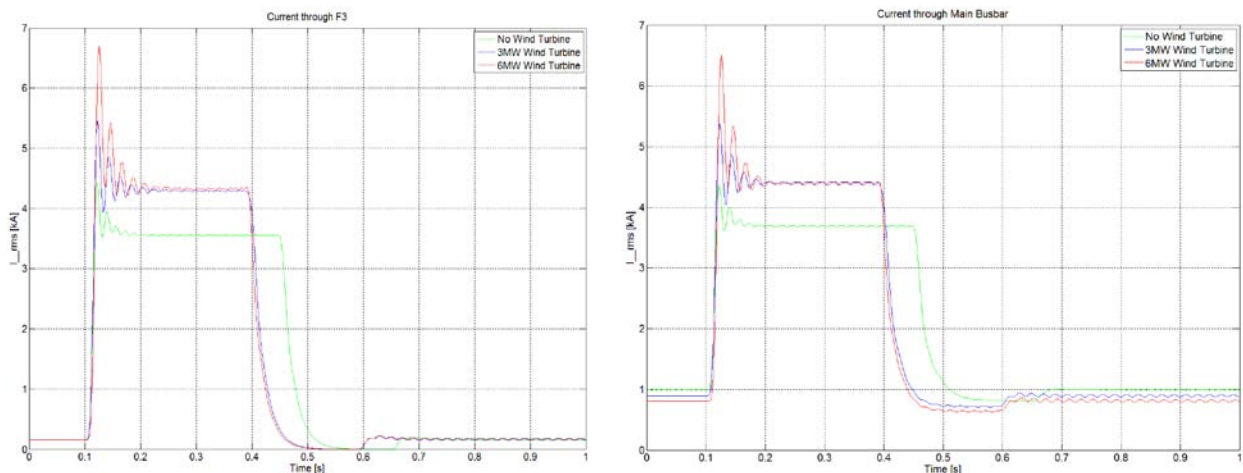
Three phase to ground fault at F3

When feeder F3 is subjected to three phase to ground fault as shown in table 4.23.

Table 4.23 Magnitudes of the fault currents at F3 when 3MW and 6MW wind turbine are attached at F12 and the time taken by the protection system to detect the fault.

Fault Location	Wind Power Capacity	Fault Type	Current through the Feeder F3			cycles
			Nominal Current (kA)	Fault Current (kA_rms)	Fault Detection Time (ms)	
F3	No Wind Power	LLLG	0.16	3.56	348.6	17.43
	3 MW Wind Power	LLLG	0.16	4.28	292.4	14.62
	6 MW Wind Power	LLLG	0.16	4.34	288.1	14.40

From table 4.23, it can be seen that the magnitude of the nominal current remains the same because of constant current load. By comparing result of table 4.19, it can be seen that the magnitude of nominal current of F2 is higher than the magnitude of F3. During fault the magnitude of F3 fault current is higher than the magnitude of fault current at F2 because of constant current load and small distance of F3 load from the main bus bar. Thus the circuit breaker of F3 detects the fault more quickly as compared to the fault at F2. Figure 4.39 shows the magnitudes of fault currents when F3 is subjected to a three phase to ground fault.



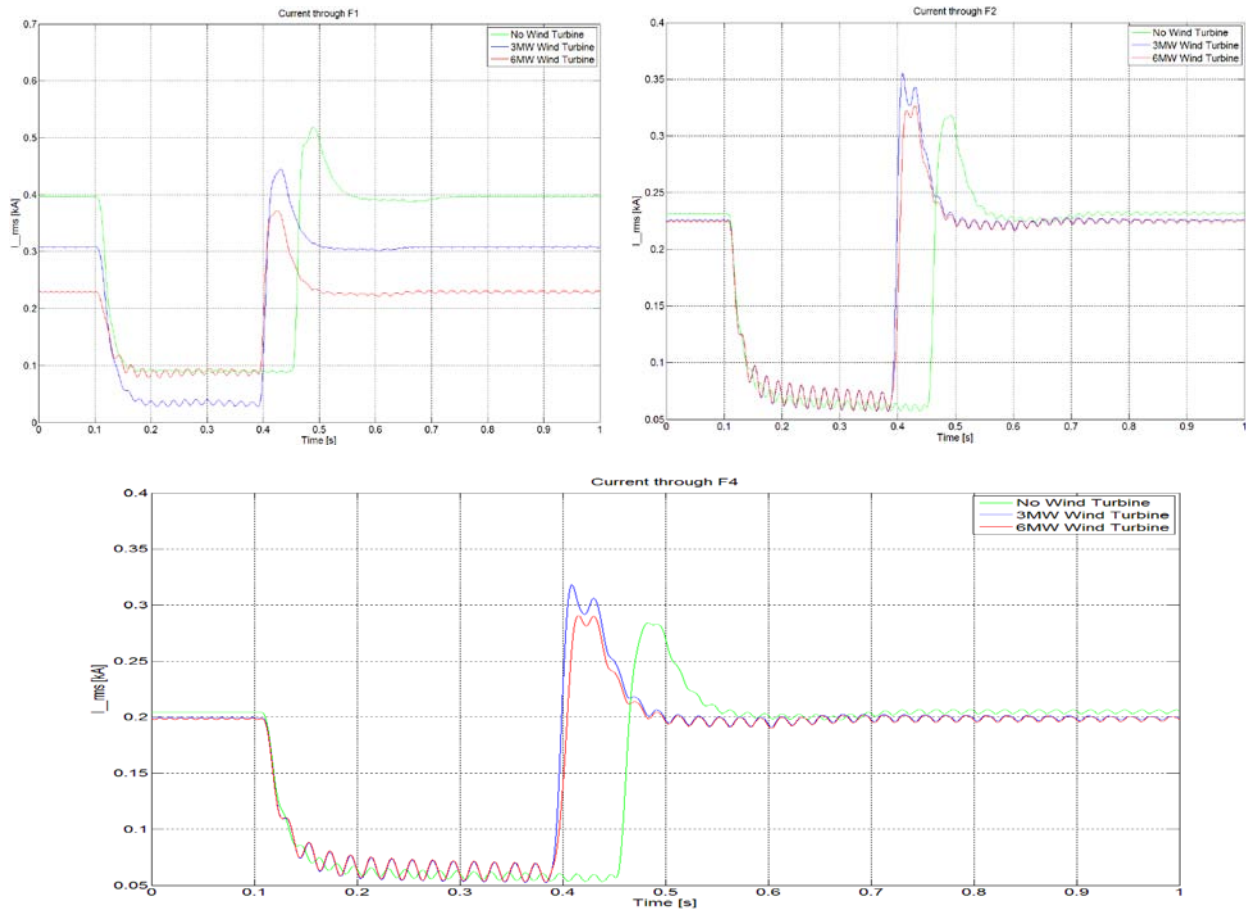


Figure 4.39: Magnitude of three phases to ground fault at F3 with 3MW and 6MW wind turbine installed at feeder F12.

The magnitudes of voltage drops at F2 during pre-fault, during fault and post-fault are shown in table 4.24.

Table 4.24: Magnitude of Voltage dips and circuit breaker tripping time at F3 for a pre-fault, during fault and post-fault when a fault is applied at the end of the feeder F3.

Fault Location	Wind Power Capacity	Fault Type	Voltage across F3 [p.u]			Fault detection Time (ms)
			Pre- Fault	During Fault	Post-fault	
F3	No Wind Power	LLLG	0.97	0.15	0.99	348.6
	3 MW Wind Power	LLLG	0.99	0.15	1.02	292.4
	6 MW Wind Power	LLLG	1.0	0.15	1.02	288.1

With 3 MW wind power capacity, the voltage drop on F2 is only 84.79% of the pre-fault voltage as compare to 84.72% voltage drop without wind turbine. In case of 6 MW wind power capacity installed in the distribution system, the voltage drop on the bus will reduce to 84.79% of the pre-fault voltage. The voltage drop of the line increases as the

converter is not able to handle the voltage drop of the three phase fault as a result the inner current controller saturates. When the inner converter saturates the outer converter loses its control, as a result the converter will not be able to limit the current and voltage, which cause an increase of fault current. Figure 4.40 shows the pre-fault, during fault and the post-fault voltages when a three phase fault is applied at F3.

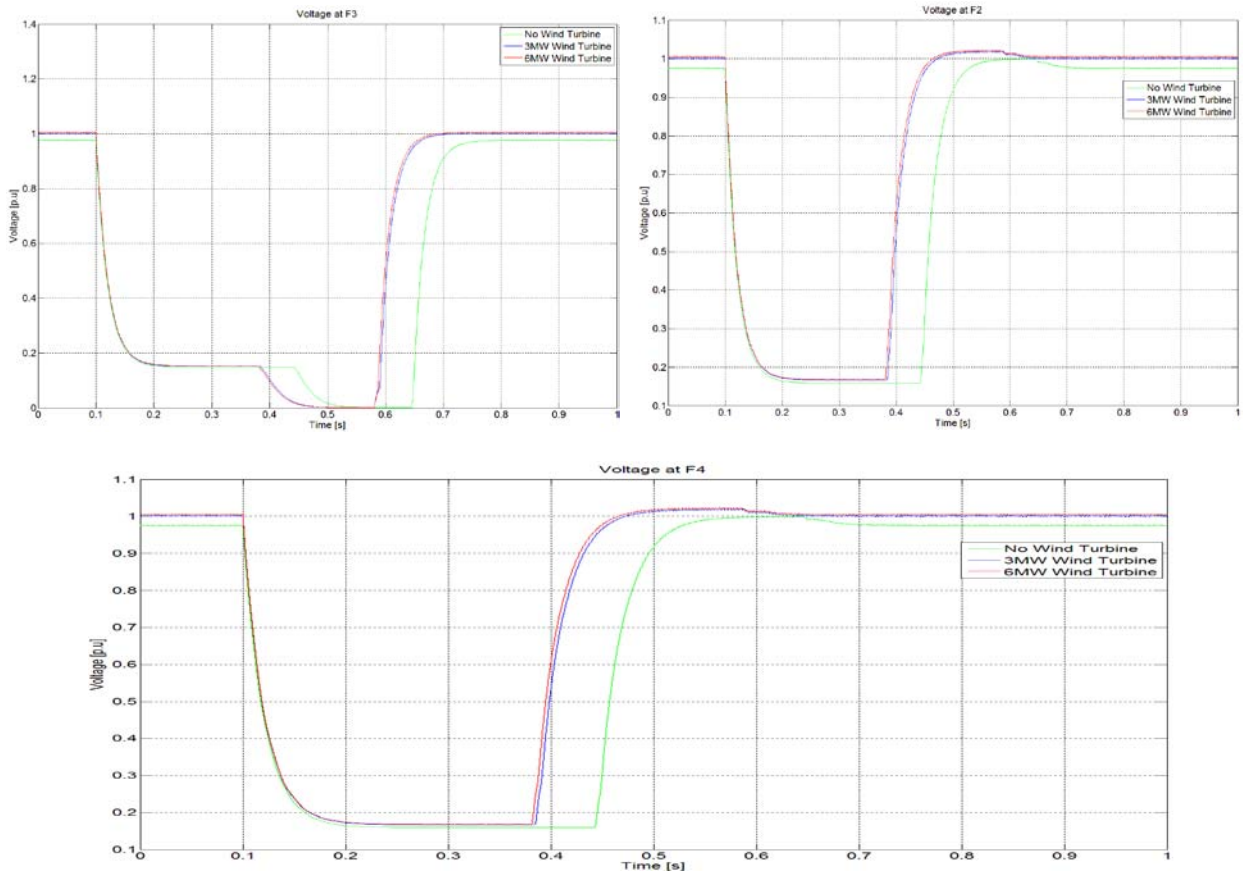


Figure 4.40: Magnitude of voltage dips when a three phase to ground fault is applied at F3

Single line to Ground Fault at F4

As feeder F4 is the shortest feeder in the network thus if a fault occurs on F4, the magnitude of the fault current will be higher as compared to the rest of the other feeders in the network. From figure 4.42, it is observed that when F4 is subjected to a fault, the circuit breaker fault detection time increases. As F4 is a constant power load, thus with the addition of DG in the network which decreases the voltage drop in the network cause a decrease in the fault current and as a result the protection system fault detection time increases.

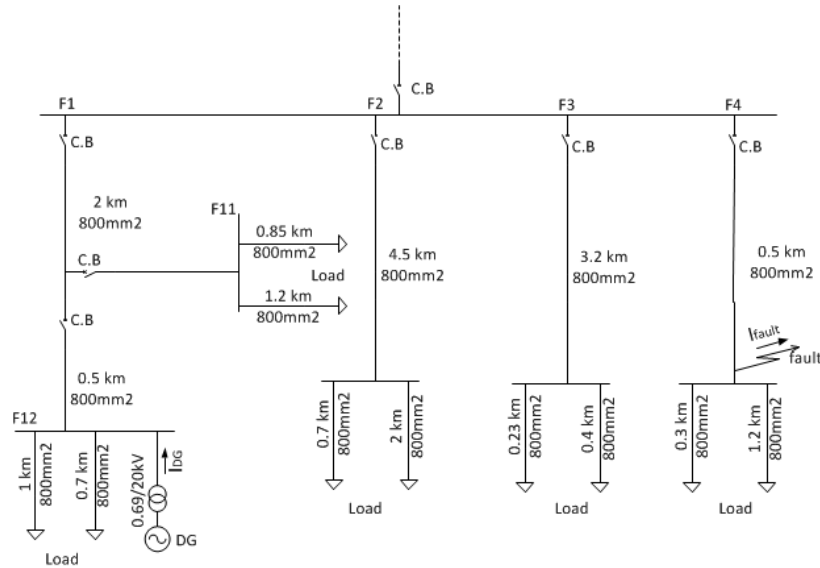


Fig 4.41: Single line diagram of the distribution system when a DG is attached at F12 and a fault is applied at F4 feeder.

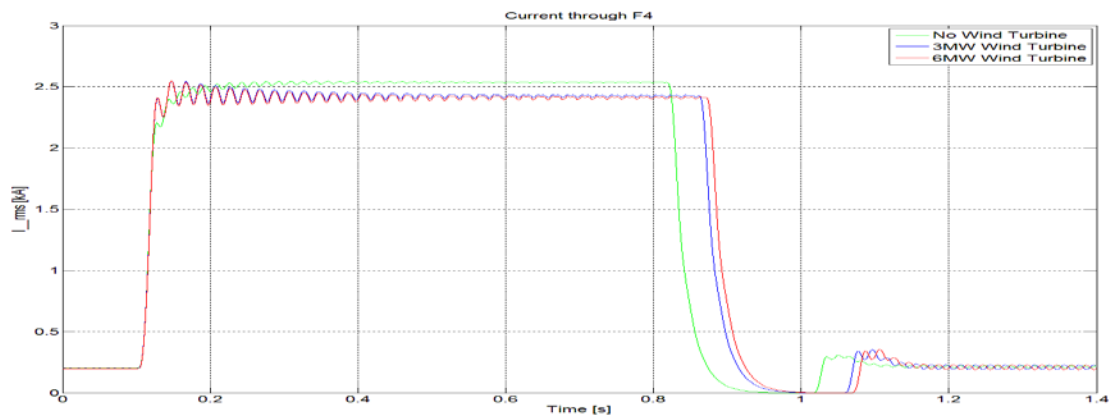


Figure 4.42: Magnitude of line to ground fault on Phase A at F4 with 3MW and 6MW wind turbine installed at feeder F12.

The nominal current of F4 approximately remains the same regardless of any DG in the distribution system. As shown in table 4.26, the magnitudes of the fault current increase as compared to line to ground fault at F3.

Table 4.25: Magnitude of Phase “A” fault current at F4 when 3MW and 6MW wind turbines are attached at F12 and the time taken by the protection system to detect the fault.

Fault Location	Wind Power Capacity	Fault Type	Current through the Feeder F4			cycles
			Nominal Current (kA _{rms})	Fault Current (kA _{rms})	Fault Detection Time (ms)	

F4	No Wind Power	LG	0.21	2.54	718.8	35.94
	3 MW Wind Power	LG	0.20	2.43	762	38.1
	6 MW Wind Power	LG	0.19	2.39	772.5	38.62

The magnitude of the fault current of phase “A” for rest of the feeders when a line to ground fault is applied at phase “A” of F4 are shown in figure 4.43.

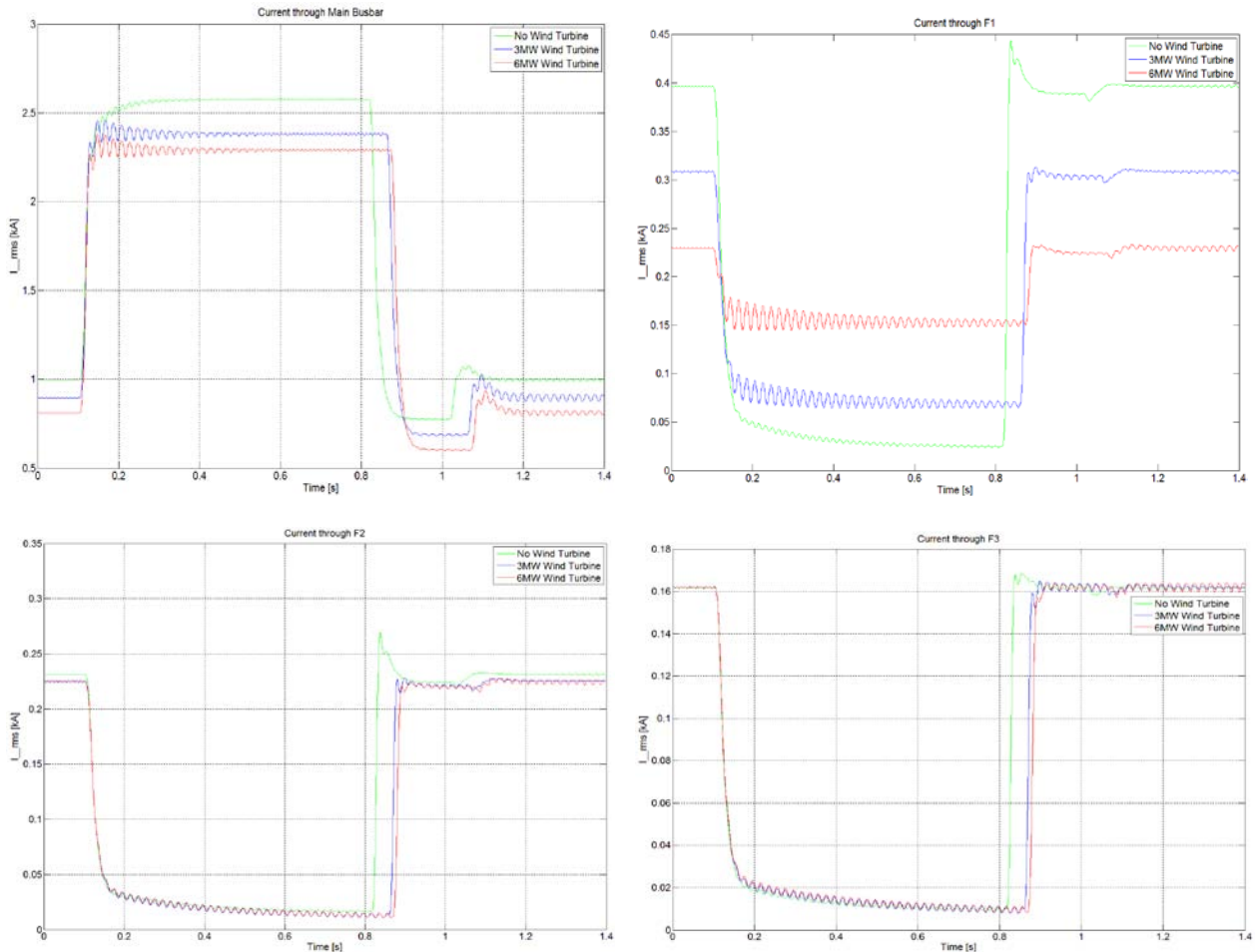


Figure 4.43: Magnitude of line to ground fault on Phase “A” at F4 with 3MW and 6MW wind turbine installed at F12.

The magnitude of the voltage dip at F4 during pre-fault, during fault and post-fault are shown in table 4.26. With 3MW wind power, the voltage drop on F3 is only 11.01% of the pre-fault voltage as compare to 18.26% voltage drop without a wind turbine. In case of 6MW wind power capacity in the distribution system, the voltage drop on the bus will reduced to 10.73% of the pre-fault voltage. Table 4.26 shows the pre-fault, during fault and the post-fault voltages when a line to ground fault is applied at F4.

Table 4.26: Magnitude of Voltage dips and circuit breaker tripping time at F4 for a pre-fault, during fault and post-fault when a fault is applied at the end of the feeder F4.

Fault Location	Wind Power Capacity	Fault Type	Voltage across F4 [p.u]			Fault detection Time (ms)
			Pre- Fault	During Fault	Post-fault	
F4	No Wind Power	LG	0.98	0.80	1.0	718.8
	3 MW Wind Power	LG	0.99	0.88	1.02	762
	6 MW Wind Power	LG	1.0	0.89	1.03	772.5

The magnitude of voltage dips at F4 and rest of the other feeders when a single line to ground fault is applied at the end of the feeder F4 are shown in figure 4.44.

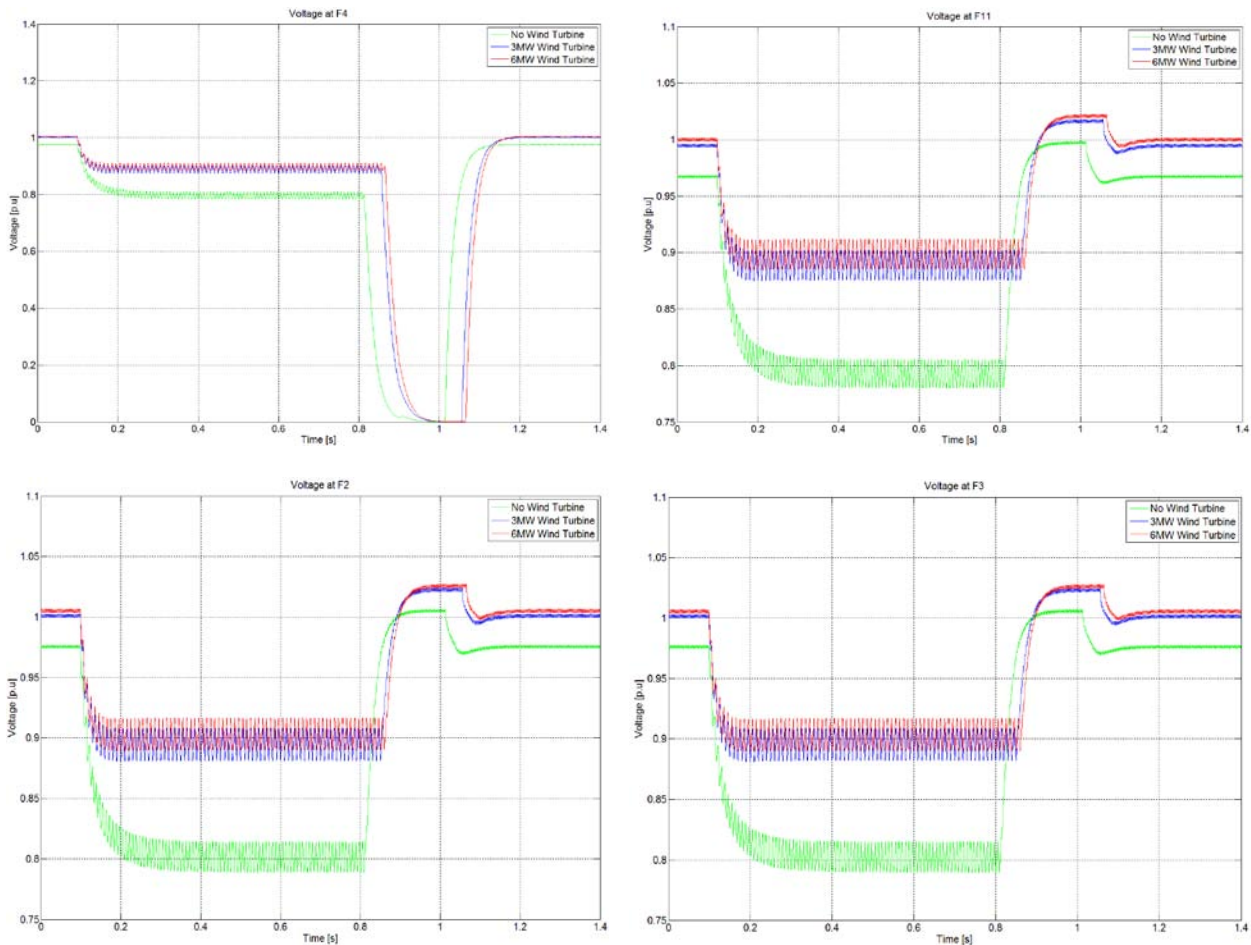


Figure 4.44: Magnitude of voltage dips when a Line to ground fault is applied at F4

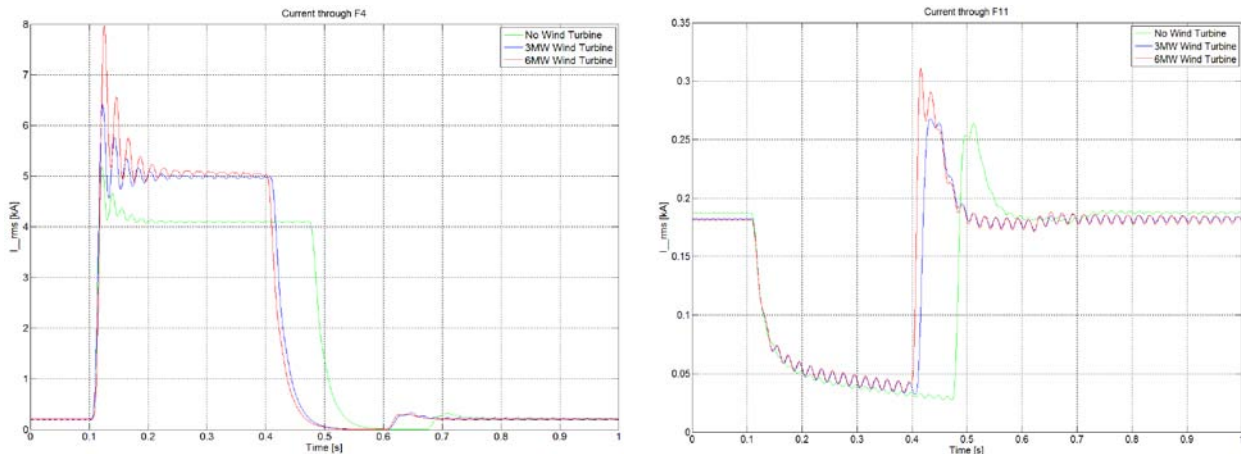
Three phase to ground fault at F4

When F4 is subjected to a three phase fault the magnitudes of fault current increase, as a result the tripping time of the circuit breaker decreases. The wind turbine also contributes to the fault to an extent depending upon the capacity of the converter and the turbine. Table 4.27 yield the result of a three phase to ground fault at the end of feeder F4. As the wind turbine is attached at F12, thus the nominal current of the feeder F4 will approximately remain the same. A small decrease in the nominal current occurs because of the characteristic of constant power load as explained in the previous sections.

Table 4.27: Magnitude of three phase fault current at F4 when 3MW and 6MW wind turbine are attached at F12 and the time taken by the protection system to detect the fault.

Fault Location	Wind Power Capacity	Fault Type	Current through the Feeder F4			cycles
			Nominal Current (kA_rms)	Fault Current (kA_rms)	Fault Detection Time (ms)	
F4	No Wind Power	LLLG	0.21	4.10	373.8	18.69
	3 MW Wind Power	LLLG	0.20	4.97	308.8	15.44
	6 MW Wind Power	LLLG	0.19	5.06	300.8	15.04

By comparing the results with table 4.23 the magnitude of the fault current increases. Figure 4.45 shows the magnitude of fault current at F4 and rest of the other feeders.



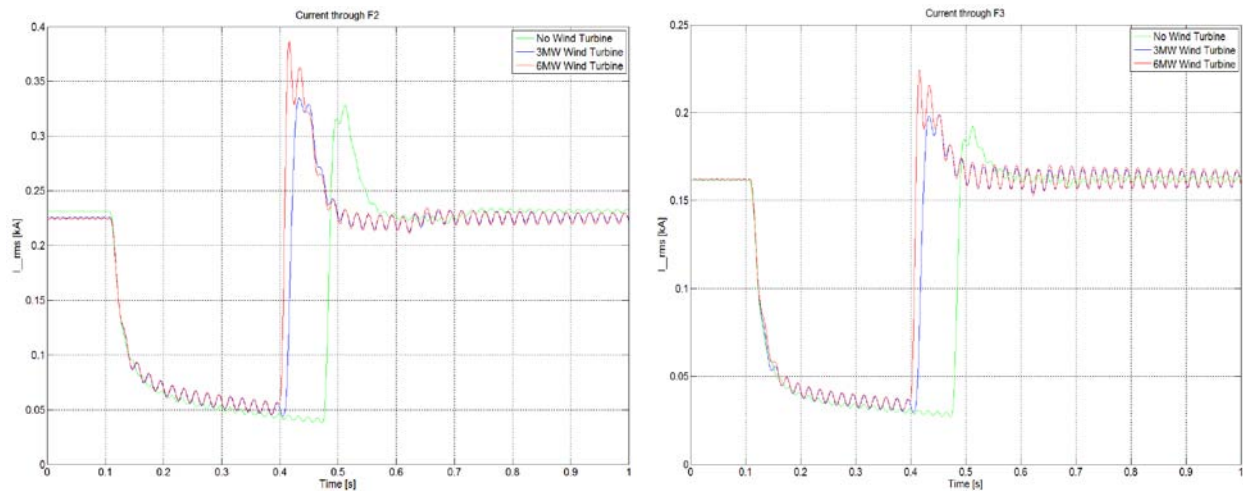


Figure 4.45: Magnitude of fault current of Phase “C” when F4 is subjected to three phase to ground fault with 3 MW and 6 MW wind turbine installed at F12.

The magnitude of pre-fault, during fault and the post-fault voltage dips are shown in table 4.28. It is observed that during three phases to ground fault the magnitude of the voltage dip is much more at F4 as compared to the rest of the other feeders in the network. Since F4 is the shortest feeder thus if a fault occur on F4 it will cause a deep voltage dip on the whole network as shown in case of three phase fault at F4. It is observed that the magnitude of the voltage dip is 97% of the pre-fault voltage in all the three cases as depicted in table 4.28.

Table 4.28: Magnitude of Voltage dips and circuit breaker tripping time at F2 for a pre-fault, during fault and post-fault voltages when a fault is applied at the end of the feeder F2.

Fault Location	Wind Power Capacity	Fault Type	Voltage across F4 [p.u]			Fault detection Time (ms)
			Pre- Fault	During Fault	Post-fault	
F4	No Wind Power	LLLG	0.98	0.03	1.0	373.8
	3 MW Wind Power	LLLG	0.99	0.03	1.02	308.8
	6 MW Wind Power	LLLG	1.0	0.03	1.03	300.8

The magnitude of the voltage dip at F4 and rest of the other feeders are shown in figure 4.46. It can be seen that when a faulted area is removed from the network, the post-fault voltage of the network increases as shown in figure below.

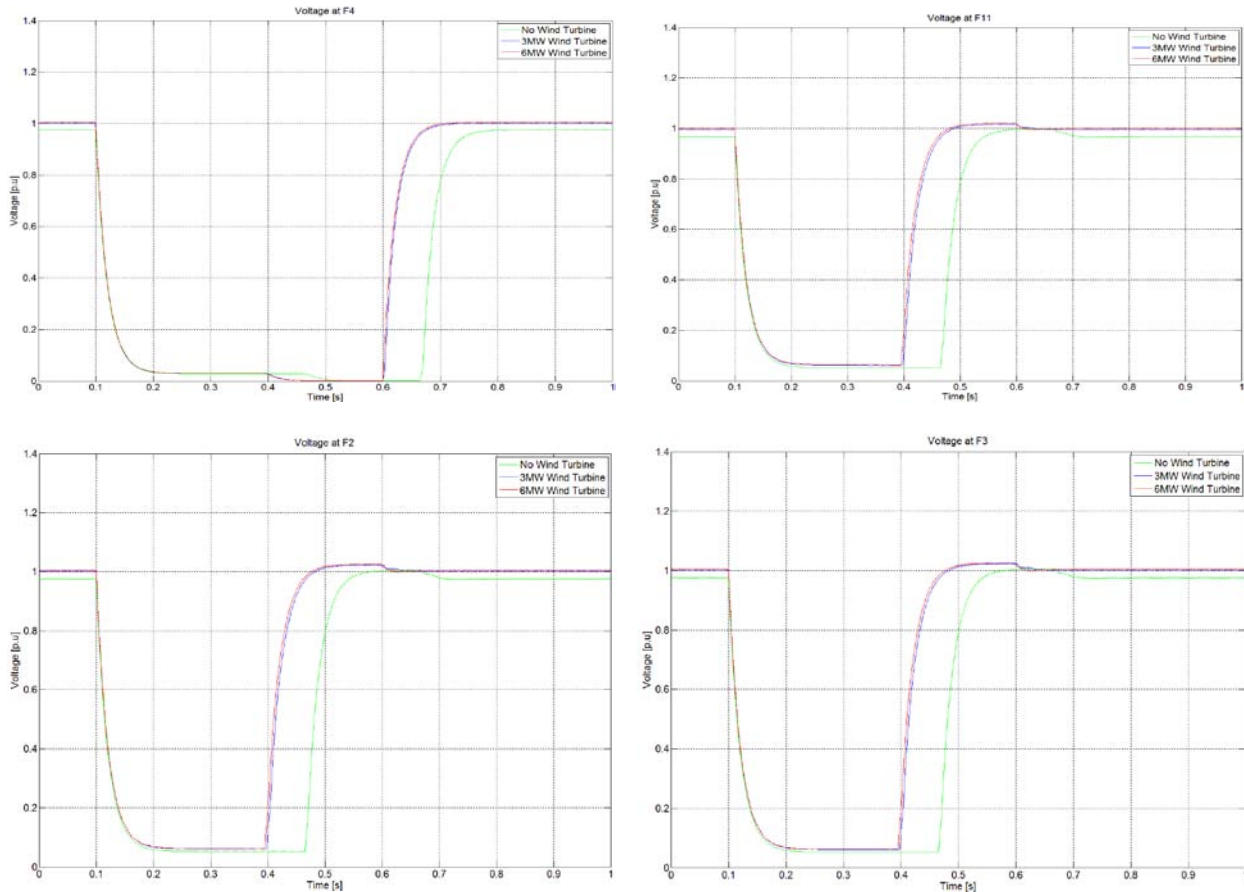


Figure 4.46: Magnitude of voltage dips when a three phase fault is applied at F4.

4.3.3. DG attached at Feeder F2

From the previous analysis, it is observed that the worst case occurs when a fault is applied on the feeder where the DG is attached as a result the magnitude of fault current decreases because of the contribution of DG current in the fault. As the magnitude of fault current decreases the circuit breaker will take longer time to detect the fault in the network. Thus in this section and the rest of other sections, the fault analysis is done only on those areas where the DGs are attached.

Single line to Ground Fault at F2

As F2 is the longest feeder in the network with 4.5km of cable. Thus the protection system will take longer time to detect any fault at F2 as compared to the rest of the other feeders in the network. From table 4.6 it is shown that the circuit breaker at F2 will take 1.0123s to detect the line to ground fault. In case when a DG is also attached at the same feeder, the circuit breaker detection time of the fault will be increased. The simulation with DG yield the following results

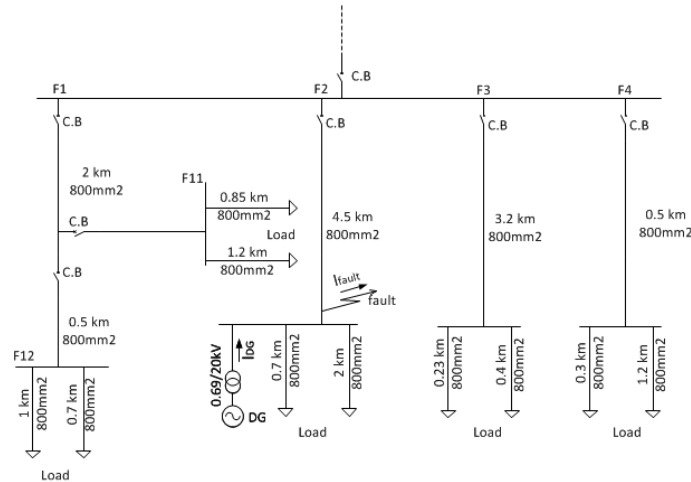


Fig 4.47: Single line diagram of the distribution system when a DG is attached at F2 and a fault is applied at F2.

Table 4.29: Magnitude of fault currents at F2 when 3MW and 6MW wind turbines are attached at F2 and the time taken by the protection system to detect the fault.

Fault Location	Wind Power Capacity	Fault Type	Current through the Feeder F2			cycles
			Nominal Current (kA)	Fault Current (kA _{rms})	Fault Detection Time (ms)	
F2	No Wind Power	LG	0.23	2.31	1028	51.4
	3 MW Wind Power	LG	0.22	2.23	1083	54.15
	6 MW Wind Power	LG	0.21	2.13	1164	58.2

From table 4.29, it can be seen that the fault current is reduced by DG which is contributing current in the opposite direction of fault current (to grid), which as a result decreased the fault current of F2 and increases the fault detection time of the circuit breaker. By comparing Table 4.29 with Table 4.17, it can be seen that the magnitude of the fault current is decreased due to the effect of DG. The magnitude of fault current at F2 and rest of the other feeders are shown in figure 4.48.

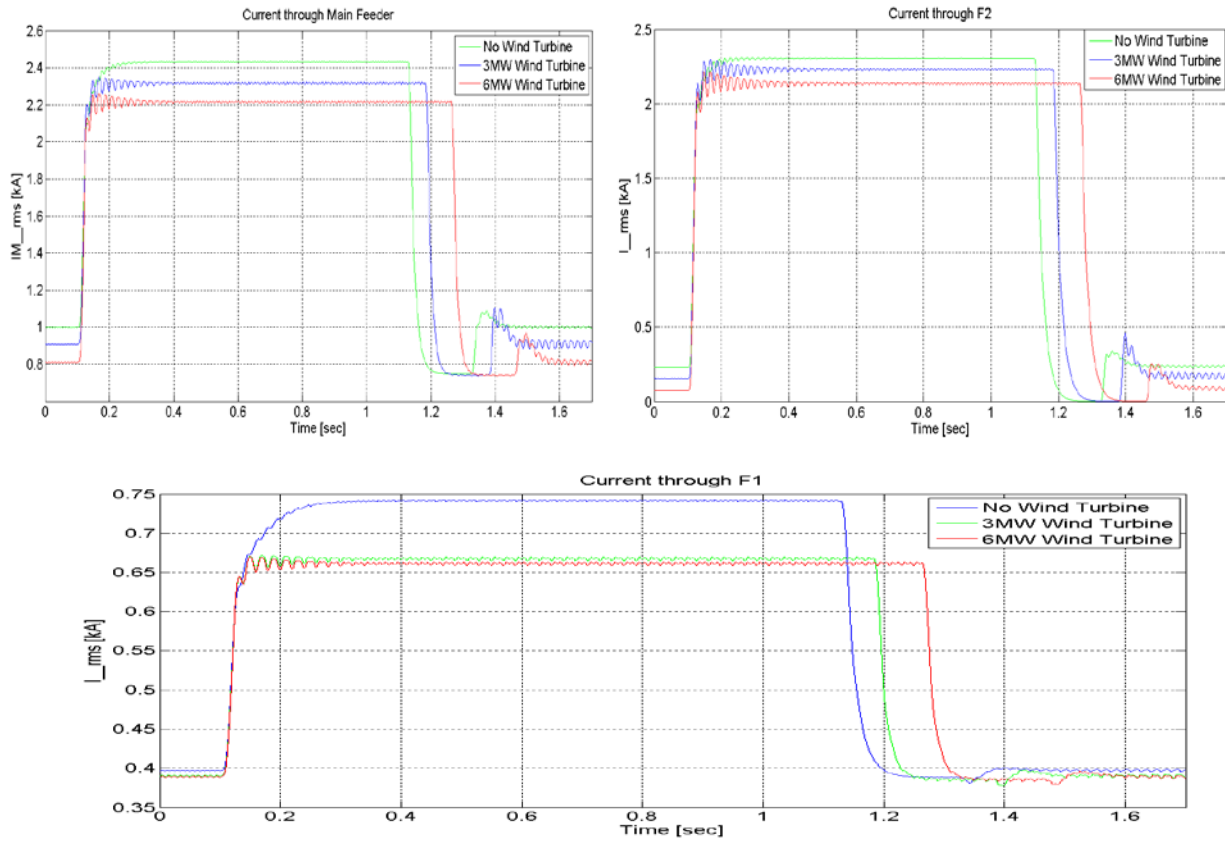


Figure 4.48: Magnitude of line to ground fault at F2 with 3MW and 6MW wind turbine installed at feeder F2.

The magnitudes of the voltage drops at F2 during pre-fault, during fault and post-fault are shown in table 4.30. With 3 MW wind power capacity, the voltage drop on F2 is only 11.7% of the pre-fault voltage as compared to 18% voltage drop without wind turbine. In case of 6 MW wind power capacity installed in the distribution system, the voltage drop on the bus will reduce to 10.22% of the pre-fault voltage. Table 4.30 shows the pre-fault, during fault and the post-fault voltages and the tripping time of the circuit breaker.

Table 4.30: Magnitude of Voltage dips and circuit breaker tripping time at F2 for a pre-fault, during fault and post-fault voltages when a fault is applied at the end of the feeder F2.

Fault Location	Wind Power Capacity	Fault Type	Voltage at F2 [p.u]			Fault detection Time (ms)
			Pre- Fault	During Fault	Post-fault	
F2	No Wind Power	LG	0.98	0.80	1.01	1028
	3 MW Wind Power	LG	0.99	0.87	1.02	1083
	6 MW Wind Power	LG	1.0	0.90	1.02	1164

The magnitude of voltage dip at F2 and rest of the other feeders are shown in figure 4.49. It can be seen that when a fault load is removed from the network, the post-fault voltage of the network increases.

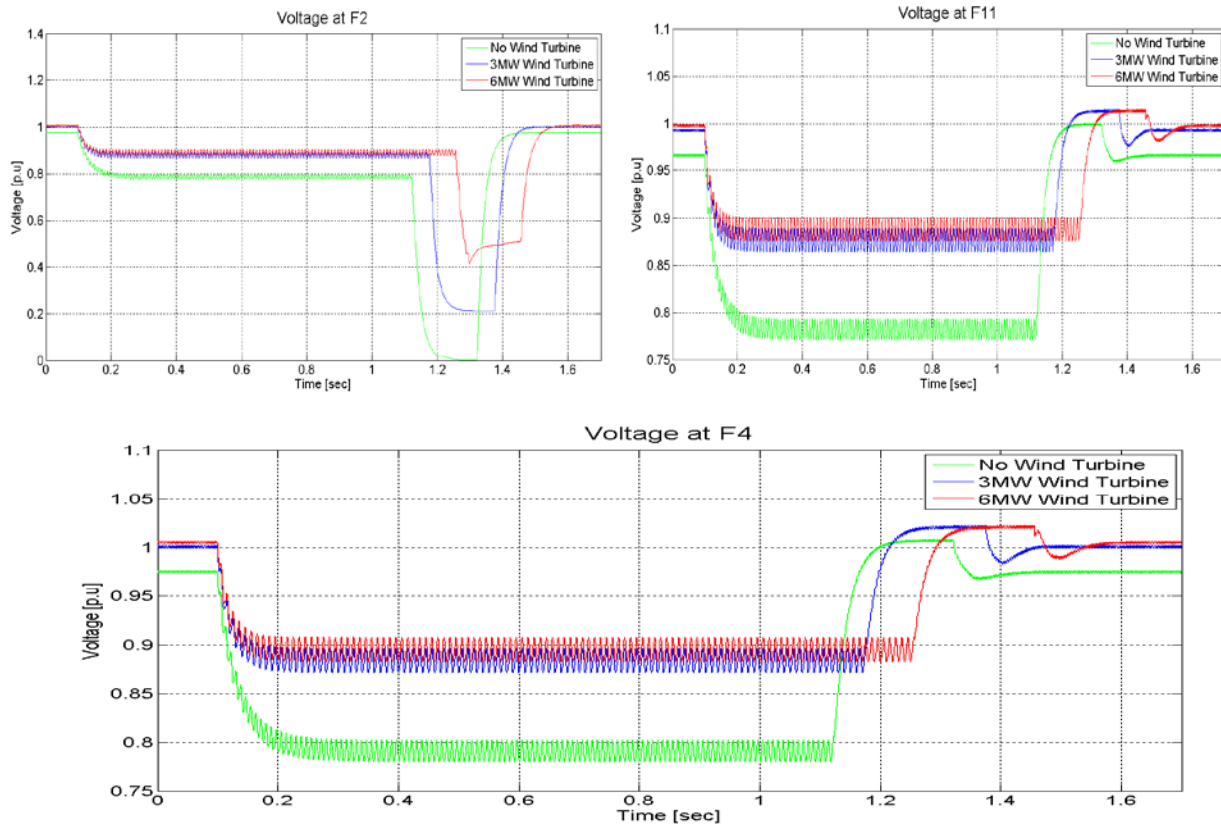


Figure 4.49: Magnitude of voltage dips when a line to ground fault is applied at F2

It can be seen that the circuit breaker will take 1.028sec to detect the fault at F2 in case when there is no wind power installer at F2. The voltage dip of the line increases when there is no wind power installed on the network. With the addition of wind power the voltage dip of the line decreases as shown in the above figure.

Three phase to ground fault at F2

When feeder F2 is subjected to three phase to ground fault, the wind turbine will also contribute in the fault. During three phase fault the voltage of the network goes to zero as a result the turbine active power will go to zero and only provide reactive power in order to bring the voltage of the network close to 1 p.u. As the voltage dip is deep thus the turbine will not be able to recover the voltage as a result the converter will take more reactive power from the grid in order to cover it loss, which is the cause of the increase of fault current in three phase fault. Table 4.31 yield the result of a three phase to ground fault.

Table 4.31: Magnitude of fault current at F2 when 3 MW and 6 MW wind turbine are attached at F2 and the time taken by the protection system to detect the fault.

Fault Location	Wind Power Capacity	Fault Type	Current through the Feeder F2			cycles
			Nominal Current (kA_rms)	Fault Current (kA_rms)	Fault Detection Time (ms)	
F2	No Wind Power	LLLG	0.23	3.36	554	27.7
	3 MW Wind Power	LLLG	0.14	4.0	441.3	22
	6 MW Wind Power	LLLG	0.07	4.06	421.07	21.07

Figure 4.50 shows the magnitudes of the fault currents at F2 and the rest of the other feeders. It is observed that the nominal current of the network decreases by the injection of wind turbine current in the same feeder.

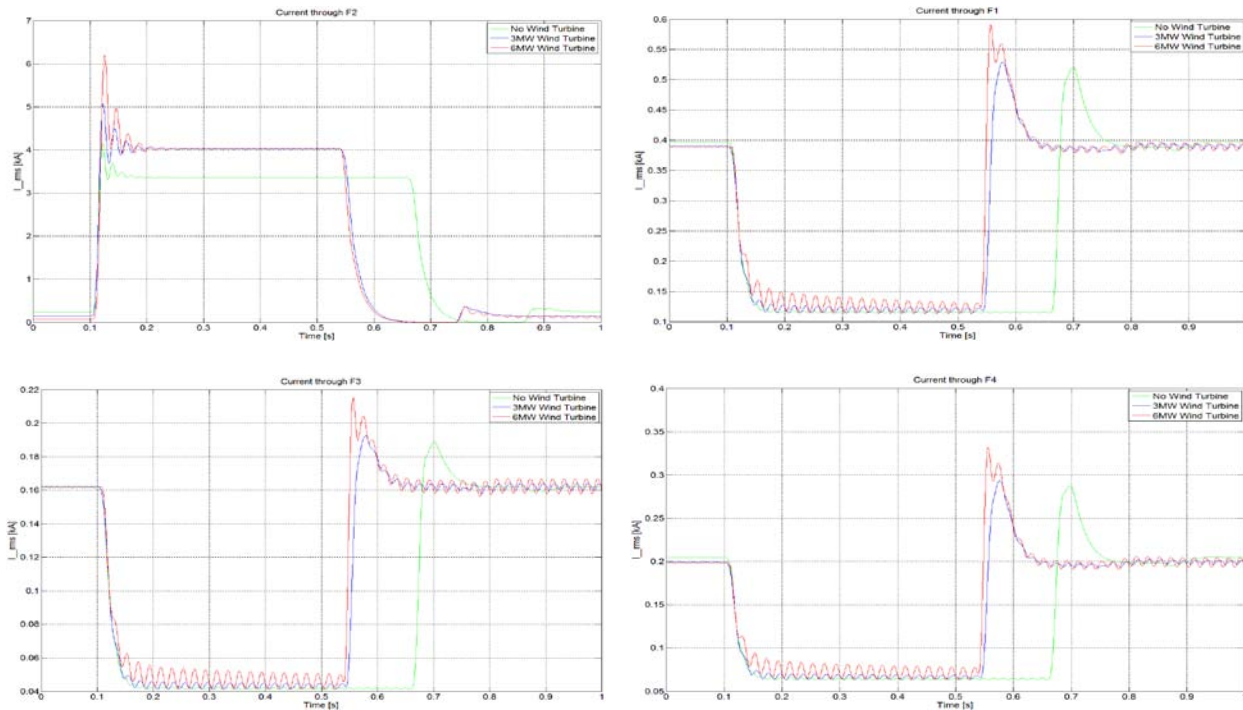


Figure 4.50: Magnitude of three phases to ground fault at F2 with 3 MW and 6 MW wind turbine installed at feeder F2.

The magnitudes of the voltage drops at F2 during pre-fault, during fault and post-fault are shown in table 4.32. It is observed that during three phase fault the magnitude of

voltage dip is 80% of the pre-fault voltage in all the three cases. The main reason is that as the feeder F2 is the longest feeder in the network thus during three phase fault which is the severe fault in the network, the wind turbine cannot handle the fault in order to bring the voltage back to its pre-fault condition, thus as a result the net voltage drop on the line remain the same. Table 4.32 shows the pre-fault, during fault and the post-fault voltages and the tripping time of the circuit breaker.

Table 4.32 Magnitude of Voltage dips and circuit breaker tripping time at F2 for a pre-fault, during fault and post-fault voltages when a fault is applied at the end of the feeder F2.

Fault Location	Wind Power Capacity	Fault Type	Voltage across F2 [p.u]			Fault detection Time (ms)
			Pre- Fault	During Fault	Post-fault	
F2	No Wind Power	LG	0.98	0.20	1.01	554
	3 MW Wind Power	LG	1.0	0.20	1.02	441.3
	6 MW Wind Power	LG	1.01	0.20	1.02	413.9

The magnitude of voltage dip at F2 and rest of the other feeders are shown in figure 4.51. It can be seen that when a fault area is remove from the network by disconnection of load through circuit breaker, the post-fault voltage of the network increases as shown in figure below.

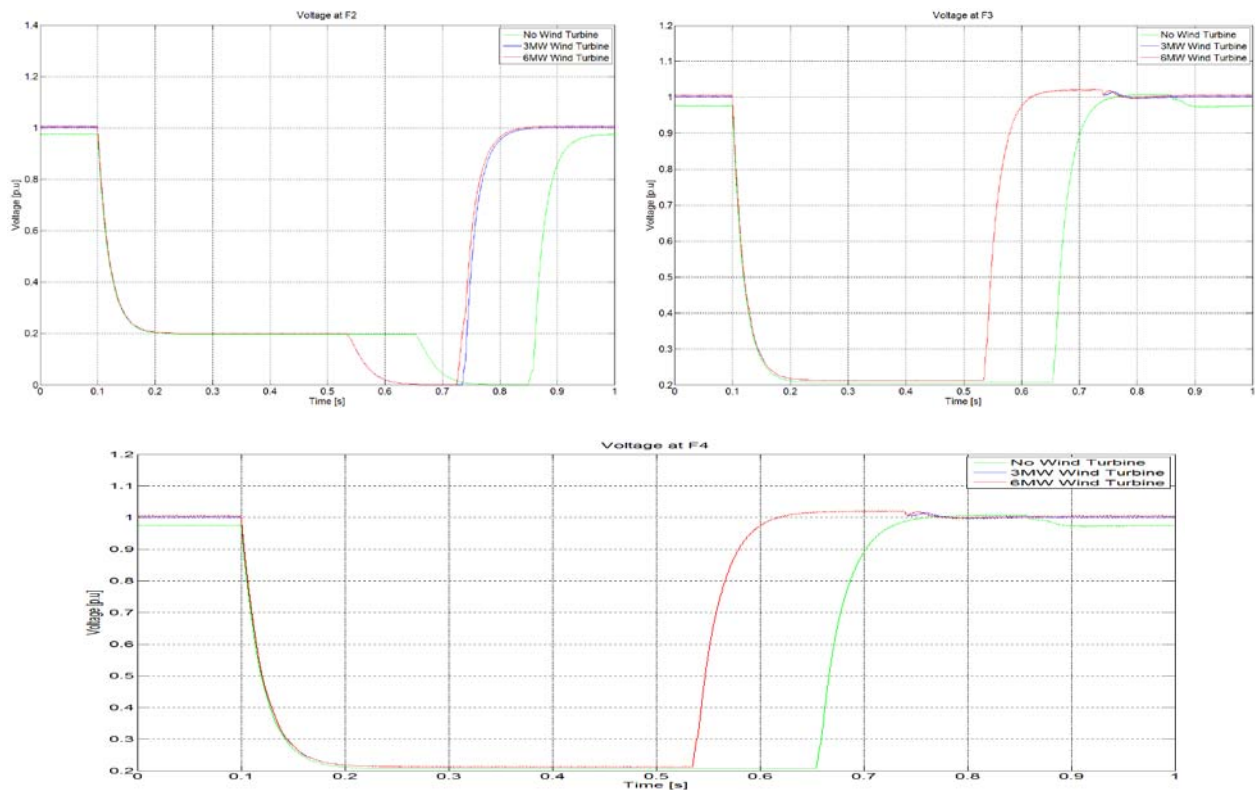


Figure 4.51: Magnitude of voltage dips when a line to ground fault is applied at F2

4.3.4. DG attached at Feeder F3

Single line to Ground Fault at F3

The load at F3 is a constant current load with a total cable length of 3.2 km from the main bus bar. When F3 is subjected to a line to ground fault at phase A, the magnitude of current at phase “A” increases. As a circuit breaker is installed on each phase of the line, thus the circuit breaker will take 612 ms to detect a fault on the line. In case of DG attached at the same feeder F3, the magnitude of nominal current and fault current of F3 decreases with the same magnitude and as a result the circuit breaker fault detection time increases.

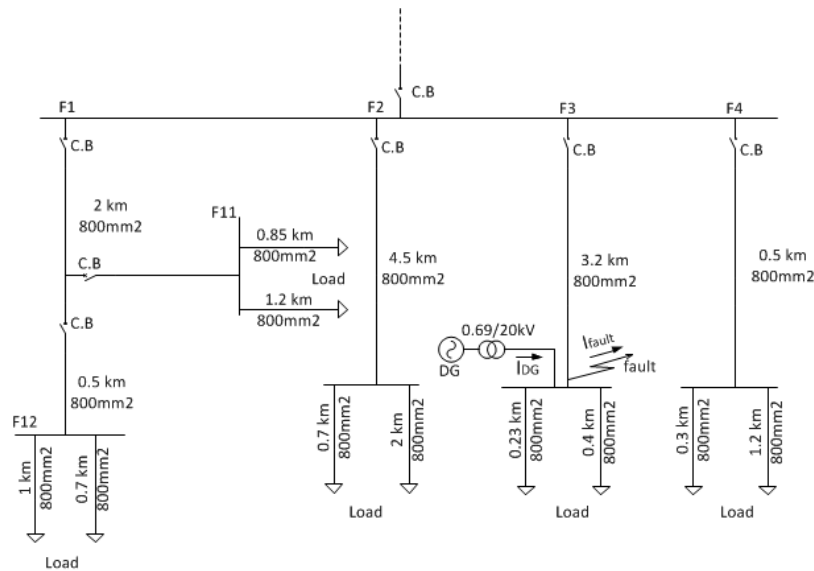


Fig 4.52: Single line diagram of the distribution system when a DG is attached at F3 and a fault is applied closed to feeder F3.

As F3 is the second longest feeder in the network with 3.2 km of cable. Thus the protection system will also take longer time to detect any fault at F3 as compare to the feeders F1 and F4 in the network. From table 4.5 it is shown that the circuit breaker at F3 will take 1.0123s to detect the line to ground fault. In case when a DG is also attached at the same feeder, the circuit breaker detection time of the fault will be increased. The simulation with DG yields the following results as shown in Table 4.34. The magnitude of fault current and the nominal current decreased because of the contribution of DG current in opposite of the current coming from the grid. As DG is installed on each feeder with a maximum of 50% of the load capacity, thus F3 is less dependent on grid. Table 4.33 shows the magnitude of nominal current, fault current and the circuit breaker fault detection time when a line to ground fault is applied at F3 phase A.

Table 4.33 Magnitude of line to ground faults at phase “A” of F3 with 3MW and 6MW wind turbine are attached at F3 and the time taken by the protection system to detect the fault.

Fault Location	Wind Power Capacity	Fault Type	Current through the Feeder F3			cycles
			Nominal Current (kA)	Fault Current (kA _{rms})	Fault Detection Time (ms)	
F3	No Wind Power	LG	0.16	2.30	612	30.6
	3 MW Wind Power	LG	0.08	2.20	646.7	32.3
	6 MW Wind Power	LG	0.05	2.12	682.4	34.14

The result of Table 4.33 is yield from figure 4.53 which shows the magnitudes of the fault currents at F3 and the rest of the other feeders.

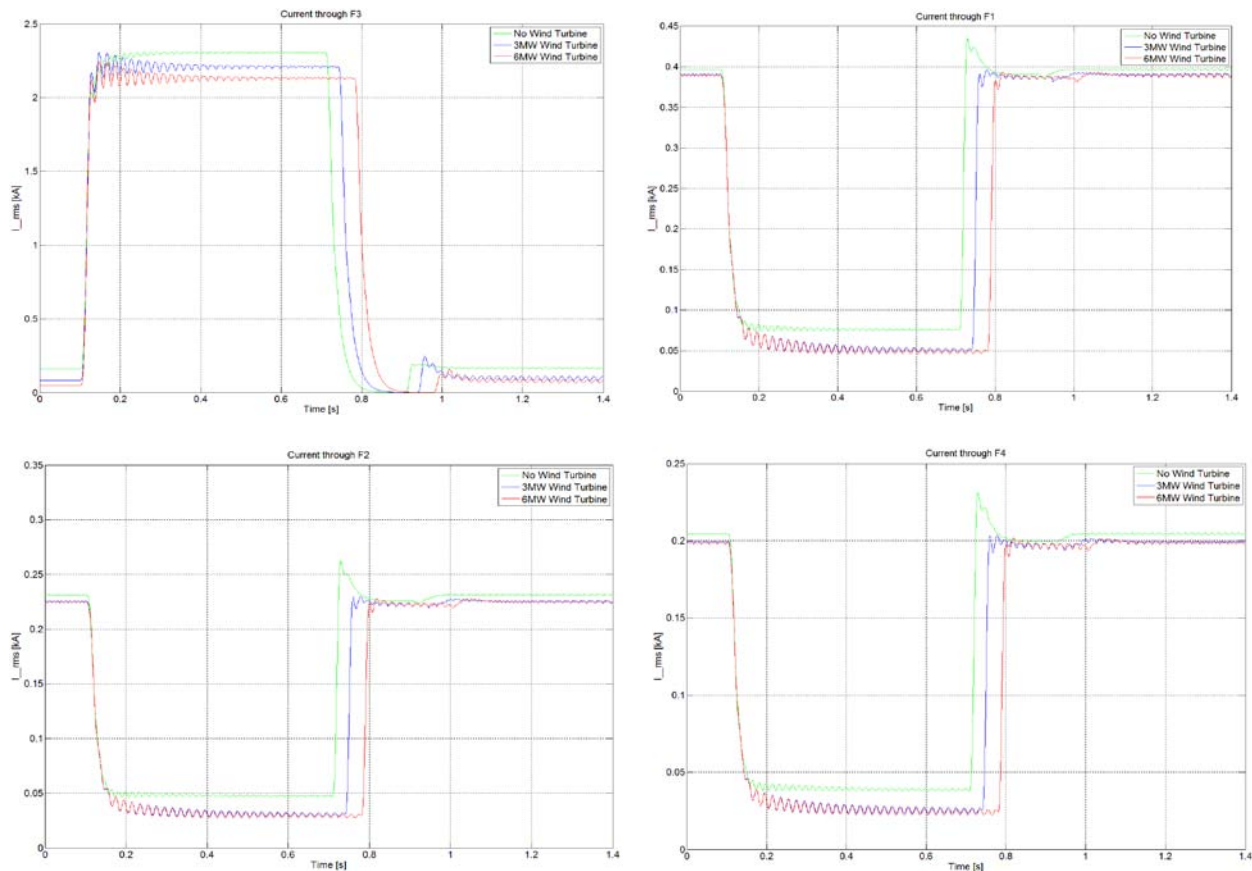


Figure 4.53: Magnitude of line to ground fault current at phase A of F3 with 3MW and 6MW DG installed at the same feeder.

The magnitudes of the voltage dips at F3 during pre-fault, during fault and post-fault are shown in table 4.34 . With 3MW wind power capacity installed at F3, the voltage drop on

is only 12% of the pre-fault voltage as compare to 18.36% voltage drop without DG. In case of 6MW wind power capacity installed in the distribution system, the voltage drop on the bus will reduce to 9.9% of the pre-fault voltage. Table 4.34 shows the pre-fault, during fault and the post-fault voltages and the tripping time of the circuit breaker.

Table 4.34: Magnitude of Voltage dips and circuit breaker tripping time at F3 for a pre-fault, during fault and post-fault voltages when a fault is applied at the end of the feeder F3.

Fault Location	Wind Power Capacity	Fault Type	Voltage across F3 [p.u]			Fault detection Time (ms)
			Pre- Fault	During Fault	Post-fault	
F3	No Wind Power	LG	0.98	0.80	1.0	612
	3 MW Wind Power	LG	1.0	0.88	1.02	646.7
	6 MW Wind Power	LG	1.01	0.91	1.02	682.4

The magnitude of voltage dip at F3 and rest of the other feeders are shown in figure 4.54. It can be seen that with the addition of DG in the network, the magnitude of voltage dip decreases.

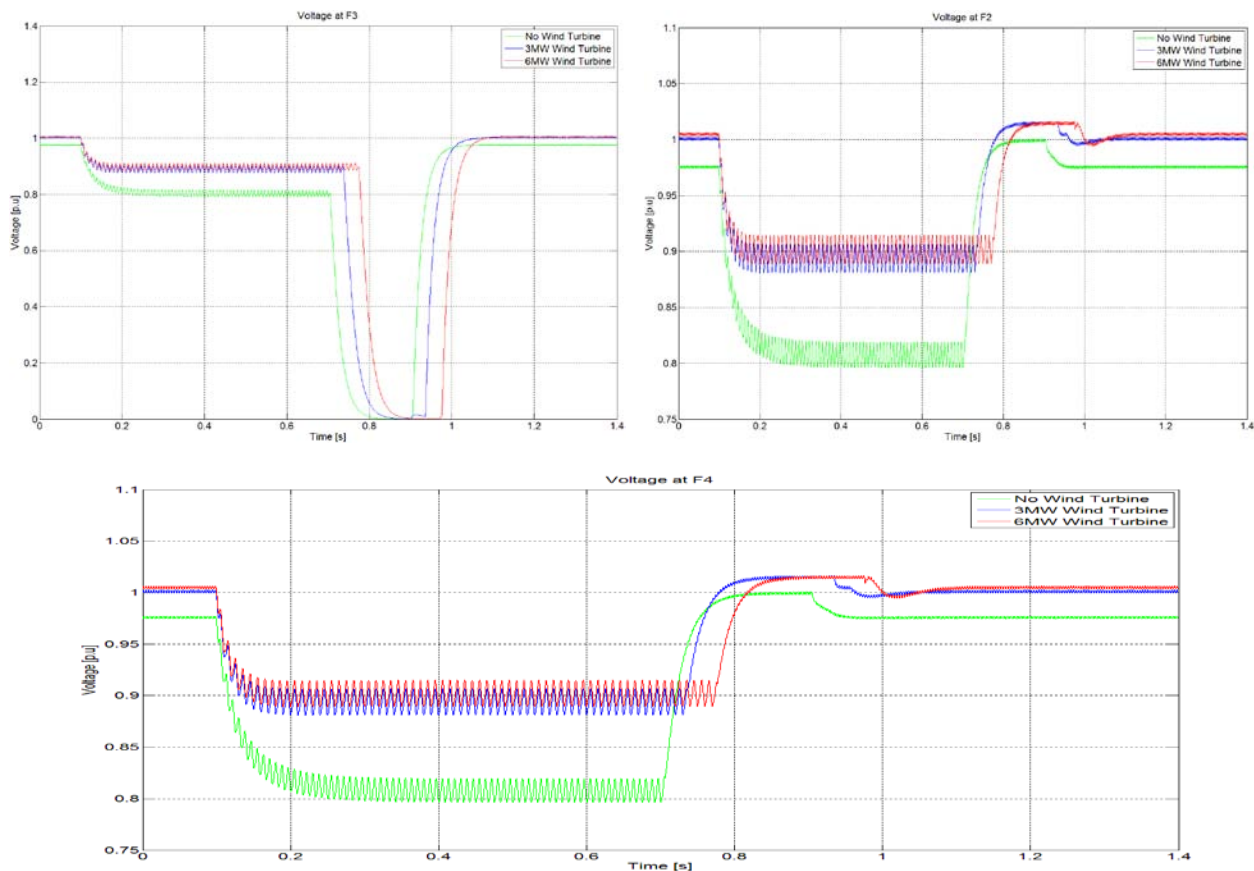


Figure 4.54: Magnitude of voltage dips when a line to ground fault is applied at F3

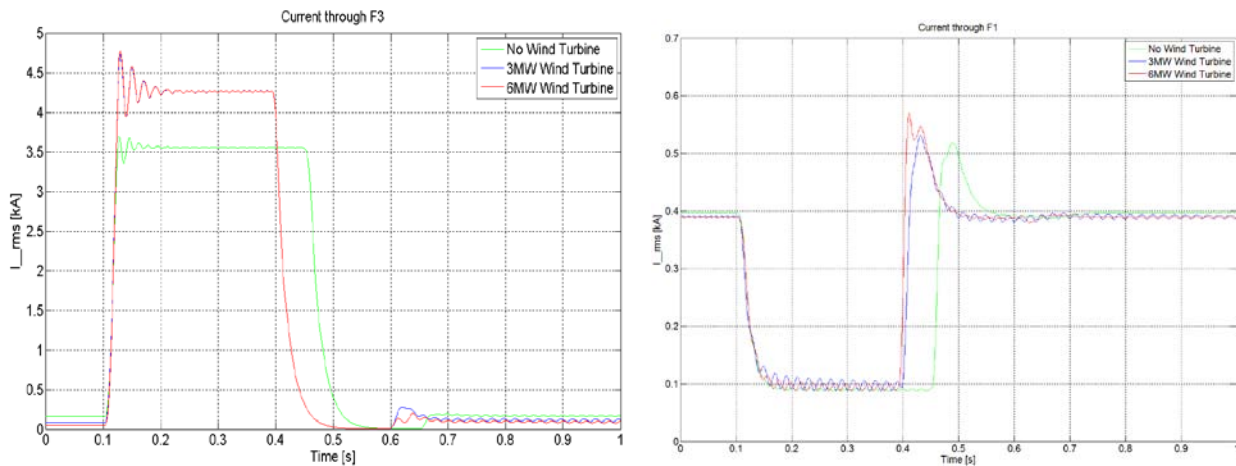
Three phase to ground fault at F3

In case of a three phases to ground fault at F3, the magnitudes of the fault currents increase. With the addition of DG in the network the magnitudes of the fault currents increase as a result the circuit breaker fault detection time decreases. Table 4.35 yield the result of three phases to ground fault at F3.

Table 4.35: Magnitude of fault current at F3 when 3MW and 6MW wind turbine are attached at F3 and the time taken by the protection system to detect the fault.

Fault Location	Wind Power Capacity	Fault Type	Current through the Feeder F3			cycles
			Nominal Current (kA_rms)	Fault Current (kA_rms)	Fault Detection Time (ms)	
F3	No Wind Power	LLLG	0.16	3.56	352.3	17.63
	3 MW Wind Power	LLLG	0.08	4.24	294.3	14.72
	6 MW Wind Power	LLLG	0.05	4.27	293.1	14.66

Figure 4.55 shows the magnitudes of the fault currents at F3 and the rest of the other feeders. It is observed that the nominal current of the network decreases by the injection of the wind turbine currents in the same feeder.



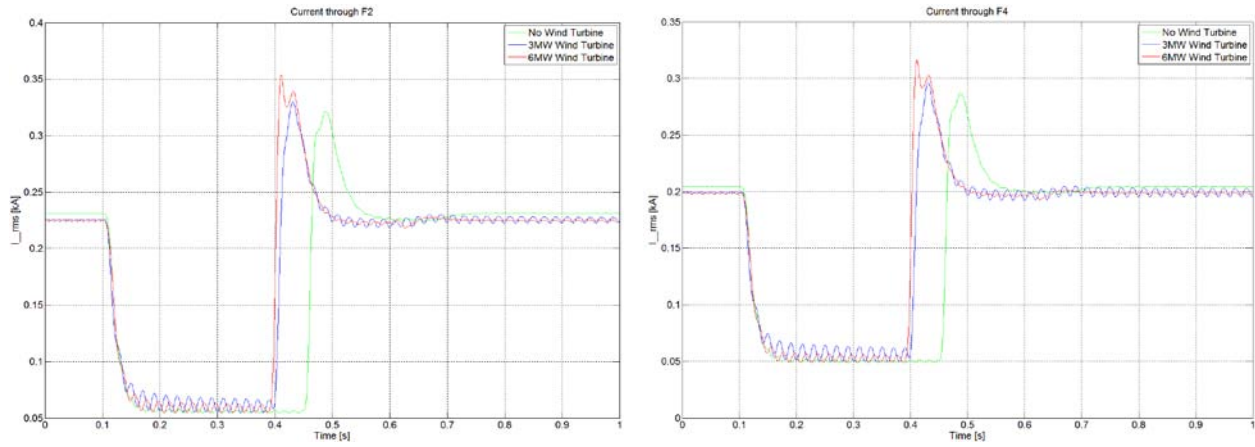


Figure 4.55: Magnitude of three phases to ground fault at F3 with 3MW and 6MW wind turbine installed at F3.

The magnitudes of the voltage drops at F3 during pre-fault, during fault and post-fault are shown in table 4.36. It is observed that during the three phase fault the magnitude of voltage dip is approximately 85% of the pre-fault voltage in all the three cases. As F3 is a shorter feeder than F2 thus during a three phase fault it will cause more voltage drop on the network as compared to F1 and F2. With such a high voltage drop in the network the wind turbine will not be in the position to handle the fault thus the net voltage dip in the network remain the same in all the three cases during a three phase fault. Table 4.33 shows the pre-fault, during fault and the post-fault voltages and the tripping time of the circuit breaker.

Table 4.36 Magnitude of Voltage dips and circuit breaker tripping time at F3 for a pre-fault, during fault and post-fault voltages when a 3 phase fault is applied at the end of the feeder F3.

Fault Location	Wind Power Capacity	Fault Type	Voltage across F3 [p.u]			Fault detection Time (ms)
			Pre- Fault	During Fault	Post-fault	
F3	No Wind Power	LLLG	0.98	0.15	1.0	612
	3 MW Wind Power	LLLG	1.0	0.15	1.02	646.7
	6 MW Wind Power	LLLG	1.01	0.15	1.02	682.4

The magnitudes of the voltage dips at F3 and rest of the other feeders are shown in figure 4.56.

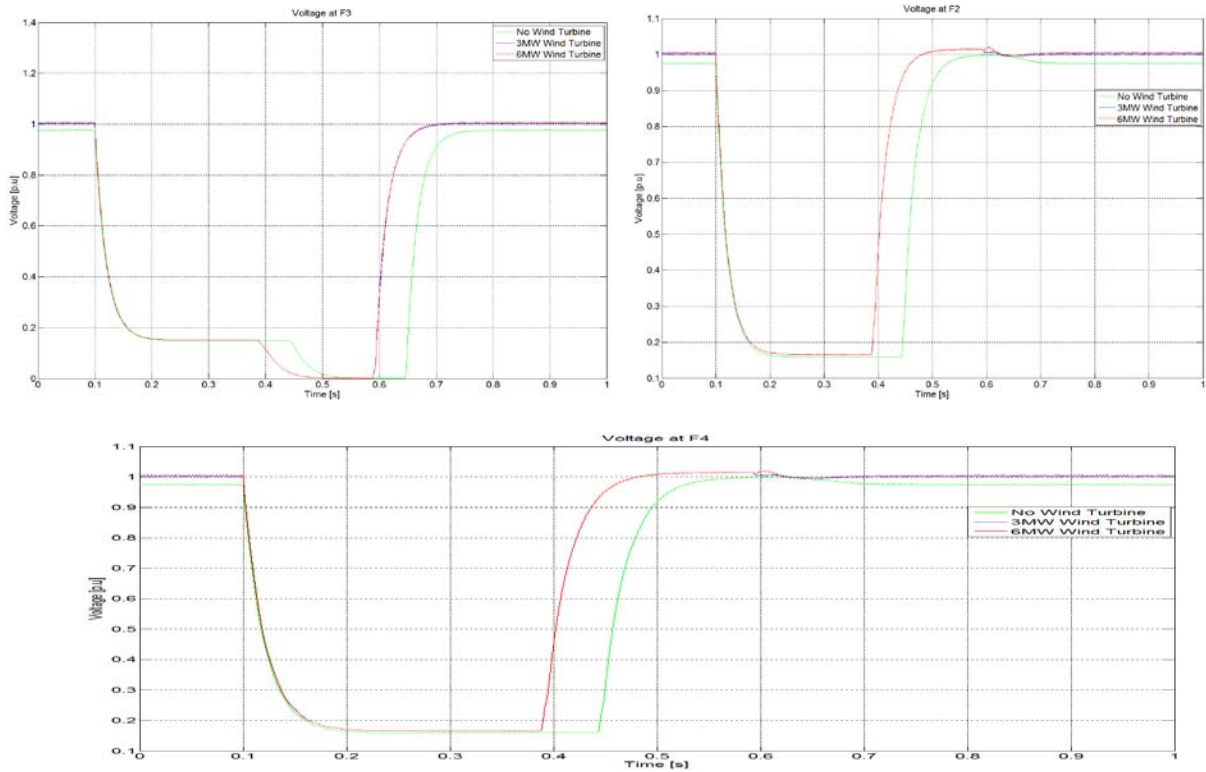


Figure 4.56: Magnitude of voltage dips when a three phase to ground fault is applied at F3

4.3.5. DG attached at Feeder F4

Single line to Ground Fault at F4

As F4 is the shortest feeder in the network with a 0.5km distance from the main bus bar, thus if a fault occur on the line, it will produce a deep voltage dip in the distribution system and high fault currents. When F4 is subjected to line to ground fault at phase A, the magnitude of fault current at phase A and the circuit breaker fault detection time is calculated and shown in table 4.37.

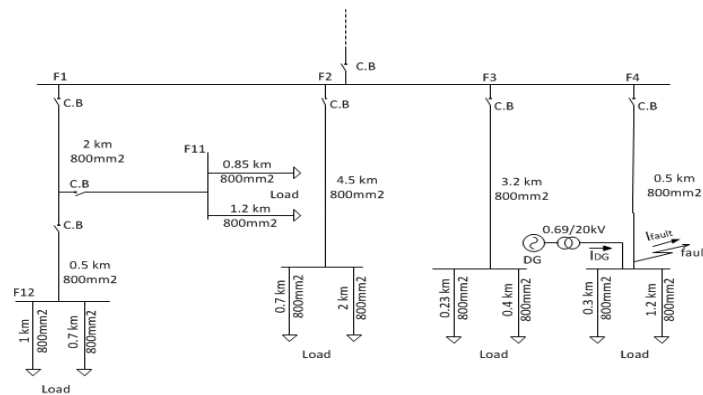


Fig 5.57: Single line diagram of the distribution system when a DG is attached at F4 and a fault is applied at F4.

Table 4.37: Magnitude of fault current at F4 when 3MW and 6MW wind turbine are attached at F4 and the time taken by the protection system to detect the fault

Fault Location	Wind Power Capacity	Fault Type	Current through the Feeder F4			cycles
			Nominal Current (kA_rms)	Fault Current (kA_rms)	Fault Detection Time (ms)	
F4	No Wind Power	LG	0.21	2.52	718.9	35.94
	3 MW Wind Power	LG	0.12	2.39	791.4	39.57
	6 MW Wind Power	LG	0.06	2.27	842.9	42.15

By comparing the result of table 4.37 with table 4.29, it can be seen that the magnitude of the nominal current of F2 without wind turbine in the network is 0.2315A which is higher than the nominal current of F4 but during a fault the magnitude of the fault current of F4 is higher than F2 which cause the circuit breaker to trip faster than as compared to a fault at F2. From the above result it is analyze that as the fault is close to the grid, the more severe and high fault current will flow in the network. The magnitude of the fault current of phase A of F4 and the rest of the other feeders are shown in figure 4.58.

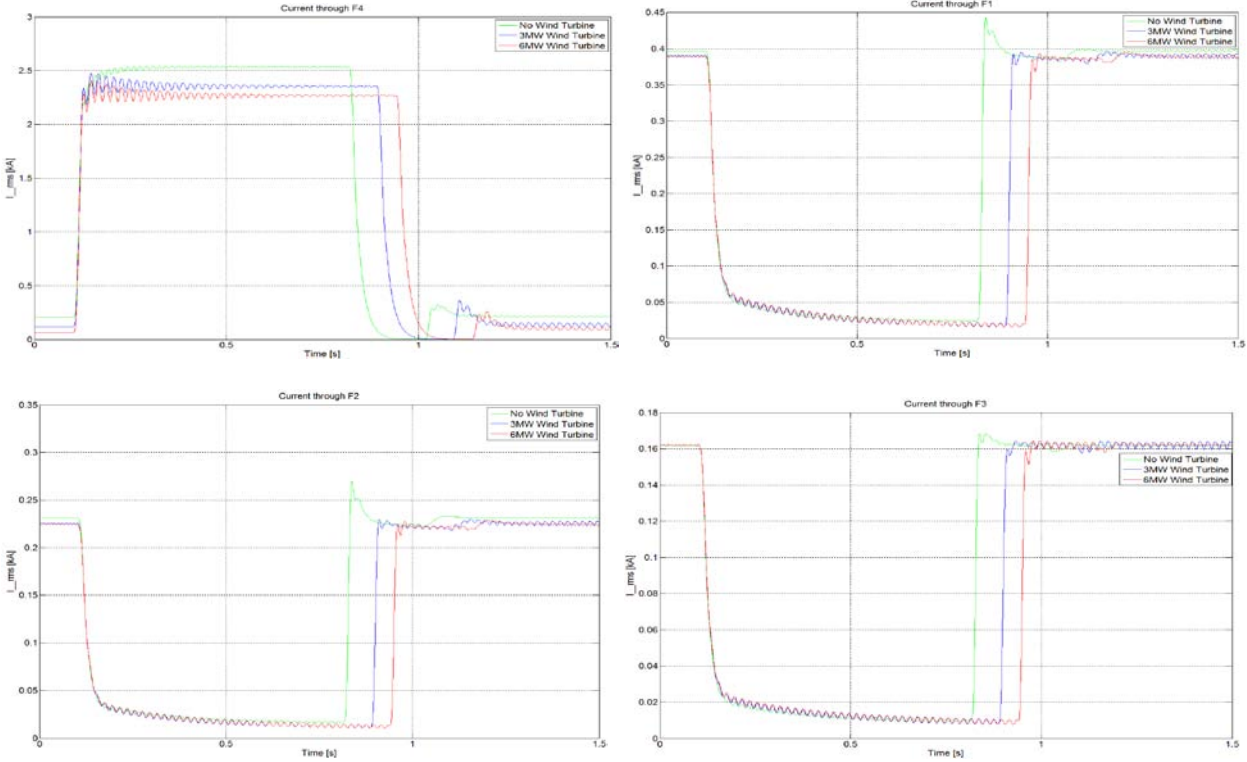


Figure 4.58: Magnitude of line to ground fault current at phase A of F4 with 3MW and 6MW wind turbine installed at the same feeder.

The magnitudes of the voltage drops at F4 during pre-fault, during fault and post-fault are shown in table 4.39. With 3MW wind power capacity, the voltage drop on F4 is only 12.58% of the pre-fault voltage as compared to 19.8% voltage drop without wind turbine. In case of 6MW wind power capacity installed in the distribution system, the voltage drop on the bus will reduce to 12.1% of the pre-fault voltage. Table 4.38 shows the pre-fault, during fault and the post-fault voltages and the tripping time of the circuit breaker.

Table 4.38 Magnitude of Voltage dips and circuit breaker tripping time at F2 for a pre-fault, during fault and post-fault voltages when a fault is applied at the end of the feeder F2.

Fault Location	Wind Power Capacity	Fault Type	Voltage across F4 [p.u]			Fault detection Time (ms)
			Pre- Fault	During Fault	Post-fault	
F4	No Wind Power	LG	0.98	0.78	1.01	1028
	3 MW Wind Power	LG	1.0	0.88	1.02	1083
	6 MW Wind Power	LG	1.01	0.89	1.02	1164

From the above calculation, it is analyzed that the magnitudes of the voltage dips increase as compared to a fault at F2. Thus the closer the fault to the main grid or substation, the more severe will be the voltage dip in the network. The magnitudes of the voltage dips at F4 and the rest of the other feeders are shown in figure 4.59.

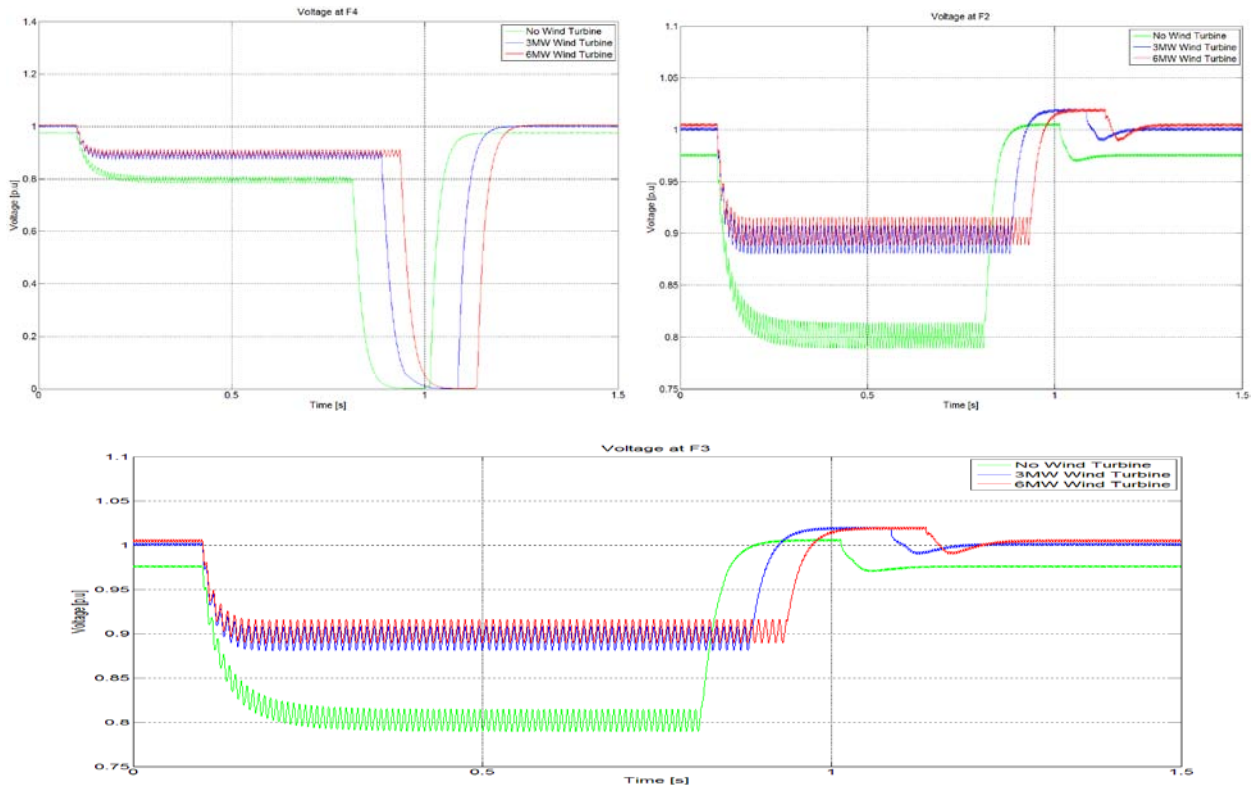


Figure 4.59: Magnitude of voltage dips when a line to ground fault is applied at F4.

Three phase to ground fault at F4

When feeder F4 is subjected to a three phase to ground fault, it can be seen that the magnitude of the fault current increases and as a result the circuit breaker fault detection time decreases.

By comparing the values of table 4.39 with table 4.30, the magnitudes of the fault currents increase which as a result trip the circuit breaker faster as compared to fault at F2. Figure 4.60 shows the magnitudes of the fault currents at F4 and the rest of the other feeders. It is observed that the nominal current (pre-fault current) of the network decreases by the injection of wind turbine current in the same feeder.

Table 4.39: Magnitude of fault current at F4 when 3MW and 6MW wind turbine are attached at F4 and the time taken by the protection system to detect the fault.

Fault Location	Wind Power Capacity	Fault Type	Current through the Feeder F4			cycles
			Nominal Current (kA_rms)	Fault Current (kA_rms)	Fault Detection Time (ms)	
F4	No Wind Power	LLLG	0.20	4.10	370.1	18.5
	3 MW Wind Power	LLLG	0.12	4.88	307.2	15.36
	6 MW Wind Power	LLLG	0.06	4.92	305.1	15.25

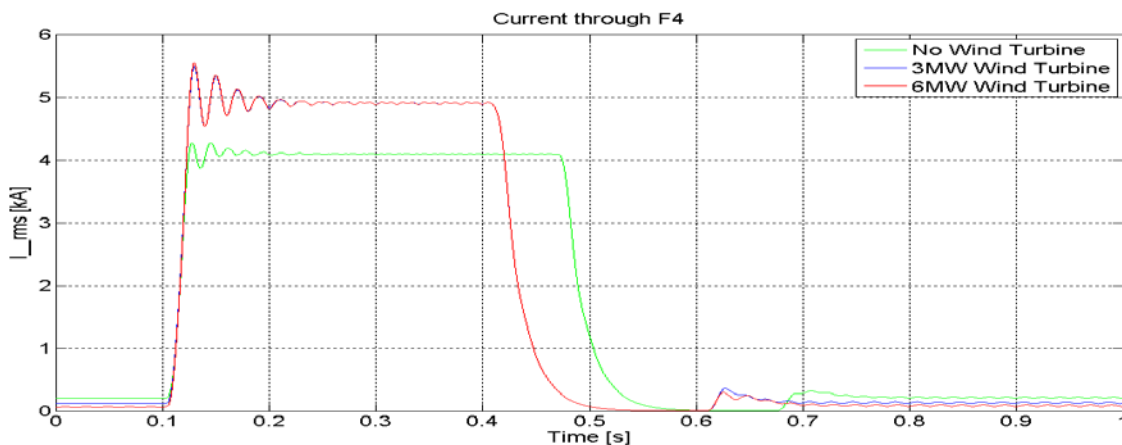


Figure 4.60 Magnitude of three phases to ground fault at F4 with 3MW and 6MW wind turbine installed at F4.

The magnitudes of the voltage drops at F4 during pre-fault, during fault and post-fault are shown in table 4.40. It is observed that during a three phase fault the magnitude of

voltage dip is 97.16% of the pre-fault voltage in all the three cases which cause a high voltage dip in the whole network as compare to fault at F1, F2 and F3.

Table 4.40: Magnitude of the Voltage dips and circuit breaker tripping time at F4 for a pre-fault, during fault and post-fault voltages when a 3 phase fault is applied at the end of the feeder F4.

Fault Location	Wind Power Capacity	Fault Type	Voltage across F4 [p.u]			Fault detection Time (ms)
			Pre- Fault	During Fault	Post-fault	
F4	No Wind Power	LLLG	0.98	0.03	1.01	612
	3 MW Wind Power	LLLG	1.0	0.03	1.02	646.7
	6 MW Wind Power	LLLG	1.01	0.03	1.02	682.4

The magnitudes of the voltage dips at F4 and the rest of the other feeders are shown in figure 4.61.

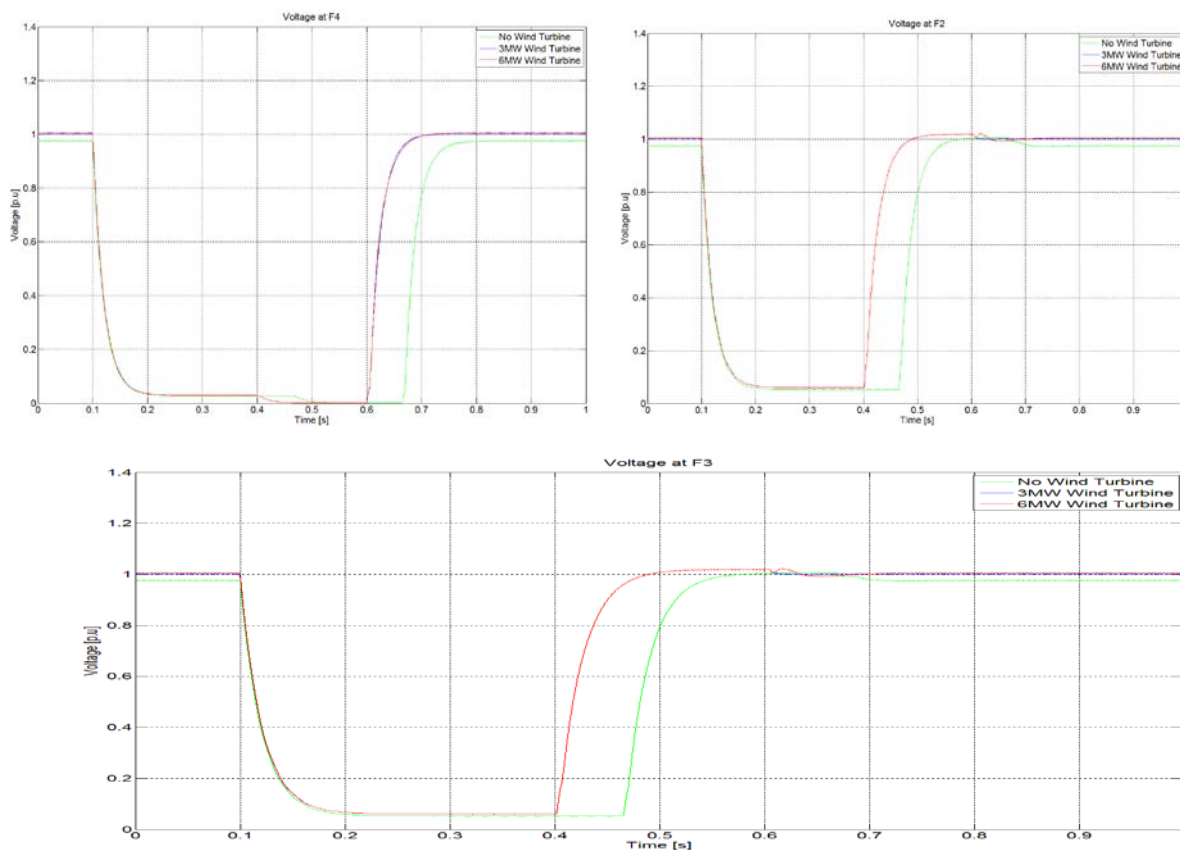


Figure 4.61: Magnitude of voltage dips when a three phase to ground fault is applied at F4

In this study, a fast switching device like the Is-limiter of ABB application is studied to overcome these problems. The purpose of the Is-limiter is to limit the very first rise of short circuit current and make a decision in 0.5ms whenever the tripping of the Is-limiter is necessary. In order to make the decision, the instantaneous current and the rate of current rise at the Is-limiter are continuously observed and measured. When the set point is reached or exceeded the Is-limiter trips. The major feature of Is-limiter is that it avoids voltage drop and do not contribute to the peak short circuit current [9].

Figure 4.62 shows the operation of Is-limiter during a fault. Thus during a fault the Is-limiter will remove the fault with first rise of the short circuit current.

Now the application of the Is-limiter is implemented by applying the logic of Is-limiter on the PCC location where the DG will be attached with the distribution system. Thus whenever a fault occurs in the network, the Is-limiter will remove the DG from the network thus as a result the DG will not be able to contribute in the fault area, it will avoid the mis-coordination of the circuit breakers during faults as stated in the previous section.

Thus to apply this scenario a worst case has been selected as stated in the previous section 4.3. As it is already observed that a worst case occurs when a fault is applied on the same node where a DG is attached. From figure 4.7 it is observed that a worst case occurs when a DG is attached at F11 and a line to ground fault is applied at the same location. As a result the circuit breaker will take longer time to detect the fault in the line because of the reduction of fault current. The fault will remain in the line for a longer duration. The magnitudes of the fault current are shown in table 4.7.

When an Is-limiter is installed with the wind turbine as shown in figure 4.63, it is

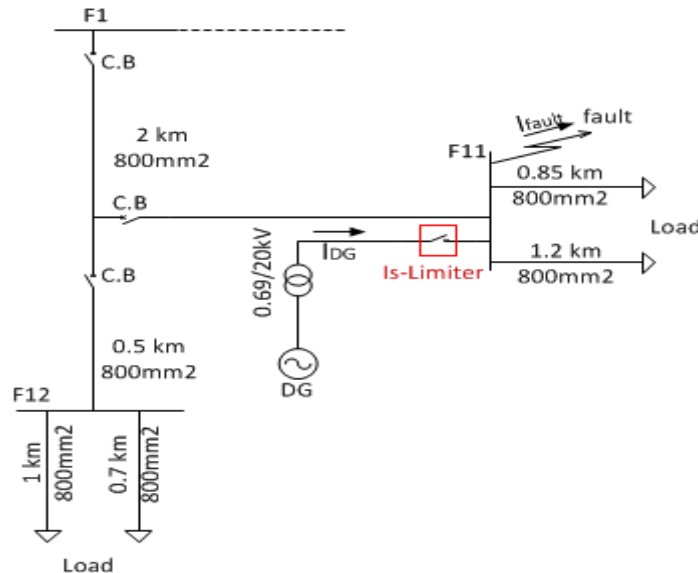


Figure 4.63 Installation of Is-limiter with DG

observed that during a fault, before the first rise peak of short circuit current, the Is-limiter will remove the wind turbine from the network. As a result the protection system will take the same amount of time to detect the fault in the line when there was no external wind turbine installed in the network. The results are shown in figure 4.64.

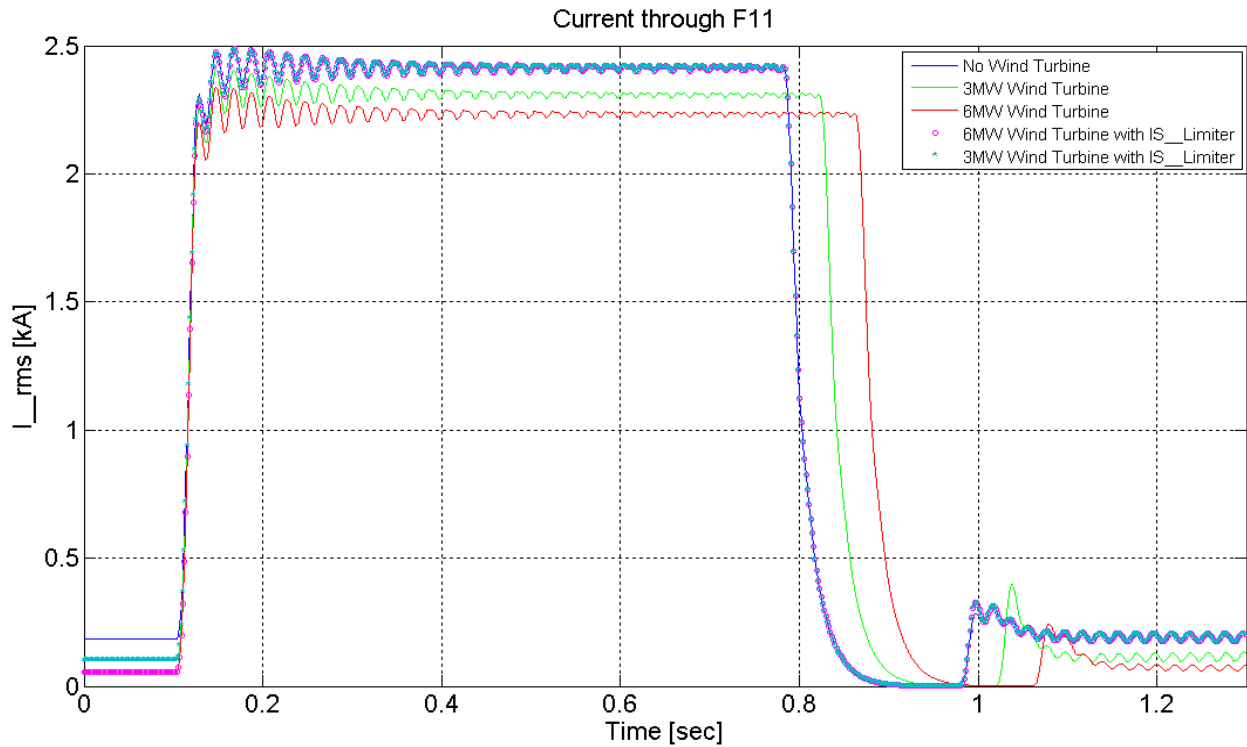


Figure 4.64 Magnitude of single line to ground fault at phase A of F11 with 3MW and 6MW wind turbine installed at F11.

From figure 4.64, it is observed that the even with the addition of 3MW and 6MW wind turbine installed in the network, the circuit breaker will take the same amount of time as seen in the case when the network is without wind turbine. With the application of Is-limiter at the PCC point, whenever a fault occurs, the fast switching device (Is-limiter) will remove the fault before the first rise of the peak. As a result the output waveform will follow the same current magnitude as in case when there was no wind power installed in the network.

5. CONCLUSION AND FUTURE WORK

The project contains two essential goals. One is to develop guidelines for constructing a full power converter based wind turbine and its integration with the distribution network and to find out how the DG is contributing in fault conditions. The major advantage of the full power converter is that the active and reactive power can be controlled independently. The full power converter with inner current controller and outer voltage and power controller has been implemented in chapter 3. The modeling of the grid connected total power converter based wind turbine was well designed, analyzed not only from the voltage level and the power flow during normal operation, but also during fault conditions such as single line to ground fault and three phase to ground fault.

The subsequent goal is to find the impact of DG on the distribution system coordination and protection system (circuit breaker) and the application of fast switching devices to overcome these problems. According to the results presented in section 4, the most severe voltage dip is caused by three phase to ground fault close to the PCC which causes mis-coordination of the circuit breaker and the increase of fault current level. As a result, it affects the thermal limits of insulation as well as the cable system.

In the scenario of single line to ground fault conditions as seen in section 4, the most severe effect of circuit breaker mis-coordination occurs when the fault is close to the PCC which causes decline in the fault current magnitude. As a result, the circuit breaker of the distribution system takes longer time to detect the fault in the network.

It has also become evident that the turbine at shorter radial feeders are exposed to more severe voltage dips while longer radial feeders result in less severe voltage dips.

By using fault current limiters such as super conductor fault current limiters or the Is-limiter depicted in section 4.4, the contribution of DG current in the faulted area and mis-coordination of circuit breakers can be avoided by limiting the very first rise of short circuit current. Thus, by using the fast switching devices, the mis-coordination of circuit breakers can be avoided by disconnecting the DG from the network during the fault.

Since the major purpose of this thesis is to find out the application of fast switching devices for individual small rating wind turbines as seen in section 4, it is observed that the wind turbine of 3MW and up to 6MW can cause mis-coordination of protection for faults close to the PCC. Usually a converter based DG cannot produce worse effects on the distribution system because of a hard limiter in the converter which can limit the fault current and low power capacity of the wind turbine.

Thus the best recommendation for fast switching devices for wind power system is to use in grid side converters where the power rating of wind turbine is up to 40MW or higher.

FUTURE WORK

Some point from this work could be the basis of future studies:

- The study has been based on variable speed PMSG full power converter. A similar study could be done on variable speed DFIG without converter. The generator and transformer current will play an important role in this study.
- When evaluating the fault ride through in a wind turbine, a more realistic detailed model for a wind park with distribution system is needed. A detail model of distribution system with large number of Wind Park should be studied.
- In this study only the need of reactive power of wind turbine has been studied during fault cases. Further study should be required for the study of reactive power controller (SVC and STATCOM) with wind turbines.
- The application of fast switching devices fault current limiter for individual wind turbine. The study of fast switching devices should be required for a grid connected base wind park system.

BIBLIOGRAPGY

- [1] IEEE std 1159-1995 "IEEE Recommended Practice for Monitoring Electric Power Quality".
- [2] Equipment failures caused by power quality disturbances By Bendre, A. Divan, D. Kranz, W. Brumsickle. This paper appears in: Industry Applications Conference, 2004. 39th IAS Annual Meeting. Conference Record of the 2004 IEEE.
- [3] IEEE Application Guide for IEEE Std 1547™, IEEE Standard for Interconnecting Distributed Resources with Electric Power Systems.
- [4] Jaap Daalder and Tuan A. Le ENM 050 Power System Analysis (Course Compendium: Chalmers University Of Technology).
- [5] Richard Roeper "Short Circuit Current in Three Phase System" by Siemens
- [6] The impact of distributed generations on the power system stability in the Singapore power system yu Chin Guan, Tan.
- [7] Effect of DG capacity on the coordination of protection system of distribution system by J. Sadeh, M. Bashir, E. Kamyab.
- [8] Superconducting FCL: Design and Application by Vladimir Sokolovsky, Victor Meerovich, Istvan Vajda.
- [9][http://www05.abb.com/global/scot/scot235.nsf/veritydisplay/8fb94bb3948fa74fc1257720003ebfb9/\\$file/2243%20Is-Limiter_EN.pdf](http://www05.abb.com/global/scot/scot235.nsf/veritydisplay/8fb94bb3948fa74fc1257720003ebfb9/$file/2243%20Is-Limiter_EN.pdf)
- [10] http://www.electricenergyonline.com/?page=show_article&mag=22&article=173
- [11] Analysis of fault detection and location in medium voltage radial networks with distributed generation. By J.I. Marvik, A. Petterteig and H.K. Hoidalen.
- [12] J.Daalder, T. A. Le. ENM050 Power System Analysis.(Course Compendium). Goteborg, Sweden: Chalmers University of Technology.
- [13] PSCAD/EMTDC course ABB by Dennis Woodford and Garth Irwin Electranix Corporation.
- [14] Massimo Bangiorno, Jan Svensson and Ambra Sannino "An advance cascade Controller for Series-connected VSC for Voltage Sag Mitigation", IEEE Industrial Application Society (IAS).
- [15] Power Electronics Converters, applications, and design by Mohan, Undeland, Robbins.

- [16] Control of variable speed drives by lennart Harnfors (Course Compendium). Chalmers University of Technology, Goteborg, Sweden.
- [17] Voltage source converters in power systems, modeling, control and applications by Amirnasir Yazdani and Reza Irvani.
- [18] IEEE standard Inverse-Time characteristic equations for over current Relay IEEE std C37. 112-1996.

Appendix A

A.1 Introduction

This appendix presents the designing and calculation of cable parameters to implement it in PSCAD to analyze the cable behavior. Both the full section model and pi-section model are presented in this appendix.

A.2 Determining Cable Parameters

In PSCAD the cable can be designed by two ways, by using cable geometry or by using equivalent pi-section model. Both the models have been designed to represent cable behavior. The output of equivalent pi-section models did not include the reflection phenomenon which makes it easy to design. Thus in pi-section model, only the RDC, C and L parameters are required for the designing of the cable.

As a pi-section model does not simulate reflection in the cable, thus it is only used for simulating steady state condition and only low frequency behavior can be analyzed. As according to our system requirement, an equivalent 132kV 2000mm² XLPE and 30kV 800mm² XLPE cable has been selected from ABB catalog. The data of the cable is shown in table A.1.

Cross-section of conductor	Diameter of conductor	Insulation thickness	Diameter over insulation	Cross-section of screen	Outer diameter of cable	Cable weight (Al-conductor)	Cable weight (Cu-conductor)	Capacitance	Charging current per phase at 50 Hz	Inductance		Surge impedance
												
mm ²	mm	mm	mm	mm ²	mm	kg/m	kg/m	μF/km	A/km	mH/km	mH/km	Ω
2000	54.4	15.0	89.4	95	106.1	11.8	24.2	0.34	8.1	0.32	0.47	18.3

Our standard for IEC 30 kV						
Cross section		Insulation		Outside diameter	Weight of complete cable with	
Conductor	Screen	Thickness	Diam.		Aluminium conductor	Copper conductor
mm ²	mm ²	mm	mm	mm	kg/m	kg/m
95	25	8	28.6	39	1.4	2.0
120	25	8	30.2	41	1.6	2.4
150	35	8	31.7	42	1.9	2.8
185	35	8	33.4	44	2.1	3.2
240	35	8	35.7	46	2.3	3.8
300	35	8	37.9	48	2.6	4.5
400	35	8	41.3	52	3.0	5.5
500	35	8	44.4	56	3.5	6.6
630	35	8	48.2	59	4.0	8.0
800	35	8	52.9	65	4.9	10.0

Table A.1: Cable data for 130kV 2000mm² and 30kV 800mm² XLPE cables [1]

For the designing of the cable it is necessary that the correct geometric parameters have been entered into the simulation program. It will be shown in the following section how the geometric parameter of the cable affects the electrical parameters (C, L, and RDC) of the cable.

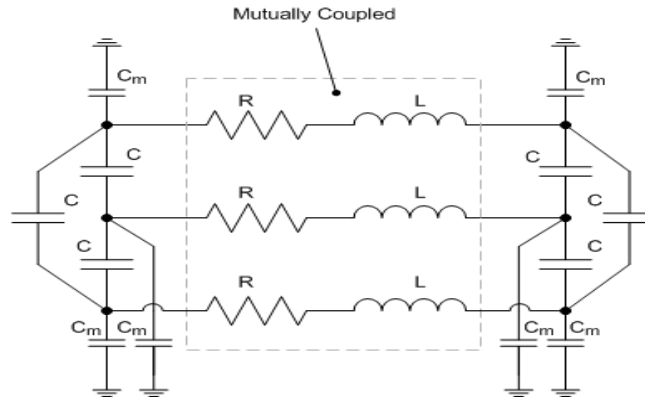


Figure A.1: Couple Pi-section model in PSCAD

In order to simulate a three phase system with three phase single core cable. PSCAD require certain parameters for the designing of the cable like conductor, insulator and sheath as shown in figure A.2.

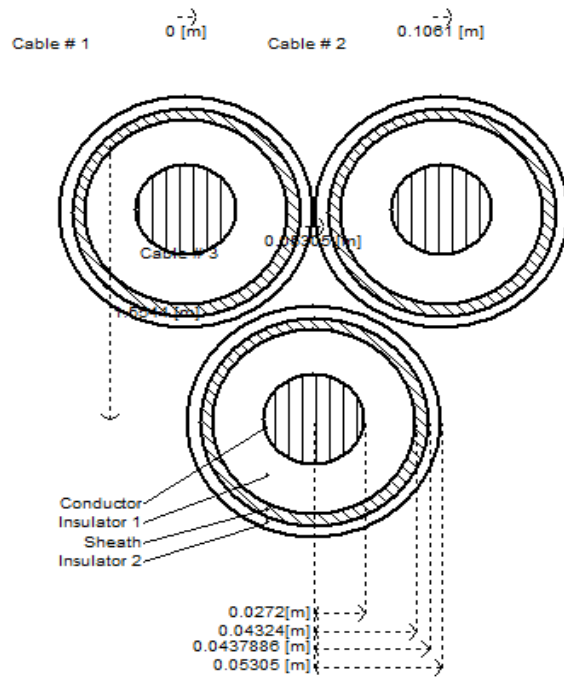


Figure A.2: Cable model geometry in PSCAD

The above PSCAD cable geometry is too simple but the real cable geometry is quite complex, it include the layers like conductor screen (semi-conductor), insulation, insulation screen, metallic sheath, fillers, beddings and outer sheath (cover).

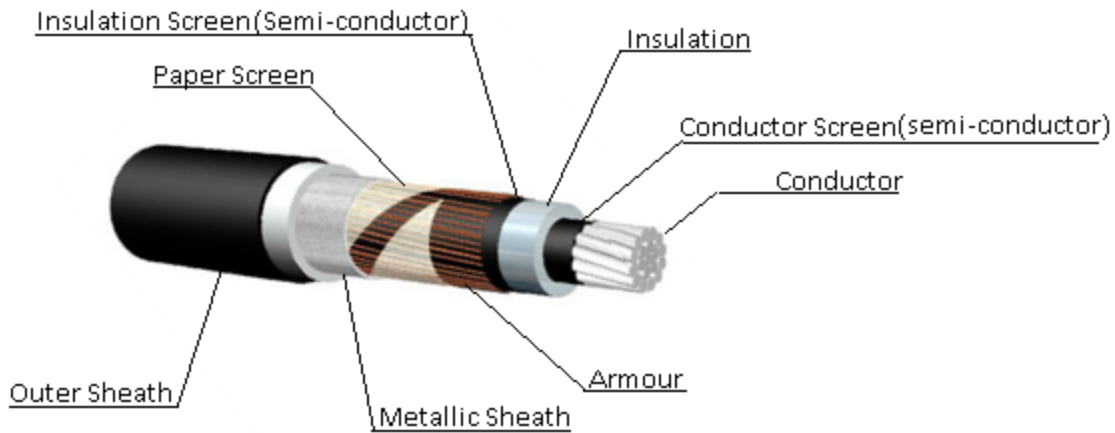


Figure A.3: XLPE cable Construction

The inner shield is used to make a uniform electric field across the conductor surface. The major purpose of specifying individual layer and its detail in the simulation is to get best possible result in the simulation.

A.3 Capacitance Calculation

As compared to overhead lines, cables have high capacitance which mainly depends upon the thickness between the two conductive elements in the cable, the conductor and the semiconductor screen.

The nominal capacitance per unit length for single core cable geometry can be calculated as,

$$C = \frac{2\pi\epsilon}{\ln(b/a)} \quad (A-1)$$

Where,

a = outer radius of conductor + semiconductor thickness.

b = External radius of Insulation.

For geometry of 3-core cable as shown in figure A.2, the capacitance for such geometry can be calculated as

$$C = \frac{\epsilon}{18 \ln\left(\frac{b}{a}\right)} \quad (A-2)$$

For an XLPE cable $\epsilon = 2.3$. Knowing the exact thickness of the inner semiconductor is difficult but taking the hint from the ABB cable catalog one can easily determine the outer radius of semiconductor layer by using the expression as,

$$\text{Semi-conductor layer outer radius} = R_1 = \frac{\text{Diameter over Insulation} - 2(\text{Insulation thickness})}{2}$$

Thus

$$\text{Thickness of the semiconductor screen} = R_1 - \frac{\text{Diameter of conductor}}{2}$$

From eq. (A-2) the external radius of insulation can be calculated as by putting the value of capacitance from cable catalog,

$$b = a \exp \frac{2.3}{18C} \quad (\text{A-3})$$

A.4 Inductance calculation

Since the calculation of inductance is the most difficult part because it include both the self-coupling and the mutual coupling of the magnetic field. The later term is more difficult to calculate thus for simplicity its effect will be neglected. The self-inductance of the cable per unit length can be defined as,

$$L = \frac{\mu_0 \mu_r}{2\pi} \ln \left(\frac{b}{a} \right) + \frac{1}{8\pi} \mu_0 \mu_r \quad (\text{A-4})$$

Where,

a = radius of inner conductor.

b = radius of inner surface of outer conductor (Screen).

For an underground cable with a depth of 1.5m in ground, the screen area will be 150mm² as given in ABB cable catalog [1]. Thus by knowing the screen area the radius of the screen can be calculated by using the expression,

$$A_{\text{screen}} = \pi (\text{radius over the screen}^2 - \text{external radius of insulation}^2)$$

$$A_{\text{screen}} = \pi (R_{\text{screen}}^2 - b^2)$$

$$R_{\text{screen}} = \sqrt{\frac{A_{\text{screen}}}{\pi} + b^2} = \sqrt{\frac{150}{\pi} + 43.24^2}$$

Thus the thickness of the screen will be 0.5486mm.

For simplicity let suppose that no armor is used, thus the radius over the last layer of insulation can be calculated from the outer diameter of the cable.

$$A_{\text{screen}} = \frac{\text{outer diameter of cable}}{2} = 53.05\text{mm}$$

We suppose that the outer layer is made of XLPE, thus the thickness of the outer layer will be 8.96mm. By using a three core cable with trefoil formation as shown in figure A.2, the inductance can be calculated by using the expression

$$L = 0.05 + 0.2 \ln\left(\frac{k \cdot s}{r_c}\right)$$

Where,

For trefoil formation $k = 1$

S = distance between conductor axes

r_c = conductor radius

The capacitance C of the cable can be calculated by substituting the value in eq (A-2), we get

$$C = \frac{\epsilon}{18 \ln\left(\frac{b}{a}\right)} = \frac{2.3}{18 \ln\left(\frac{43.24}{\frac{54.4}{2} + 2.5}\right)}$$

A.5 Determining other Parameters

After calculation inductance and capacitance of the line, the other important parameter of the line is the surge impedance loading or SIL. It is the maximum MW loading of the transmission line at which a maximum active power flow occur with reactive power flow balance. The amount of reactive power (MVAR) produced by the transmission line depends on the capacitive reactance (X_c) and voltage at which the line is energized, which is required by the transmission line to support its magnetic field. In the equation the above expression will be written as,

$$\text{MVAR Produced} = \text{MVAR Used}$$

$$\frac{V^2}{X_c} = I^2 X_L$$

Thus SIL is the MW loading at which the line MVAR produce is equal to used. In general form it can be written as,

$$SIL = Z_0 = \sqrt{\frac{L}{C}} = 30.78 \Omega$$

The reactance of the transmission line will be calculated in order to fulfill the criteria for pi-model designing in PSCAD.

$$X_C = 1/2\pi f C$$

$$X_L = 2\pi f(L/1000)$$

A.6 Skin Effect

The size of the conductor is very important factor to define skin effect in cable designing. The skin effect is caused by high frequency component. At low frequency, the electromagnetic field penetrates through the conductor thus all the current flows through the cross section area of the conductor. Hence the resistance will be small and computed as DC resistance. The resistance of the conductor is simply defined as,

$$R_{DC} = \frac{\rho}{A} = 1.41 \times 10^{-5} \Omega/m$$

Where

ρ = resistivity of the conductor,

A = area of the conductor.

Now as the frequency increases the electromagnetic field penetration through the conductor decreases and the field pushes the current at the skin of the conductor thus at high frequency all the current flows through the skin of the conductor. The penetration depth (skin depth) is defined as

$$\delta = \sqrt{\frac{\rho}{\pi f \mu}}$$

Where

f = frequency

μ = permeability of the conductor.

The skin effect thus causes an addition ac resistance to be added with the dc resistance, thus [2]

$$R_{AC} = \omega L_{AC} = \frac{\rho}{2\pi r \delta}$$

Where

r = the radius of the conductor.

The dc resistance depends upon the area of the conductor whereas the ac resistance depends upon frequency.

A.7 Result Comparison

In this section two different cable models have been analyze from the result of previous section. The “equivalent Pi-Model” that is design in PSCAD has been understand from the theory given in [3].

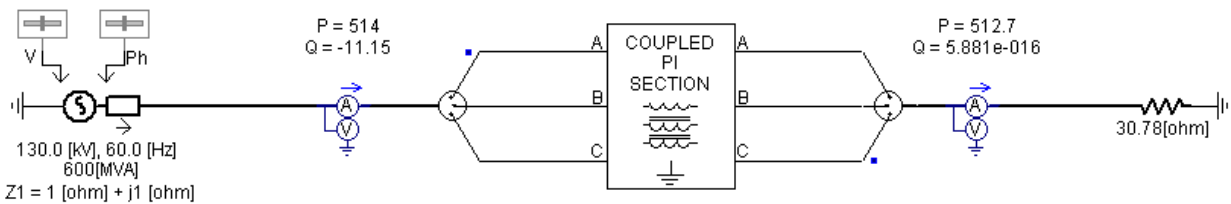


Figure A.4: Couple Pi-Model

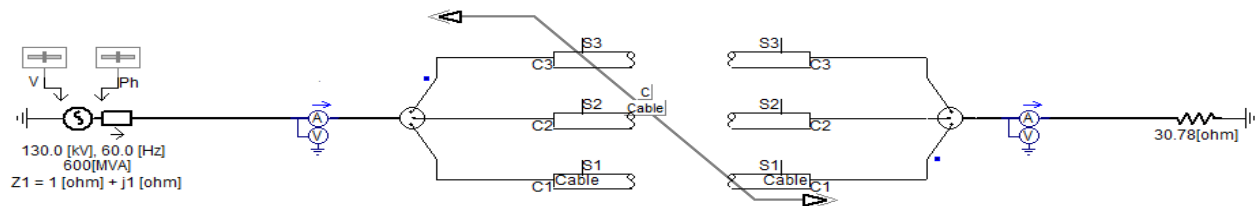


Figure A.5: Full Cable Model

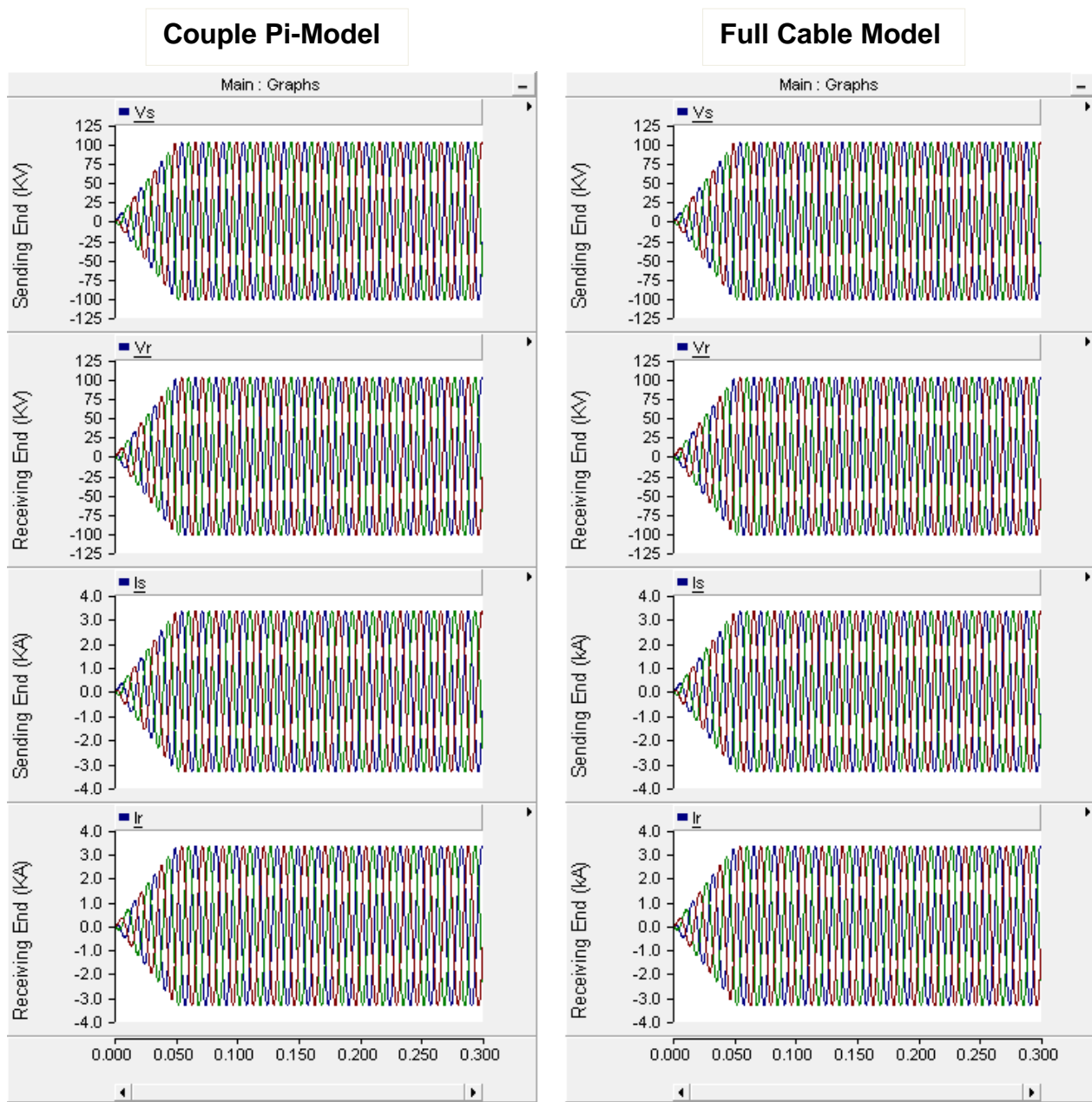


Figure A.6: Result for voltage and current magnitude in Cable

With a total cable length of 5.5 km loaded at the end with a SIL value of 30.78Ω . From the graph output the result of the full cable model is fairly different from the couple Pi-Model. The reason for it is that the cable model takes the DC resistance as well as the AC resistance whereas the Pi-model only takes the DC resistance. Thus in pi-model the magnitude of voltage and active power is higher than the full cable model. [2]

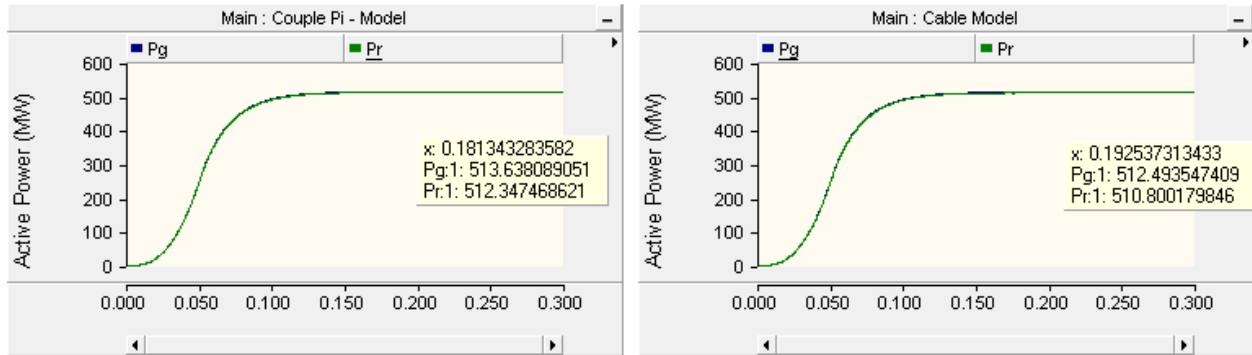


Figure A.7: Result of Active Power flow

As it has been observed in figure A.7, the magnitude at the receiving end is higher in pi-model as compared to the full cable model in PSCAD. The power losses in the full cable model is 1.68MW whereas from I^2R the losses are only 864kW, the reason for the higher losses are due to the fact that the cable model take the DC as well as the AC resistance in PSCAD whereas during our analytical calculation in previous section only the DC resistance is taken into account. The result is therefore expected.

The same calculation procedure has been done for 30kV XLPE cable.

BIBLIOGRAPGY

- [1] "ABB XLPE cable guide" available from <http://www.abb.com/product/us/9AAF401951.aspx?country=SE>
- [2] Skin Effects models for Transmission Line Structures using Generic SPICE Circuit Simulators by Bidyut K. Sen and Richard L. Wheele.
- [3] Power System stability and control by Prabha Kundur.